THROMBORESISTANT SILICONES AND POLYURETHANES PREPARED WITH AMPHIPHILIC SURFACE-MODIFYING ADDITIVES

A Dissertation

by

BRYAN KHAI DINH NGO

Submitted to the Office of Graduate and Professional Studies of
Texas A&M University
in partial fulfillment of the requirements for the degree of

DOCTOR OF PHILOSOPHY

Chair of Committee,	Melissa A. Grunlan
Committee Members,	Gerard L. Coté
	Daniel L. Alge
	James D. Batteas
Head of Department,	Michael J. McShane

May 2020

Major Subject: Biomedical Engineering

ABSTRACT

Silicones and polyurethanes (PUs) are often used in blood-contacting medical devices; however, their hydrophobicity makes them susceptible to non-specific protein adsorption and subsequent thrombosis. In this work, amphiphilic poly(ethylene oxide) (PEO)-based surface modifying additives (SMAs) were evaluated for their capacity to enhance surface hydrophilicity and thromboresistance. In prior studies, these PEO-silane amphiphiles [PEO-SA; α-$(EtO)_3$-Si-$(CH_2)_2$-$ODMS_m$-*block*-PEO_n-CH_3] exhibited rapid, substantial surface restructuring and protein resistance in a condensation cure silicone. Various SMA structures were assessed, including those of differing PEO (n = 3 – 16) and oligo(dimethyl siloxane) (ODMS; m = 0 – 30) repeat units. PEO-SAs with (*XL diblock*) and without (*Diblock*) the crosslinkable triethoxysilane (TEOS) group were also assessed to determine the impact on SMA modified silicone stability (e.g. water uptake and leaching). The TEOS group was determined to be unnecessary, particularly with a longer, m = 30, ODMS tether.

Herein, both *XL diblock* and *Diblock* PEO-SAs were prepared with ODMS lengths of m = 13 or 30, and constant PEO length (n = 8). As SMAs in a condensation cure silicone (5 – 100 μmol/g), these were assessed similarly to determine their minimum effective concentration and stability. PEO-SA modified silicones ≥ 25 μmol/g showed enhanced hydrophilicity and protein resistance that was sustained following aqueous conditioning. All modified silicones also had minimal water uptake and leaching, further indicating the TEOS group is not needed with a sufficiently long ODMS tether. Following this, the *XL*

diblock, m =13 and *Diblock, m = 30* PEO-SAs were tested as SMAs in silicone against whole human blood. Under both static and dynamic conditions, PEO-SA modified silicones showed effective resistance to protein adsorption and platelet adhesion at 10 µmol/g or greater.

Finally, the *XL diblock, m = 13* PEO-SA was incorporated as SMAs in PU (5 – 100 µmol/g) to assess hydrophilicity, stability, and thromboresistance. PEO-SAs showed some immiscibility in PUs; however, the resulting modified PUs (at concentrations ≥ 25 µmol/g) exhibited increased hydrophilicity and good stability (i.e. low water uptake and leaching) following aqueous conditioning. Lastly, PEO-SA modified PUs (at concentrations ≥ 10 µmol/g) showed significantly reduced protein adsorption and platelet adhesion from whole human blood under static conditions.

DEDICATION

To Natsuki

Moving to Texas to complete my doctoral studies was as daunting a choice that I have ever made. Throughout the many long days, nights, and weekends these past few years, you have always been there for me. Thank you so much for your love, support, and belief in me. I truly could not have done it without you.

ACKNOWLEDGEMENTS

I would first like to thank my committee chair, Prof. Melissa Grunlan. Before arriving at Texas A&M, I had little polymer chemistry knowledge and a non-engineering background. Even so, Prof. Grunlan welcomed me into her research group and believed in my passion and ability to succeed on this project. Since then, Prof. Grunlan has been an excellent advisor and continues to be exceedingly patient and supportive. I would not be where I am today, if it was not for her mentorship, and I am incredibly grateful. I would also like to thank my committee members, Prof. Gerard Coté, Prof. Daniel Alge, and Prof. James Batteas for their support and guidance throughout my doctoral studies.

I would like to thank my friends, colleagues, as well as the faculty and staff of the Biomedical Engineering department. They truly shaped my experience at Texas A&M and made it one I could never forget. I have been fortunate to make life-long friends and would like to thank former and current Grunlan lab members for their support: Dr. Melissa Hawkins, Dr. Marc Rufin, Dr. Lindsay Woodard, Dr. Kristen Means, Dr. Jakkrit Suriboot, Michaela Pfau, Ping Dong, Mike Frassica, Felipe Beltran, Alec Marmo, and Connor Demott. I owe thanks especially to the undergraduate students who assisted in conducting this work, including Jessica Johnson, Kendrick Lim, Mikayla Barry, and Andrea Brunal.

Finally, thank you to my family for their encouragement and support, not only during my doctoral studies, but also throughout my life. To my mom, my dad, and my sisters, thank you for your unwavering love and support. No matter how far away you are, you inspire me to do and be the best that I can every day.

CONTRIBUTORS AND FUNDING SOURCES

Contributors

This work was supervised by a dissertation committee consisting of Professor Melissa A. Grunlan [advisor] as well as Professor Gerard L. Coté and Professor Daniel L. Alge of the Department of Biomedical Engineering, and Professor James Batteas of the Department of Chemistry.

The data in Chapter II for Figure 2-6 was collected and analyzed by Shane Stafslien of the Office of Research & Creative Activity at North Dakota State University. The studies done with human blood in Chapters III and IV were facilitated by former and current students, David Luna and Tanmay Mathur, under the advisement of Professor Abhishek Jain of the Department of Biomedical Engineering at Texas A&M University. This included access to human blood, as well as use of a BSL-2 lab space and microscope for image analysis. The Chandler Loop construct and protocols were designed and fabricated by Dr. Nick Sears and Mikayla Barry of the Department of Biomedical Engineering at Texas A&M University. The poly(2-oxazoline)s utilized in Chapter V was synthesized, characterized, and provided by Joachim Van Guyse under the advisement of Professor Richard Hoogenboom in the Department of Organic and Macromolecular Chemistry at Ghent University.

All work for the dissertation was completed by the student, under advisement of Professor Melissa A. Grunlan of the Department of Biomedical Engineering.

Funding Sources

This work was made possible in part by the National Science Foundation (NSF) Engineering Research Center for Precise Advanced Technologies and Health Systems for Underserved Populations (PATHS-UP) under Award Number 1648451, and the Texas A&M Engineering Experiment Station (TEES). Its contents are solely the responsibility of the authors and do not necessarily represent the official views of institutions.

TABLE OF CONTENTS

Page

Page

Page

LIST OF FIGURES

Page

Page

Page

Page

LIST OF TABLES

Page

CHAPTER I

INTRODUCTION: PROTEIN RESISTANT POLYMERIC BIOMATERIALS*

1.1. Overview

Toward improving implantable medical devices as well as diagnostic performance, the development of polymeric biomaterials having resistance to proteins remains a priority. Herein, we highlight key strategies reported in the recent literature that have relied upon improvement of surface hydrophilicity via direct surface modification methods or with bulk modification using surface modifying additives (SMAs). These approaches have utilized a variety of techniques to incorporate the surface hydrophilization agent, including physisorption, hydrogel network formation, surface grafting, layer-by-layer (LbL) assembly and blending base polymers with SMAs. While poly(ethylene glycol) (PEG) remains the gold standard, new alternatives have emerged such as polyglycidols, poly(2-oxazoline)s (POx), polyzwitterions, and amphiphilic block copolymers. While these new strategies provide encouraging results, the need for improved correlation between *in vitro* and *in vivo* protein resistance is critical. This may be achieved by employing complex protein solutions as well as strides to enhance the sensitivity of protein adsorption measurements.

---

*Reprinted with permission from "Protein Resistant Polymeric Biomaterials" by Ngo, B.K.D. and Grunlan, M.A., 2017. *ACS Macro Lett.*, 6, 992-1000, Copyright 2017 American Chemical Society.

1.2. Introduction

Upon implantation of blood-contacting medical devices, adsorption of plasma proteins occurs immediately and initiates a thrombosis cascade and bacterial infection.[1-6] These ultimately lead to reduced device efficacy and safety.[7,8] Similarly, protein adsorption leads to biofouling and limits the sensitivity and lifetime of diagnostics and implanted biosensors.[9-12] Polymeric biomaterials used for medical devices are largely selected on the basis of their bulk mechanical properties, rather than the suitability of their surface properties. Poor protein resistance is often associated with surface hydrophobicity. For example, hemodialysis catheters are commonly prepared from silicones and polyurethanes (PU) that offer a desired combination of flexibility and strength.[13] Unfortunately, these and other commonly employed polymeric materials are hydrophobic and thus highly susceptible to nonspecific protein adsorption.[14] While there is a vast body of literature regarding protein resistant materials strategies,[15-19] thrombosis remains a significant problem for devices. Herein, we highlight key strategies that have emerged in the recent literature which seek to improve the protein resistance of polymeric biomaterials using direct surface modification as well as bulk modification with surface-modifying additives (SMAs).

The conversion of a hydrophobic surface to one that is hydrophilic is a common, albeit nonexclusive theme among protein resistant biomaterials strategies.[20] In the biological environment, a hydrophobic surface generates a high surface energy that the body relieves via protein adsorption.[21] Proteins undergo a conformational change to associate their hydrophobic domains with the material and their hydrophilic domains with

the biological environment to create a substantial reduction in surface energy. This reduction outweighs the entropic cost of the conformational change, thermodynamically favoring protein adsorption to a material surface.[22] Therefore, increased surface hydrophilicity can reduce the high interfacial energy and make protein adsorption less favorable. The technique by which surface hydrophilicity is imparted and the chemical nature of the surface hydrophilization agent varies. Historically used surface modification techniques have highlighted the challenges of producing protein resistant polymeric biomaterials. Coupled with various hydrophilization agents, each surface modification technique is associated with its own advantages and disadvantages. These features have been drivers for the development of newer protein resistant surface modification strategies.

Among the commonly utilized techniques to incorporate chemical modifiers onto a surface are physical adsorption (physisorption), hydrogel network formation, surface grafting, layer-by-layer (LbL) assembly, and blending with SMAs (**Figure 1-1**). However, many of these strategies have been demonstrated on model surfaces (e.g. glass, gold, and silicon wafer) and subsequently may not perform with the same efficacy on polymeric biomaterial substrates. Common to many of these strategies is the incorporation of poly(ethylene glycol) (PEG) or poly(ethylene oxide) (PEO) at the surface. Extensively studied, PEG is largely considered the gold standard for protein resistant applications.[23-26] PEG strategies utilize a passive mechanism to increase surface hydrophilicity and resist protein adsorption. PEGs hydrophilic polymer chains can hydrogen bond with large amounts of water to form a hydration layer.[27] This layer is sustained by the presence of a

hydration pressure that serves as an energetic barrier to nonspecific protein adsorption.[28] In addition, the polyether backbone of PEG is inherently flexible. When presented as polymer brushes on a substrate, these flexible chains create configurational mobility that blocks potential sites of protein adsorption due to steric excluded volume effects (**Figure 1-2**). Protein resistance is achieved since the entropic energy cost to surpass these chains is too high for proteins to favorably adsorb to the surface.[29]

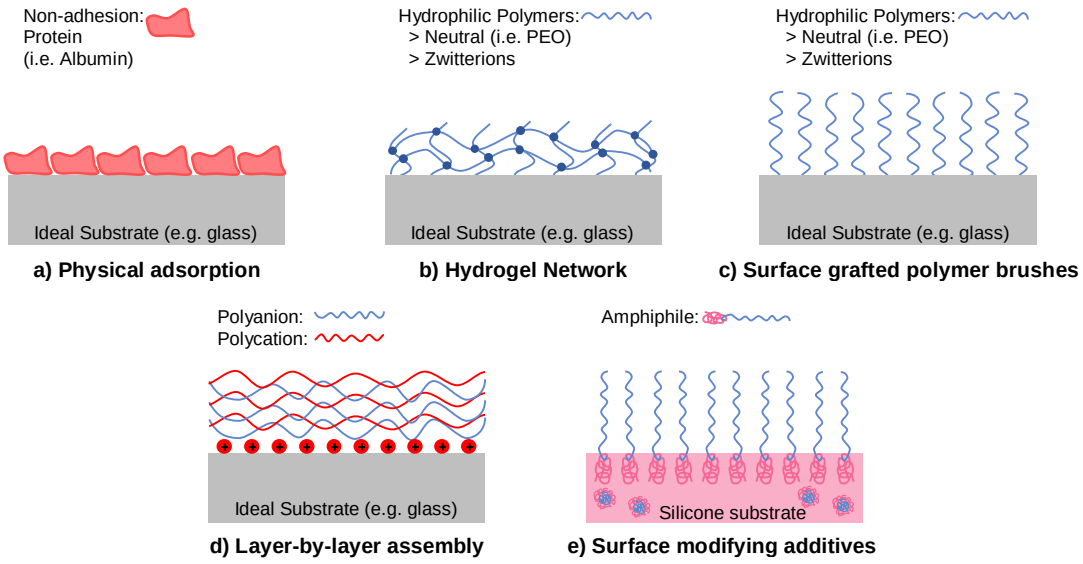

Figure 1-1. Summary of techniques for protein resistant applications. Direct surface modification techniques include: (a) physical adsorption, (b) hydrogel network formation, (c) surface grafted polymer brushes, and (d) layer-by-layer (LbL) assembly. Bulk modification techniques involve blending of (e) surface modifying additives (SMAs) into the base polymer substrate.

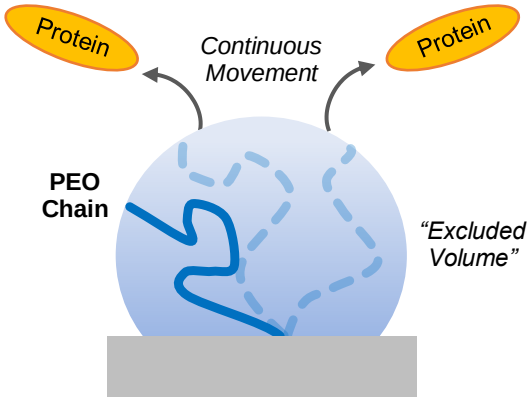

Figure 1-2. Schematic of the steric excluded volume effects of surface grafted PEG chains. Flexible and continuously moving PEG chains create a physical barrier to protein adsorption.

The simplest surface modifying strategy is the formation of a surface coating using physical adsorption (i.e. physisorption). This strategy utilizes secondary forces such as van der Waals forces to associate with a substrate to form a coating. While simple in its methodology, the use of relatively weak secondary bonds typically gives rise to poor long-term stability of physisorbed substances.[30,31] Reported decades ago, a notable physisorption strategy involved the preadsorption of albumin onto a surface. Both albumin and fibrinogen are common plasma proteins with strong affinities for hydrophobic surfaces. Unlike fibrinogen, albumin is a nonadhesion protein that does not present recognizable sites to platelets and cells upon adsorption to the material surface. Therefore, it was hypothesized that preadsorption of albumin onto a material surface would physically block adsorption of other adhesion proteins such as fibrinogen. In addition to several *in vitro* studies demonstrating their effectiveness in thromboresistance,[32,33] these coatings were also used clinically for artificial kidneys.[34] While physisorbed albumin was

able to improve thromboresistance initially, the effect was only retained for a few hours after implantation.[35] It is believed that the loss of efficacy was due to the Vroman effect in which the preadsorbed albumin was quickly displaced by fibrinogen due to the latter's higher affinity for the material surface. To overcome this, chemical modifications were used as well as a multilayering of albumin. For instance, Matsuda et al.[36] studied PU coated with numerous layers of albumin and found them to be effective at reducing thrombogenicity. Unfortunately, delamination of these layers can occur over time and lead to a reduction in thromboresistance. These findings indicate that physisorption techniques, though simple, are likely insufficient for long-term implantable medical devices.

In contrast, surface grafting is a technique that utilizes covalent bonds to form a coating on the material with improved long-term stability. To achieve protein resistance, the grafted polymers are often hydrophilic and flexible (e.g. PEG), allowing formation of a hydration layer and utilization of steric excluded volume effects. There are two types of surface grafting: the "graft-to" method, and the "graft-from" method. In "graft-to", flexible, hydrophilic end-functionalized polymers are directly grafted to a surface to impart protein resistance.[26,37-40] Unfortunately, these coatings are typically effective only at high graft densities. This is often difficult to achieve with the "graft-to" method due to the steric hindrance of the neighboring polymer chains.[27,41,42] The "graft-from" method is where the flexible, hydrophilic polymer chains are formed through an *in situ* surface-initiated (SI) polymerization.[42] This technique allows for improved graft density and, thus, protein resistance;[43] however, steric effects remain, potentially leading to a broad range of polymer chain lengths. Recent advances in SI polymerization techniques [e.g. reversible

addition-fragmentation chain transfer (RAFT),[44] atom transfer radical polymerization (ATRP),[45] etc.] have shown potential to reduce the polydispersity of grafted chains.[46,47] Irrespective of technique, once grafted to surfaces, exposure to shear forces of blood flow may mechanically disrupt the grafted surface resulting in loss of protein resistance. Though promising, challenges in surface grafting remain for blood-contacting devices and, thus, inspire the use of more elaborate surface modification techniques.

The formation of a hydrogel layer on a surface is another technique explored to achieve protein resistance. Hydrogels are lightly cross-linked polymer networks that have the capacity to swell and interact with large amounts of water.[27] Similar to PEG grafted chains, this can lead to formation of a hydration layer, which increases surface hydrophilicity and establishes a barrier to nonspecific protein adsorption (**Figure 1-3**). Naturally PEG was a prime candidate for incorporation into hydrogels and was successful at conferring protein resistance *in vitro*.[48] Other studies have also shown that increased water content through this mechanism corresponds to a reduction in thrombus formation on these hydrogel surfaces.[49,50] However, a study by Ratner et al.[49] also found that higher water content gels corresponded to an increase in blood platelet damage, due to the direct interactions of plasma proteins and the strongly hydrophilic interface of the gels. These results dispute the idea that hydrophilicity is the only requirement toward achieving protein resistance and suggest other factors are involved as well.

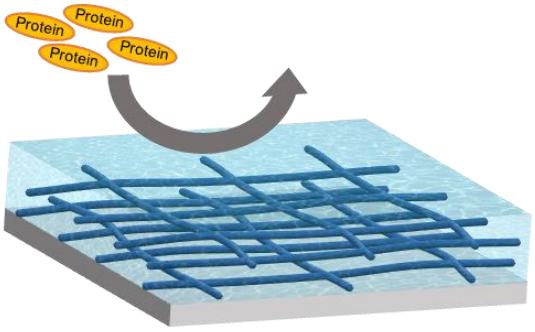

Figure 1-3. Schematic of hydration layer formation of a hydrogel. The network chains interact strongly with water to form a hydrophilic barrier to protein adsorption.

LbL deposition and SMAs are two relatively new techniques to achieve protein resistance. LbL involves a sequential "stacking" of thin layers of polymer chains onto a material surface using secondary or electrostatic interactions.[51] By developing chemistries that allow for effective attachment of the initial layer, subsequent layers are then able to stack independent of the original material substrate.[51,52] In addition, the layering mechanism enables nanoscale control of coating thickness.[53] SMAs are blended into the base polymer material but undergo water-driven surface restructuring to enhance surface hydrophilicity.[54,55] Typically, SMAs are block copolymers comprised of blocks with affinity to the base material as well as blocks with affinity to the aqueous environment. Exposure of the bulk-modified material to the biological, aqueous environment ideally drives the migration of hydrophilic "protein repellant" blocks to the surface whereas the hydrophobic blocks interact with the base polymer to inhibit leaching.[56] LbL and SMAs have been shown to be promising platforms for some of the new chemistries and strategies of protein resistance discussed below.

1.3. New Chemistries and Strategies

1.3.1. Hydrophilic Polymers

Newer approaches to impart surface hydrophilicity and subsequent protein resistance to polymeric biomaterials combine various surface modification techniques with new chemistries. While PEG-based strategies have been historically regarded as the most effective, concerns exist regarding the use of PEG. Recent studies have displayed the potential immunogenicity of PEG, with as much as 25% of the population containing anti-PEG antibodies.[57] In addition, there are questions regarding the oxidative stability of the polyether backbone of PEG (**Figure 1-4a**). The poor oxidative stability of PEG *in vivo* has been repeatedly shown,[58,59] although a recent study found that PEG can be oxidatively stable *in vivo*.[60] These concerns have prompted research into alternative hydrophilic polymers. One such alternative is polyglycerols (PG), also known as polyglycidols (**Figure 1-4b**), which are very similar in structure to PEG. In addition to a polyether backbone, polyglycidols also have hydroxymethyl pendant groups that allow for multifunctional characteristics. This class of polymers has shown similar, often superior, protein resistance compared to PEG in both its linear form[61-63] as well as its hyperbranched form.[64-66] For example, Lukowiak et al.[65] grafted hyperbranched PG to a polypropylene (PP) surface to improve protein resistance. They utilized a "graft-to" method with a hyperbranched, amine-functionalized PG and a brominated PP surface. Using fluorescent microscopy, they found that these "PG-lated" surfaces substantially reduced adsorption of fluorescein isothiocyanate (FITC)-labeled bovine serum albumin (BSA) and fibrinogen, comparable to those of their PEG control. In addition to effective resistance to protein

adsorption, polyglycidols also exhibit higher thermal and oxidative stability versus PEG.[67] Paired with the multifunctional aspect of its structure, PGs are showing their versatility and potential to supplant PEG in protein resistant applications.

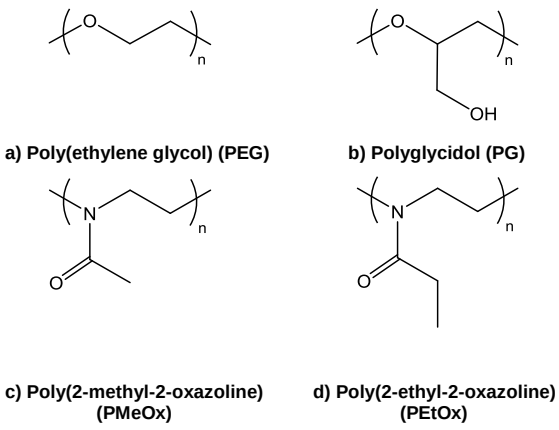

Figure 1-4. Chemical structures of neutral, hydrophilic polymers commonly used as surface hydrophilization agents for protein resistant applications.

Another class of polymers which may be an alternative to PEG is poly(2-oxazoline) (POx), particularly the two hydrophilic variations, poly(2-methyl-2-oxazoline) (PMeOx; **Figure 1-4c**) and poly(2-ethyl-2-oxazoline) (PEtOx; **Figure 1-4d**).[68] Similar to PEG, these hydrophilic polymers can form a hydration layer and use steric excluded volume effects to achieve protein resistance.[69] PMeOx has also been found to have good physiological stability.[70] These similarities prompted Konradi et al.[71] to compare PEG and PMeOx which were first graft copolymerized with poly(L-lysine) (PLL) to form PLL-*g*-PEG and PLL-*g*-PMeOx and adsorbed onto a negatively charged niobium oxide substrate.

When exposed to full human serum, both had comparable protein resistance (< 2 ng cm^{-2}) when evaluated with optical waveguide light-mode spectroscopy (OWLS), whereas the PMeOx system showed enhanced oxidative stability. Likewise, Zhu and Li[72] evaluated the protein resistance of PMeOx when copolymerized with poly(dimethyl siloxane) (PDMS). Varying PDMS−PMeOx macromer concentrations (0 – 50 wt %) were incorporated into hydrogels with 3-bis(trimethylsilyloxy) methylsilylpropyl glycerol methacrylate (SiMA; 20 – 70 wt %) and 2-hydroxyethyl methacrylate (HEMA; 30 wt %). Using a bicinchoninic acid assay with a BSA solution, the 50 wt % PMeOx-PDMS hydrogel significantly reduced adsorption (3.76 μg cm^{-2}) compared to the 0 wt % control (> 60 μg cm^{-2}). Thus, with improved oxidative stability and comparable protein resistance, PMeOx and poly(2-oxazolines) alike may be viable alternatives to PEG.

Another alternative to PEG is hydrophilic zwitterionic-based polymers or polyzwitterions. Zwitterions are neutral molecules that contain separate positive and negative charges. When used in surface modification, they can improve surface hydrophilicity and protein resistance of a material. Similar to PEG, surface-grafted polyzwitterions utilize steric exclusion effects and can also form a hydration layer through their strong electrostatic interactions with water in order to achieve protein resistance.[73] One class of polyzwitterions, known as polybetaines (**Figure 1-5**), have been widely studied for protein resistant applications, particularly poly(sulfobetaine methacrylate) (PSBMA) and poly(carboxybetaine methacrylate) (PCBMA).[74-80] These can be independently grafted to a material, or incorporated into other platforms such as hydrogels or LbL deposition. For example, Chang et al.[81] grafted PSBMA brushes to a

poly(vinylidene fluoride) (PVDF) membrane via atmospheric plasma-induced surface copolymerization. Protein adsorption was measured via ELISA with a human fibrinogen (HF) solution. The PSBMA-grafted membranes demonstrated marked reduction in HF adsorption (~ 90%) compared to a PVDF control. The Jiang group grafted PCBMA brushes onto glass and gold substrates and subsequently demonstrated their low fibrinogen adsorption via ELISA, relative to a glass control,[82] and surface plasmon resonance (SPR) (< 0.3 ng cm^{-2}),[83] respectively. In addition, Jiang and Ratner et al. evaluated the host response of a PCBMA-based hydrogel implanted subcutaneously in rats.[84] After three months, the PCBMA hydrogels were found to resist fibrous capsule formation, thereby demonstrating their antifouling properties.

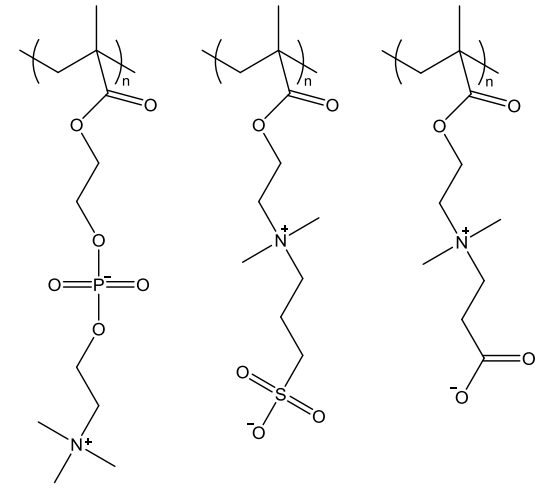

Figure 1-5. Chemical structures of polybetaines commonly used as surface hydrophilization agents for protein resistant applications.

These studies prompted a more in-depth investigation of polyzwitterions, specifically in regard to charge. Though generally considered neutral, a zwitterion can vary in charge depending on its isoelectric point (pI) and the environment in which it resides. To maintain neutrality in the body, desirable for protein resistance, the pI of a zwitterion should generally be at or near physiological pH, 7.4.[75] For example, PSBMA brushes have shown consistent protein resistance *in vitro*.[73] However, the sulfonate ($pK_a \sim 2$)[85] and quarternary amine ($pK_b \sim 5$)[86] groups of PSBMA form a pI ~ 5.5, meaning they lack charge neutrality at physiological pH, which could potentially limit success *in vivo*. In a recent study, Guo et al.[87] sought to tune the pI of PSBMA through copolymerization with a cationic monomer, methacryloylethyltrimethylammonium chloride (METAC). Notably, with less than 2 wt % METAC, a tunable pI range from 5-10 was obtained by simply adjusting monomer ratios. In addition, the protein resistance of these copolymers was compared against traditional PSBMA brushes likewise grafted onto a silica wafer substrate using a modified dye-interaction test and showed similarly low levels of BSA and lysozyme adsorption (< 10 μg cm^{-2}). This is a crucial development for PSBMA and potentially other protein resistant polyzwitterions, since a tunable pI would allow these to remain charge neutral in the body.

In concert with LbL, polyzwitterion integration can help improve hydrophilicity and protein resistance. For example, Chien et al.[88] grafted PSBMA and PCBMA chains to a trilayer polyelectrolyte (TLP) film to improve the protein resistance of PDMS and polysulfone (PSF) substrates. The cross-linked TLP film was composed of poly(ethylene-imine) (PEI) and poly(acrylic acid)-*graft*-azide (PAA-*g*-AZ) in a PEI/PAA-*g*-AZ/PEI

scheme and provided a functionalized surface for conjugation of the polyzwitterions using a "graft-to" method. Using an ELISA assay, they found that both the PSBMA and PCBMA grafted TLP films were able to drastically reduce fibrinogen adsorption from plasma, relative to a TLP control. A similar study examined polyzwitterionic copolymers, namely, azide- and alkynyl-functionalized PSBMA for use in "click chemistry-enabled" LbL deposition onto PSF.[89] The polyzwitterionic, covalent LbL network was able to reduce BSA and bovine serum fibrinogen adsorption to less than 4 and 2 μg cm^{-2}, respectively. These results demonstrate the versatility and effectiveness of combining LbL deposition and polyzwitterions in protein resistant applications.

1.3.2. Superhydrophobic Approach

Aside from hydrophilic approaches, superhydrophobic surfaces have recently been explored for protein resistance. These surfaces exhibit a degree of roughness and are generally characterized as those with water contact angles greater than 150 degrees.[90] The unique topographies help to minimize interactions with water and contaminants for prevention of fouling.[91] Shirtcliffe and Roach examined this effect by testing for BSA adsorption on glass surfaces of varying roughness.[92] They confirmed that increasing roughness (i.e. smaller surface features) leads to reduced BSA adsorption under flow conditions. Likewise, superhydrophobic polymeric biomaterials such as PU with increased surface roughness led to reduced protein adsorption.[93] In addition to roughness, another consideration of topography is the surface curvature. A curved surface is thought to prevent stable adsorption of proteins and facilitate shear removal of any deposited on the surface.[94] Thus, continued research on superhydrophobic surfaces must also consider

topographical aspects such as curvature. One such approach is a biomimetic-inspired superhydrophobic surface, Sharklet AF (**Figure 1-6**). The topographical design was inspired from shark skin, a natural antifouling surface. Sharklet AF has a unique pattern with ribs spaced 2 μm apart, which are 2 μm wide with lengths that range from 4−16 μm. Recently, the Sharklet AF topography was micropatterned onto thermoplastic polyurethanes (TPU) and was shown to be a promising construct for use in central venous catheters (CVC).[95] These micropatterned TPU surfaces were tested against common CVC fouling agents such as bacterial colonization (e.g. *S. aureus, S. epidermidis*) and platelet adhesion. They were able to reduce *S. aureus*, *S. epidermidis*, and platelet adhesion by 70%, 71%, and 80%, respectively. Thus, in addition to diminished thrombosis, the reduction in bacterial adhesion has the potential to decrease infection, a complication associated with increased mortality for CVC patients.[96,97] These results show the effectiveness of Sharklet AF, and more generally demonstrate the potential and versatility of superhydrophobic surfaces for protein resistant applications.

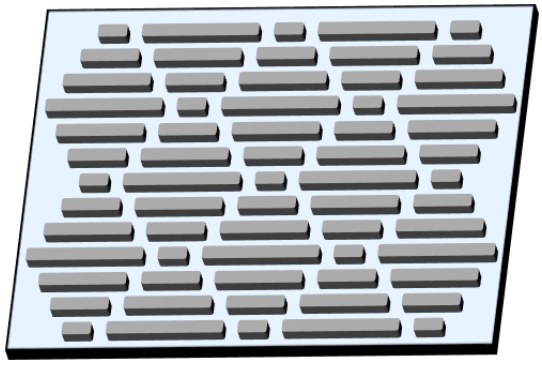

Figure 1-6. Depiction of Sharklet AF pattern. Surface feature ribs are 2 μm wide, spaced 2 μm apart, and vary in length from 4 – 16 μm.

1.3.3. Amphiphilic Materials

Amphiphilic materials, through the combination of hydrophilic and hydrophobic regions offer a unique protein resistant strategy. They may be comprised of a hydrophobic component such as PDMS or a fluoropolymer, in addition to a hydrophilic component such as PEG or zwitterions that can impart protein resistance.[98-107] For example, a recent study examined the protein resistance of an amphiphilic fluorinated diblock copolymer, poly(PEGMA-*co*-MMA)-*b*-PC_6SMA.[106] Poly(ethylene glycol) methyl ether methacrylate (PEGMA) and methyl methacrylate (MMA) comprised the hydrophilic block. The fluorinated hydrophobic block was composed of a poly(*n*-methyl-perfluorohexane-1-sulfonamide) ethyl methacrylate (PC_6SMA). Once spin-coated onto silicon wafers, adsorption of fluorescently labeled BSA was reduced on the amphiphilic surface, compared to a polystyrene-*b*-poly(ethylene-*co*-butylene)-*b*-polystyrene control. Amphiphiles have also been effective at reducing protein adsorption when applied onto polymeric substrates.[98,101,103,104] For example, Chen et al.[98] dip coated amphiphilic PDMS-*graft*-PEG to a PVDF membrane. The modified PVDF membrane showed reduced BSA adsorption under both static (22 ng cm^{-2}) and dynamic (10 ng cm^{-2}) conditions. The adsorption mass was calculated from the pre- and post-test BSA solution concentrations, BSA solution volume, and PVDF membrane area. Additionally, amphiphilic PES-*graft*-PEGMA has shown effective resistance to BSA adsorption when applied to a poly(ether sulfone) (PES) membrane.[104] The efficacy of this approach on various substrates demonstrates the potential for preparation of protein resistant surfaces.

Additionally, amphiphilic SMAs are designed to be blended into a base polymer but restructure their hydrophilic portions to the surface-biological interface. Our research group has reported amphiphilic SMAs for bulk modification of silicones in order to attain protein resistance. PEO-silane amphiphiles were prepared with a hydrophilic PEO segment, a flexible, hydrophobic oligo(dimethyl siloxane) (ODMS) tether, and a cross-linkable trialkyloxysilane group: [α-$(EtO)_3Si$-$(CH_2)_2$-$ODMS_{13}$-*block*-$(OCH_2CH_2)_8$-OCH_3].[108] Following blending into an RTV silicone and subsequent curing, exposure to an aqueous environment prompted the rapid and substantial migration of the PEO segments to the surface (**Figure 1-7**) as confirmed by temporal contact angle analysis and atomic force microscopy (AFM).[54,55] It is believed that the similar hydrophobicity and chain flexibility of the SMA's siloxane tether[109] (as well as its low overall molecular weight) improved its compatibility with the silicone matrix and enhanced its water-driven migration potential. With the incorporation of less than 2 wt % of SMA amphiphile, both BSA (27 ng cm^{-2}) and HF (175 ng cm^{-2}) adsorption were significantly reduced relative to an unmodified silicone control (BSA: 323 ng cm^{-2}; HF: 832 ng cm^{-2}), as measured by fluorescence microscopy. At higher amphiphile concentrations between 4 and 20 wt %, adsorption was less than 3 ng cm^{-2}.[108] In a separate study,[55] PEO repeat unit length was probed (n = 3, 8, and 16) at varying concentrations (5, 10, 25, 50, and 100 μmol g^{-1} in silicone) to test the restructuring capacity of the PEO-silane amphiphile. At lengths n = 8 and 16, effective restructuring was observed under aqueous exposure for protein resistance, but at length n = 3, poor protein resistance was observed. It is possible at length

n = 3, the PEO chains are not sufficient in length to impart protein resistance. These studies highlight the critical role of molecular structure to maximize efficacy of SMAs.

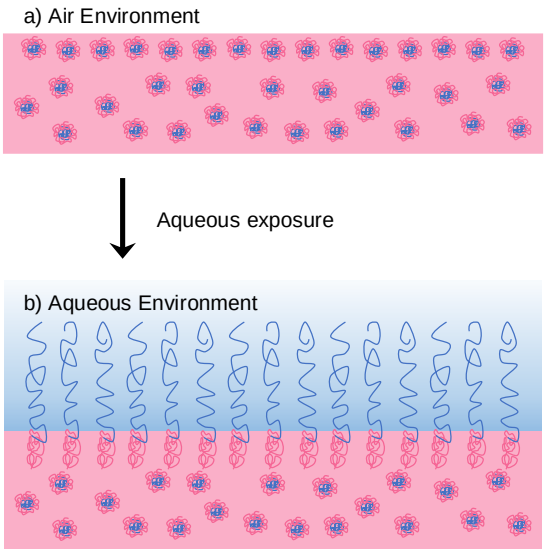

Figure 1-7. Depiction of PEO-silane amphiphile behavior once bulk-modified into silicone. (a) In air, PEO-silane amphiphiles migrate into the silicone bulk. (b) In an aqueous environment, PEO-silane amphiphiles restructure to the surface-biological interface.

1.4. Assessment of Protein Resistance

As described above, there are numerous chemistries and associated surface modification methods that have demonstrated the ability to reduce protein adsorption to very low levels *in vitro*. These results have been confirmed with various spectroscopic (e.g. fluoroscopy, UV/vis, etc.)[71,87,92,108,110] and gravimetric techniques (e.g. OWLS, quartz crystal microbalance with dissipation (QCMD)),[55,111,112] as well as biochemical assays (e.g. ELISA, BCA assay).[72,82,88] However, *in vitro* results frequently exhibit poor

correlation with *in vivo* results.[113] One contributing factor is the use of "ideal" or model substrates to analyze surfaces rather than polymeric biomaterials substrates which are ultimately used as implanted medical devices or in diagnostics and employed for *in vivo* testing. We observed this in our evaluation of conventional PEO-silanes, α-$(EtO)_3Si$-$(CH_2)_2$-$(OCH_2CH_2)_n$-OCH_3.[55] When grafted to silicon wafers, surfaces exhibited high protein resistance. However, when blended into silicone as SMAs, conventional PEO-silanes were unable to restructure to the aqueous interface and did not improve protein resistance. This highlights the importance of confirming *in vitro* protein resistance on polymeric biomaterial substrates, rather than model substrates, prior to *in vivo* testing. This could help improve the correlation between *in vitro* and *in vivo* protein resistance.

Another potential contributor to poor correlation between *in vitro* and *in vivo* results is the lack of a standardized method for protein adsorption testing. Much of the testing has been done with single protein solutions such as fibrinogen or albumin.[108,110,114] However, these fail to represent the complexity and dynamics of protein adsorption *in vivo*. In contrast, human serum and plasma are complex multiprotein solutions that result in different mechanisms of protein adsorption. Briefly, in a multiprotein mixture, adsorption becomes a competitive and dynamic process[115] that often results in poor protein resistance, relative to a single protein adsorption test. In a recent study, higher levels of fibrinogen adsorption onto a variety of substrates was observed when testing with human plasma compared to a single fibrinogen solution.[80] While *in vitro* testing with full human serum results in higher protein adsorption, this may be a better indicator of *in vivo* protein resistance. For example, in the previously noted study by Jiang and Ratner, PCBMA was

observed to effectively resist nonspecific protein adsorption and prevent capsule formation *in vivo*.[84] These results were supported by earlier *in vitro* data,[116] where PCBMA brushes showed high protein resistance when tested with full human serum. Although there are numerous factors to consider, a standardized protocol involving use of full human serum may allow for improved discernment between protein resistant materials and prediction of *in vivo* performance.

A final consideration for improved *in vitro* protein adsorption testing is the need for highly sensitive measurement techniques. Common techniques include fluorescent microscopy, ELISA, QCM-D, and SPR. These are effective at comparison of a protein resistant strategy to a control, but their lower limits of detection (LOD) may lack the sensitivity to be able to discern two highly protein resistant strategies. Studies have shown that fibrinogen adsorption in concentrations as low as 5 ng cm^{-2} can facilitate platelet adhesion.[117,118] When reported in literature, SPR generally has the lowest LOD (0.3 ng cm^{-2}),[83,119] followed by ELISA (0.5 – 4.9 ng cm^{-2}; determined from antibody LOD,[120-122] based on a 96-well plate surface area of 0.32 cm^{-2} and antibody volume of 100 μL), QCM-D (1.4 – 6 ng cm^{-2}),[123] and fluorescence microscopy (3 ng cm^{-2}).[108] This creates a particularly narrow window to compare and differentiate surfaces of exceptional protein resistance. Development of a highly sensitive technique would improve the discernment of protein resistant polymeric biomaterials, potentially leading to enhanced *in vivo* performance.

1.5. Conclusions

In summary, numerous approaches have recently been explored to create protein resistant polymeric biomaterial surfaces. Though PEG-based strategies remain the gold standard, alternatives utilizing polyglycidols, poly(2-oxazoline)s, polyzwitterions, or amphiphilic SMAs have the potential to be robust, effective options. To advance the development of new polymeric biomaterials, improved correlation between *in vitro* to *in vivo* protein resistance is needed. Toward this goal, protein resistance is ideally tested on surfaces prepared with polymeric biomaterial substrates rather than model substrates. In addition, a standardized method for protein adsorption involving full human serum rather than a single protein solution could more accurately simulate the dynamics and complexities of protein adsorption experienced *in vivo*. Other factors such as static versus dynamic testing conditions as well as the exposure time should also be considered. Finally, an increase in sensitivity to measure *in vitro* protein adsorption would allow for improved differentiation between highly protein resistant materials. Given the potential impact on medical devices and diagnostics, continued work to develop and test protein resistant polymeric biomaterials is a critical endeavor.

CHAPTER II

STABILITY OF SILICONES MODIFIED WITH PEO-SILANE AMPHIPHILES: IMPACT OF STRUCTURE AND CONCENTRATION[†]

2.1. Overview

The efficacy of poly(ethylene oxide) (PEO)-based surface-modifying additives (SMAs), following the bulk-modification of silicones, requires sustained, water-driven PEO migration to the surface to achieve hydrophilicity and subsequent reduction of protein adsorption. Herein, a condensation cure silicone was modified with PEO-silane amphiphile SMAs (5 – 100 μmol per 1 g silicone) comprised of an oligo(dimethyl siloxane) (ODMS) tether, PEO segment and optional triethoxysilane (TEOS) crosslinkable group. This allowed us to confirm that the TEOS crosslinkable group was not necessary and that the ODMS tether (m = 13 or 30) could sufficiently physically anchor the amphiphile in the silicone network. Surface hydrophilicity was examined before and after aqueous conditioning, as well as mass loss and water uptake after conditioning. Overall, silicones modified with all amphiphilic SMAs produced increasingly hydrophilic surfaces and their hydrophilicity was maintained following conditioning. At all concentrations, all amphiphilic SMA modified silicones had minimal water uptake and mass loss, comparable to that of unmodified silicone. Finally, silicones

---

modified with all amphiphilic SMAs ≥ 25 μmol exhibited exceptional protein resistance that was not appreciably diminished after conditioning.

2.2. Introduction

Silicones such as crosslinked poly(dimethyl siloxane) (PDMS) are commonly used in biomedical applications due to their nontoxicity, biostability, and elastomeric mechanical properties.[13,124,125] Unfortunately, the hydrophobic nature of silicones makes them susceptible to non-specific protein adsorption, leading to platelet adhesion as well as activation, and ultimately, thrombus formation.[2,3,5] This can be problematic for silicone-based blood-contacting devices such as hemodialysis catheters, as thrombosis can lead to device occlusion and compromised device function.[7,8,126] Thrombosis can also facilitate blood stream infection, which is a major cause of patient fatality.[3,5,127] Currently, antithrombotic agents (e.g. heparin) are used for thrombosis prevention either via pharmaceutical administration or, in the case of hemodialysis catheters, as intraluminal locking solutions.[128-131] However, these therapies are costly, often ineffective, and have been associated with high bleeding risk and potential hypersensitivity.[132-136] Thus, a materials-based strategy to manage and prevent thrombosis without the use of antithrombotic drugs would improve the safety and efficacy of silicone blood-contacting devices.

Modification of silicone with poly(ethylene oxide) [PEO; or poly(ethylene glycol) (PEG)] represents a general strategy to increase surface hydrophilicity in order to impart antifouling behavior.[30,37,137-140] PEO's exceptional protein resistance is primarily attributed

to its hydrophilicity and ability to interact with water to form a repulsive hydration layer.[27,28] The configurational mobility of the flexible PEO polymer backbone also creates a large excluded volume that sterically repels proteins and blocks underlying adsorption sites.[29] PEO's prolific use in antifouling applications stems from its biocompatibility as well as oxidative stability.[60,141] Direct surface grafting as well as bulk-modification may be considered for PEO-modification of silicone, but it is essential that PEO is initially present as well as preserved over time in sufficient concentration at the aqueous interface in order to realize antifouling behavior.[38,142] Indeed, the protein resistance of PEO has been established when directly applied to the surfaces of physically stable, model substrates (e.g. silicon wafer,[26,143-145] glass,[23,146] and gold[24,25,147,148]). In this scenario, the PEO chains are maintained at the surface, irrespective of the environment (i.e. air or aqueous). In contrast, modified silicone surfaces can undergo hydrophobic recovery due to silicone's low surface energy and high chain flexibility.[149,150] This effect is seen in plasma-treated silicones which are unable to sustain a hydrophilic surface once removed from an aqueous environment.[151] Alternatively, silicones may be bulk-modified with a PEO-based surface-modifying additive (SMA), requiring reorganization of the PEO chains to aqueous interface. However, this approach is associated with concerns regarding surface stability stemming from the leaching of the SMAs from the silicone as well as water uptake into the bulk, which may lead to migration of the PEO from the aqueous interface into the bulk and a loss of surface hydrophilicity.[152]

Our group has developed amphiphilic PEO-based SMAs for the bulk-modification of condensation-cure silicones. These PEO-silane amphiphiles contain a reactive

triethoxysilane (TEOS) crosslinking (XL) group, a highly flexible, hydrophobic oligo(dimethyl siloxane) (ODMS) tether, and a hydrophilic PEO segment: α-$(EtO)_3$-Si-$(CH_2)_2$-$ODMS_m$-*block*-PEO_n-CH_3.[153] When these amphiphilic SMAs were incorporated into the silicone, the surfaces underwent dramatically enhanced water-driven surface restructuring, resulting in hydrophilicity and protein resistance. Such behavior was not observed for silicones modified with analogous conventional, non-amphiphilic PEO-silanes [(α-$(EtO)_3$-Si-$(CH_2)_3$-PEO_n-CH_3)]. Thus, the unique restructuring ability of PEO-silane amphiphiles was attributed to the flexibility of the ODMS tether as well as its similar composition and thus compatibility with the silicone matrix. Subsequent studies explored the impact of amphiphilic SMA structural features, including ODMS tether length (*m*; *m* = 0, 4, 13, 17, 24, 30) and PEO segment length (*n*; *n* = 3, 8, 16).[55,154,155] An *n* = 8 PEO segment length paired with either an *m* = 13 or *m* = 30 ODMS tether length were found to maximize water-driven surface restructuring and protein resistance.

Most recently, PEO-silane amphiphile SMAs were prepared without the TEOS crosslinkable group to determine their ability to provide similar modification of the silicone surface, even after aqueous conditioning. Such non-crosslinkable SMAs recapitulates a scenario wherein the hydrolytically unstable crosslinks may be broken during extended aqueous exposure.[156] Additionally, the preparation of non-crosslinkable SMAs involves a mere single synthetic step compared to two for crosslinkable SMAs. Thus, for these initial studies, PEO-silane amphiphiles were prepared with and without a TEOS group (*XL diblock* and *Diblock*, respectively) and evaluated in silicone at a single concentration (50 μmol per 1 g of silicone).[157] While the PEO segment length was kept at

n = 8, both those with an *m* = 13 and an *m* = 30 ODMS tether length were evaluated as we hypothesized that the longer tether could more effectively physically anchor the SMA due to its chemical similarity to the silicone matrix. Following aqueous conditioning, silicones modified with non-crosslinkable *Diblock* amphiphiles were able to maintain effective water-driven surface restructuring and resistance to protein adsorption. Additionally, these *Diblock* amphiphile modified silicones had minimal leaching and water uptake over time. In terms of ODMS length, silicones modified with *m* = 30 SMAs had similar efficacy to those modified with *m* = 13 SMAs, but with slightly enhanced stability during aqueous conditioning (i.e. reduced leaching and water uptake). These results indicate that crosslinking of PEO-silane amphiphile SMAs may not be essential, particularly when the ODMS tether length is increased.

Given the promising preliminary results of silicones modified with these *Diblock* SMAs (i.e. non-crosslinkable PEO-silane amphiphiles), in this present study we thoroughly evaluated their efficacy against that of the corresponding *XL diblock* SMAs (i.e. with a TEOS crosslinkable group), each with *m* = 13 & 30 ODMS tether lengths, as well as against a non-amphiphilic PEO-control (**Figure 2-1a**). We sought to determine the minimum effective concentration for each SMA by bulk-modifying a medical-grade, condensation cure silicone at a range of concentrations: 5, 10, 25, 50, and 100 µmol SMA per 1 g silicone. Moreover, these surfaces were assessed for their ability to sustain hydrophilicity and protein resistance after aqueous conditioning. Both leaching of SMAs from the modified silicones and water uptake were assessed as these would be expected to diminish hydrophilicity and protein resistance, with the latter due to PEO migration

from the surface and into the bulk (**Figure 2-1b**).[157] Thorough assessment of these SMAs will ultimately establish if the crosslinkable TEOS group is not necessary and may be mitigated with a longer ODMS tether. As noted, this would allow for a simpler one-step synthetic protocol and mitigate concerns of hydrolysis of alkoxysilane groups *in vivo*.[158]

a.

SMA Concentration (μmol/g MED-1137)	5	10	25	50	100
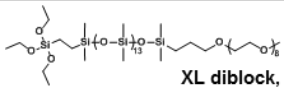 XL diblock, *m* = 13	0.9%	1.7%	4.3%	8.6%	17.1%
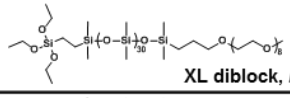 XL diblock, *m* = 30	1.5%	3.0%	7.4%	14.8%	29.7%
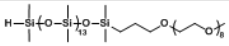 Diblock, *m* = 13	0.8%	1.5%	3.8%	7.6%	15.2%
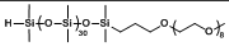 Diblock, *m* = 30	1.4%	2.8%	6.9%	13.9%	27.8%
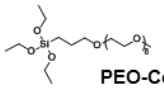 PEO-Control	0.3%	0.6%	1.5%	2.9%	5.9%

b.

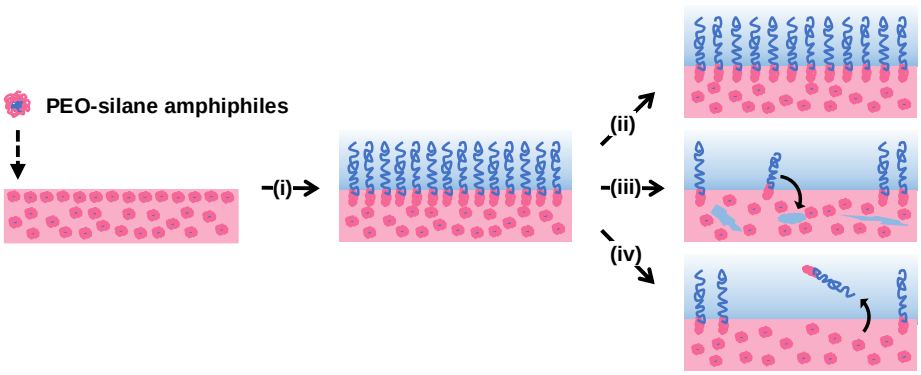

Figure 2-1. a. Table of chemical structures and concentrations of SMAs (molar concentration & corresponding weight percent) evaluated in this study. b. (**i**) Minutes following aqueous exposure, PEO-silane amphiphiles restructure to form a protein resistant surface. Upon extended exposure, modified silicones can either (**ii**) retain protein resistance, or (**iii**) exhibit water uptake, and (**iv**) leaching, which would lead to reduced PEO surface coverage and loss of protein resistance.

2.3. Materials and Methods

2.3.1. Materials

Polyglykol AM 450 [Allyl methyl PEO (AM PEO_8), M_n = 292 – 644 g mol^{-1} per manufacturer's specifications; M_n = 424 g mol^{-1} per ^1H NMR end group analysis; ^1H NMR (δ, ppm): 3.37 (s, 3H, OCH_3), 3.53-3.65 (m, 32H, OCH_2CH_2), 3.99-4.02 (d, *J* = 5.4 Hz, 2H, CH_2=$CHCH_2O$), 5.14-5.29 (m, 2H, CH_2=$CHCH_2O$) and 5.84-5.96 (m, 1H, CH_2=$CHCH_2O$)] was provided by Clariant. Tetramethyldisiloxane (TMDS), octamethylcyclotetrasiloxane (D_4), triethoxysilane (TEOS), vinyltriethoxysilane (VTEOS), Pt-divinyltetramethyldisiloxane complex in xylene (Karstedt's catalyst), and α,ω-bis-(SiH)oligodimethylsiloxane [α,ω-bis-(SiH)ODMS, ($ODMS_{13}$); M_n = 1000 – 1100 g mol^{-1} per manufacturer's specifications; M_n = 1096 g mol^{-1} per ^1H NMR end group analysis; ^1H NMR (δ, ppm): 0.05-0.10 (m, 78H, $SiCH3$), 0.18-0.19 (d, *J* = 2.7 Hz, 12H, $OSi[CH_3]_2H$) and 4.67-4.73 (m, 2H, Si*H*)] were purchased from Gelest. $ODMS_{30}$ [M_n = 2354 g mol^{-1} per ^1H NMR end group analysis; ^1H NMR (δ, ppm): 0.05-0.10 (m, 180H, $SiCH_3$), 0.18-0.19 (d, *J* = 2.7 Hz, 12H, $OSi[CH_3]_2H$) and 4.67-4.73 (m, 2H, Si*H*)] was prepared as reported via ring opening polymerization of TMDS and D_4.[154] Tris(triphenylphosphine)rhodium(I) chloride (Wilkinson's catalyst), hexamethyldisilazane, triflic acid, and solvents were purchased from Sigma-Aldrich. Solvents were dried in 4 Å molecular sieves prior to use in reactions and film casting. Medical grade, condensation cure silicone elastomer [MED-1137, per manufacturer's specifications, containing: α,ω-bis(Si-OH)PDMS, 11-21% silica, < 5% methyltriacetoxysilane, < 5% ethyltriacetoxysilane, and trace amounts of acetic acid] was

purchased from Nusil. Polystyrene 24-well plates were purchased from Corning. Human fibrinogen (HF) was purchased from Calbiochem. Glass microscope slides (75 x 25 x 1 mm), tris buffered saline with Tween 20 (TBS-T20), goat anti-fibrinogen horse radish peroxidase (HRP)-conjugated polyclonal detection antibody, and ultra 3,3',5,5'-tetramethylbenzidine dihydrochloride (TMB di-HCl) substrate solution were purchased from Thermo Fisher Scientific.

2.3.2. Synthetic Approach

All reactions were run under an inert, nitrogen atmosphere with a Teflon-covered stir bar to agitate the mixture. Chemical structures were confirmed with proton nuclear magnetic resonance (^{1}H NMR) spectroscopy using an Inova 500 MHz spectrometer operating in the Fourier transform mode and a $CDCl_3$ standard.

2.3.2.1. Synthesis of crosslinkable, diblock amphiphile ("XL diblock, m = 13", and "XL diblock, m = 30")

Crosslinkable ("XL") diblock amphiphiles (*m* = 13 & 30) were synthesized as previously reported using a two-step hydrosilylation protocol.[153] Briefly, each $ODMS_m$ (*m* = 13 or 30) tether was reacted with VTEOS (1:1 M ratio) via a Wilkinson's-catalyzed, regioselective hydrosilylation reaction. Next, each product was reacted with AM PEO_8 (1:1 M ratio) via a Karstedt's-catalyzed hydrosilylation reaction.

2.3.2.2. Synthesis of non-crosslinkable, diblock amphiphile ("Diblock, m = 13", and "Diblock, m = 30")

Non-crosslinkable diblock amphiphiles (i.e. no TEOS group; *m* = 13 & 30) were synthesized as previously reported using a one-step hydrosilylation protocol.[157] Briefly,

each $ODMS_m$ (m = 13 or 30) tether was reacted with AM PEO_8 (1:1 M ratio) via a Wilkinson's catalyzed, regioselective hydrosilylation reaction.

2.3.2.3. Synthesis of conventional PEO-silane ("PEO-control")

The non-amphiphilic PEO-control was synthesized as previously reported with a one-step hydrosilylation protocol.[153] Briefly, TEOS was reacted with AM PEO_8 (1:1 M ratio) via a Karstedt's-catalyzed hydrosilylation reaction.

2.3.3. Film Preparation

Glass microscope slides were sequentially rinsed with acetone, dichloromethane, and acetone, followed by overnight drying in a 120 °C oven. Casting solutions were prepared by combining MED-1137 with hexane (1:3 wt/wt) and mixing via vortexer until homogenous. For SMA modified silicones, each amphiphile or the PEO-control were added to individual casting solutions at various concentrations (5, 10, 25, 50, and 100 µmol of SMA per 1 g silicone). Solutions were then solvent-cast onto level glass slides (1.5 mL per slide) and covered with a Petri dish. For protein adsorption testing, solutions were solvent-cast into 24-well plates (0.25 mL per well). All films were allowed to cure for one week at room temperature (RT) and then promptly used for designated analyses.

2.3.4. Water-driven Surface Restructuring

Water-driven surface restructuring of SMA modified silicones were characterized with static water contact angle (θ_{static}) measurements using a CAM-200 goniometer (KSV instruments) equipped with an autodispenser, video camera, and drop-shape analysis software (Attention Theta).

2.3.4.1. "Air-conditioned" films (i.e. conditioned in air)

θ_{static} was measured immediately after completion of curing (1 week, RT). A 5 µL deionized (DI) water droplet was placed on the film and θ_{static} was iteratively measured over a 2 min period in 15 s intervals. The reported θ_{static} values are an average and standard deviation of three measurements made on different regions of the same film at 2 min after drop placement ($\theta_{static,\ 2\ min}$). Measurements were repeated on each film at 7 and 14 days after the initial measurement.

2.3.4.2. "Water-conditioned" films (i.e. conditioned in water)

Following initial θ_{static} measurements a separate, equivalent set of films were subjected to conditioning in DI water for subsequent θ_{static} measurements. For these, each film was sequentially submerged in ~30 mL of DI water in a plastic Petri dish, removed after a given period, briefly dried under a stream of air, and $\theta_{static,\ 2\ min}$ was measured as noted above. Following each measurement, films were re-submerged with ~30 mL fresh DI water. Measurements were made at t = 0, 6, and 15 days.

2.3.5. Water Uptake

Water uptake of each film was assessed with thermal gravimetric analysis (TGA; TA Instruments Q50). Films were prepared in triplicate and subsequently submerged in ~30 mL DI water in plastic Petri dishes. After a given period, films were removed, briefly dried with a stream of air, and patted dry with a paper towel. A 20 ± 5 mg segment of film was cut into small pieces by razor blade, and set in a platinum TGA pan. Changes in mass were monitored as each sample was heated from RT to 150 °C at a rate of 10 °C min^{-1}. Mass loss from water was observed as the peak in the mass loss derivative curve which

occurred between RT and ~140 °C. Film water uptake was defined as the percent mass loss over the bounds of that peak. Following each measurement, films were re-submerged in ~30 mL fresh DI water. Measurements were made at t = 1, 6, and 15 days for each film. The reported values are an average and standard deviation of three identically prepared films with identical submersion times.

2.3.6. Mass Loss

To monitor film mass loss, cleaned glass slides were weighed prior to film casting (W_0). Once films were cured, another weight measurement was taken and the difference versus W_0 was recorded as the initial film mass (W_i). Films were then submerged in ~30 mL DI water in a plastic Petri dish and conditioned at RT for 14 days. Following conditioning, each film was removed, briefly dried under a stream of air, and patted dry with a paper towel. Care was taken to avoid abrasion of the film surface. Films were subsequently dried at 50 °C under reduced pressure (30 in. Hg) overnight, before a final weight measurement was taken. Again, the difference versus W_0 was accounted for and recorded as the final film mass (W_f). Measurements were made on triplicate films, and mass loss is defined in **Equation 2-1**:

$$\textbf{Equation 2-1.}\ Film\ Mass\ loss\ (\%) = \left[\frac{(W_i - W_f)}{W_i}\right] x\ 100$$

2.3.7. Fibrinogen Adsorption

HF adsorption was measured using a modified immunosorbent assay.[159] Triplicate wells coated with each SMA modified silicone were exposed to 0.15 mL of HF solution prepared in phosphate buffered saline (PBS) (3.0 mg/mL) and statically incubated for 1 h at 37 °C. The HF solution was removed and each well was rinsed three times with PBS

before the addition of TBS-T20 (0.50 mL), which was statically incubated for 30 min at 37 °C. Wells were then rinsed three times with additional TBS-T20. Next, goat anti-fibrinogen (HRP)-conjugated polyclonal detection antibody (0.50 mL; 1:50,000 dilution in TBS-T20) was added to each well and statically incubated for 1 h at 37 °C. Wells were then rinsed three times with additional TBS-T20. TMB di-HCl substrate solution (0.50 mL) was added and allowed to incubate for 30 min at 37 °C. To stop the reaction, 2 M H_2SO_4 was added to each well and plates were shaken on an orbital shaker at RT for 15 min. For quantification of HF adsorbed on each surface, 0.15 mL of each resulting solution was transferred to a 96-well plate, absorbance was measured at 450 nm with a spectrophotometer (Tecan Safire^2) and the value was compared to a HF standard curve (0.01 – 1000 ng/mL). An additional well plate was prepared and underwent 14 days of water conditioning prior to being tested as described above.

2.3.8. Statistical Analysis

Statistical analysis was performed with two factor ANOVA and statistical significance was assumed with a p-value < 0.05.

2.4. Results and Discussion

In this study, the efficacy of PEO-silane amphiphiles as SMAs to invoke protein resistance of a condensation cure silicone was evaluated. Namely, we probed the necessity of the terminal crosslinkable group, hypothesizing that a longer ODMS tether could maintain the SMA at the aqueous interface by acting as a "physical anchor" to the chemically similar silicone matrix. Thus, crosslinkable, TEOS-containing *XL diblock*

amphiphiles (*m* = 13 & 30) and non-crosslinkable, silane-terminated *Diblock* amphiphiles (*m* = 13 & 30) were prepared along with a non-amphiphilic, crosslinkable PEO-control as well as an unmodified silicone control (**Figure 2-1a**). Previously these PEO-silane amphiphiles were evaluated at a single concentration of 50 µmol SMA per 1 g silicone,[55,153,154,157] but herein, concentrations were expanded to 5, 10, 25, 50, and 100 µmol to determine the minimum effective level. Water-driven surface restructuring, water uptake, mass loss, and fibrinogen adsorption were assessed following aqueous conditioning to determine the stability of SMA modified silicones.

2.4.1. Water-driven Surface Restructuring

2.4.1.1. Static contact angle, "non-conditioned" films

The efficacy of PEO-silane amphiphiles (*XL diblock*, *m* = 13 & 30; *Diblock*, *m* = 13 & 30) as SMAs in silicone for protein resistance critically rests on their ability to restructure to the aqueous interface and form a hydrophilic, PEO-rich surface. Immediately after film preparation, θ_{static} was temporally measured over a 2 min period to assess the initial ability of the surfaces to undergo water driven surface restructuring in the absence of environmental conditioning. The unmodified silicone control and SMA modified samples were hydrophobic when the droplet was initially deposited onto the film (θ_{static} = ~119°), indicating the little to no PEO was initially present at these surfaces. Two minutes post-deposition of the water droplet, contact angle ($\theta_{static,\ 2\ min}$) was recorded to determine if PEO was migrating to the surface to increase hydrophilicity (**Figure 2-2**, data marked *t* = initial). The unmodified silicone control and PEO-control modified silicones at concentrations ≤ 25 µmol remained hydrophobic ($\theta_{static,\ 2\ min}$ = ~113°). At 50 and 100

µmol, PEO-control modified silicones exhibited only a slight gain in surface hydrophilicity ($\theta_{static,\ 2\ min}$ = 95° & 73°, respectively) due to limited PEO migration. PEO-silane amphiphile SMA modified silicones at 5 µmol also had minimal restructuring and remained hydrophobic ($\theta_{static,\ 2\ min}$ = ~111°). However, at concentrations ≥ 10 µmol, all amphiphilic SMA modified silicones exhibited rapid restructuring to form hydrophilic surfaces ($\theta_{static,\ 2\ min}$ < 90°) which was generally enhanced at higher concentrations. While the tether length (*m*) did not produce substantial differences in surface hydrophilicity, non-crosslinked *Diblock* amphiphiles resulted in somewhat lower $\theta_{static,\ 2\ min}$ values compared to TEOS-containing *XL diblock* amphiphiles. For sustained protein resistance, it is crucial that silicones modified with these SMAs retain their ability to undergo water-driven surface restructuring when conditioned in both an air and an aqueous environment. Thus, this was explored as described below.

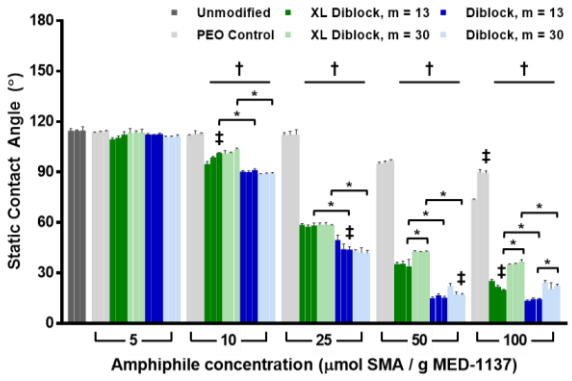

Figure 2-2. θ_{static} at 2 min is shown for each SMA modified silicone at various concentrations after prolonged conditioning in air. Bars are organized as conditioning duration from left to right: initial, 7 d, and 14 d. Statistical analysis ($p < 0.05$): ‡initial v. 14 d in a sample set; †sample v. unmodified at 14 d; *difference between sample sets at 14 d.

2.4.1.2. Static contact angle, air-conditioned films

Throughout 2 weeks of conditioning at RT in air, $\theta_{static,\ 2\ min}$ values were recorded at t = 7 and t = 14 days (**Figure 2-2**). Versus at t = 0 ("initial"), following conditioning, there was a negligible change in $\theta_{static,\ 2\ min}$ (~1° increase) for the unmodified silicone control and PEO-control modified silicones (≤ 50 µmol). At 100 µmol, the PEO-control sample showed a loss in restructuring capacity (~16° increase). The change in $\theta_{static,\ 2\ min}$ was also minimal for silicones modified with amphiphilic SMAs, irrespective of concentration (only a ~0.2° decrease). These results demonstrate that, at concentrations ≥ 10 µmol, all amphiphilic SMA modified silicones retain their capacity to undergo water-driven surface restructuring following conditioning in air.

2.4.1.3. Static contact angle, water-conditioned films

Water-driven restructuring was also examined for films after conditioning in water over a 2 week period where $\theta_{static,\ 2\ min}$ values were tested at t = 6 and t = 15 days (**Figure 2-3**). Following conditioning, the change in $\theta_{static,\ 2\ min}$ was minimal for the unmodified silicone and the PEO-control modified silicone (5 µmol; ~1.6° increase). However, at concentrations ≥ 10 µmol, PEO-control modified silicones exhibit a substantial loss in restructuring following conditioning (~17° increase). For silicones modified with amphiphilic SMAs, the increase in $\theta_{static,\ 2\ min}$ was negligible at low concentrations (5 µmol; ~1.1° increase). At concentrations of 10 µmol, $\theta_{static,\ 2\ min}$ was somewhat higher (~11° increase), but this change rendered the initially hydrophilic surfaces ($\theta_{static,\ 2\ min}$ < 90°) slightly hydrophobic ($\theta_{static,\ 2\ min}$ ~101°). However, at concentrations ≥ 25 µmol, while slightly higher $\theta_{static,\ 2\ min}$ values resulted (~7.9° increase), surfaces remained hydrophilic.

Altogether, these results show that all amphiphilic SMA modified silicones can retain substantial water-driven surface restructuring following conditioning in water, particularly at concentrations greater than 10 µmol. Notably, the crosslinkable group was not required, whether with a shorter (m = 13) or longer (m = 30) ODMS tether, to appreciably retain surface hydrophilicity following aqueous conditioning.

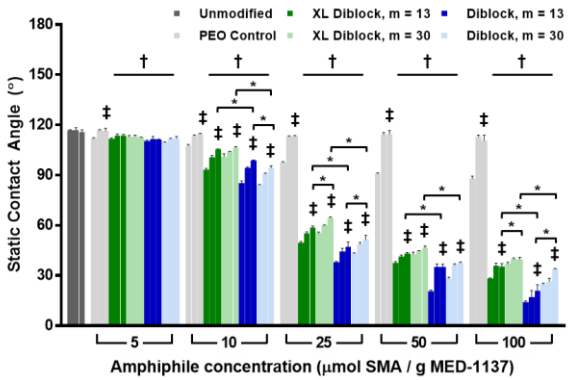

Figure 2-3. θ_{static} at 2 min is shown for each SMA modified silicone at various concentrations after prolonged conditioning in DI water. Bars are organized as conditioning duration from left to right: initial, 6 d, and 15 d. Statistical analysis ($p < 0.05$): ‡initial v. 15 d in a sample set; †sample v. unmodified at 15 d; *difference between sample sets at 15 d.

2.4.2. Water Uptake

Modified silicones were subjected to aqueous conditioning and water uptake was evaluated gravimetrically at t = 1, 6, and 15 days (**Figure 2-4**). The unmodified silicone (~0.31 wt%) and PEO-control modified silicones at concentrations ≤ 25 µmol (~0.61 wt%) had minimal water uptake, but increased for 50 and 100 µmol (~3.6 wt% & 13 wt%, respectively). This water uptake is thought to have contributed to the observed decrease

in surface hydrophilicity following aqueous conditioning (**Figure 2-3**). Silicones modified with amphiphilic SMAs at concentrations ≤ 25 µmol (~0.39 wt%) had minimal water uptake, but increased at 50 and 100 µmol (~1.9 wt% & 4.8 wt%, respectively), albeit lower levels versus the PEO-control modified silicones. At these higher concentrations, water uptake varied somewhat based on amphiphilic SMA structure. For silicones modified with *m* = 30 amphiphiles (~3.7 wt%) and *m* = 13 amphiphiles (~3.0 wt%), water uptake was quite similar. For non-crosslinkable *Diblock* amphiphile modified silicones, water uptake (~4.9 wt%) was somewhat higher compared to those modified with *XL diblock* amphiphiles (~1.7 wt%). Although these differences are discernible at high concentrations of SMAs, overall water uptake for all modified silicones was determined to be rather minimal at concentrations ≤ 25 µmol. Moreover, this level of water uptake did not substantially compromise water-driven surface hydrophilicity per **Figure 2-3**.

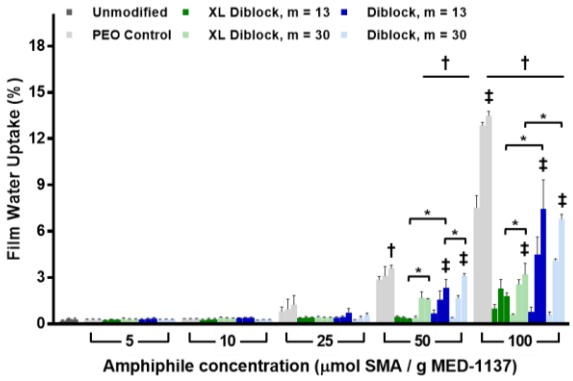

Figure 2-4. Film water uptake is shown as wt% water absorbed for each SMA modified silicone at various concentrations after prolonged conditioning in DI water. Bars are organized as conditioning duration from left to right: 1 d, 6 d, and 15 d. Statistical analysis ($p < 0.05$): $^{\ddagger}t$ = 1 d v. 15 d in a sample set; †sample v. unmodified at 15 d; *difference between sample sets at 15 d.

2.4.3. Mass Loss

To assess water-induced leaching of SMAs from the silicones, changes in specimen mass were noted after 14 days of aqueous conditioning and calculated using **Equation 2-1** (**Figure 2-5**). The unmodified silicone had minimal mass loss (< 0.30 wt%), while all SMA modified silicones generally had concentration dependent increases in mass loss following water-conditioning. PEO-control modified samples exhibited the most prominent changes, with the 100 µmol sample losing almost 4.0 wt% following water conditioning. Though amphiphilic SMA modified silicones also had increased mass loss, overall loss for samples at concentrations ≤ 25 µmol was minimal (< 0.85 wt%) and remained relatively low at higher concentrations (< 1.8 wt%). At these high concentrations (50 & 100 µmol), silicones modified with m = 30 amphiphiles (~0.87 wt %) and m = 13 amphiphiles (~1.4 wt%) exhibited similar weight loss. Silicones modified with *XL diblock* amphiphiles had similar mass loss (~1.1 wt%) as those modified with *Diblock* amphiphiles (~1.2 wt %). Thus, for amphiphilic SMA modified silicones, especially at concentrations ≤ 25 µmol, SMA leaching via mass loss was minimal and did not substantially compromise water-driven surface hydrophilicity (**Figure 2-3**).

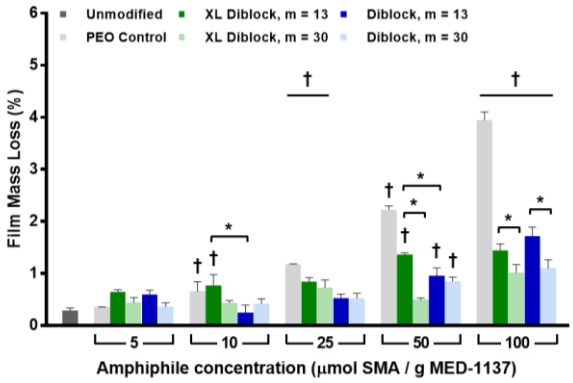

Figure 2-5. Film mass loss is shown for each SMA modified silicone at various concentrations after 14 days of conditioning in DI water. Statistical analysis ($p < 0.05$): †sample v. unmodified at 14 d; *difference between sample sets at 14 d.

2.4.4. Fibrinogen Adsorption

HF adsorption was measured on SMA modified silicones, both before and after 14 days of aqueous conditioning (**Figure 2-6**). As expected, the unmodified silicone as well as the PEO-control modified silicones (all concentrations) showed substantial HF adsorption before and after water-conditioning (>250 ng/cm^2). This is attributed to the lack of water-driven surface restructuring of PEO to induce hydrophilicity, both before and after water-conditioning (**Figure 2-3**). Similarly, amphiphilic SMA modified silicones, at only 5 µmol, showed high levels of HF adsorption (>270 ng/cm^2) before and after water-conditioning. However, when the amphiphilic SMA concentration was increased to 10 µmol, modified silicones showed significantly reduced HF adsorption initially (~73 ng/cm^2), but appreciably increased following water-conditioning, rising most substantially for *Diblock, m* = 13 (~210 ng/cm^2) versus ~120 ng/cm^2 for all other SMAs, including *Diblock, m* = 30. Upon increasing the amphiphilic SMA concentration

to 25 µmol, all modified silicones showed significantly reduced HF adsorption, before and after water-conditioning (< 39 ng/cm^2). Overall, compared to the unmodified control, amphiphilic SMA modified silicones at concentrations ≥ 10 µmol had significantly reduced HF adsorption that was sustained throughout water-conditioning. Moreover, SMAs did not require a crosslinkable group, whether with a shorter (*m* = 13) or longer (*m* = 30) ODMS tether, to appreciably maintain exceptional protein resistance after aqueous conditioning.

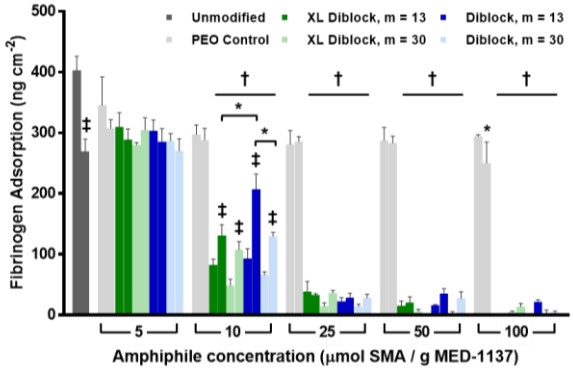

Figure 2-6. HF protein adsorption is shown for each SMA modified silicone before and after 14 days of conditioning in DI water. Statistical analysis ($p < 0.05$): ‡initial v. 14 d in a sample set; †sample v. unmodified at 14 d; *difference between sample sets at 14 d.

2.5. Conclusions

The hydrophobicity of silicones results in poor resistance to protein adsorption, leading to subsequent platelet adhesion and thrombus formation. Bulk modification of condensation cure silicones with hydrophilic, protein resistant PEO critically relies on the ability of PEO to restructure to the aqueous/biological interface, including during

prolonged aqueous conditioning. In this study, a condensation cure silicone was modified with PEO-silane amphiphiles comprised of an ODMS ("siloxane") tether and PEO segment (n = 8). Herein, we evaluated whether a crosslinkable TEOS group was necessary and if this depended on ODMS tether. Thus, crosslinkable, TEOS-containing *XL diblock* amphiphiles (m = 13 & 30) and non-crosslinkable, silane-terminated *Diblock* amphiphiles (m = 13 & 30) were prepared along with a non-amphiphilic, crosslinkable PEO-control. These modified silicones were prepared with each SMA at several concentrations (5, 10, 25, 50, and 100 μmol SMA per 1 g silicone). Following aqueous conditioning, irrespective of amphiphilic SMA structure, all modified silicones at concentrations ≥ 25 μmol retained their surface hydrophilicity with only minor increases in contact angle. Since leaching and water uptake would promote reduced hydrophilicity and protein resistance, these were assessed to confirm their appreciable absence. At all concentrations, amphiphilic SMA modified silicones had minimal water uptake and mass loss, comparable to that of unmodified silicone. Finally, HF protein adsorption was also assessed before and after aqueous conditioning. The unmodified silicone and PEO-control samples, at all concentrations, showed significant HF adsorption. Amphiphilic SMA modified silicones ≥ 25 μmol exhibited extremely low levels of HF adsorption and this resistance was retained after aqueous conditioning. Overall, this study confirms that PEO-silane amphiphiles are effective SMAs for silicones, achieving surface hydrophilicity and protein resistance, even following aqueous conditioning. Additionally, the TEOS crosslinkable group does not appear to be essential for retention of this behavior, irrespective of ODMS tether length. Thus, both tether lengths (m = 13 & 30) serve as effective "physical anchors"

to retain the amphiphiles in the silicone network. Such non-crosslinkable PEO-silane amphiphiles alleviates concerns of crosslink hydrolysis as well as simplifies the synthesis to just one step. Thus, these SMAs show potential to achieve protein resistant silicones that are stable in aqueous environments.

CHAPTER III

THROMBORESISTANCE OF SILICONES MODIFIED WITH PEO-SILANE AMPHIPHILES[‡]

3.1. Overview

The antifouling properties of poly(ethylene oxide) (PEO)-silane amphiphiles as surface-modifying additives (SMAs) in a condensation cure silicone have been previously demonstrated against simple protein solutions. Comprising an oligo(dimethyl siloxane) tether (m = 13 or 30) and PEO segment (n = 8), sustained protein resistance was achieved even in the absence of a crosslinkable triethoxysilane group, particularly when comprising the longer tether. To probe their potential for thromboresistance, PEO-silane amphiphile SMAs were used to bulk-modify silicones and evaluated for adhesion resistance against whole human blood under both static and dynamic conditions. Both a crosslinkable (XL diblock, m = 13) and a non-crosslinkable (Diblock, m = 30) SMA were evaluated at various concentrations (5 – 50 µmol SMA/g silicone) in a condensation cure silicone. Under static conditions, silicones modified with either SMA at concentrations of 10 µmol/g or greater were effective in reducing adhesion of human fibrinogen and platelets. Dynamic testing further showed that modified silicones were able to reduce protein adsorption and thrombus formation. This occurred at 5 µmol/g and 10 µmol/g for silicones

---

[‡]Reprinted with permission from "Thromboresistance of Silicones Modified with PEO-Silane Amphiphiles" by Ngo, B.K.D.; Barry, M.E.; Lim, K.K.; Johnson, J.C.; Luna, D.J.; Pandian, N.K.R.; Jain, A. and Grunlan, M.A., 2020. *ACS Biomater. Sci. Eng.*, (in press) doi: 10.1021/acsbiomaterials.0c00011, Copyright 2020 American Chemical Society.

modified with XL diblock, *m* = 13 and Diblock, *m* = 30 SMAs, respectively. Combined, these results indicate the effectiveness of PEO-silane amphiphiles as SMAs in silicone for improved thromboresistance.

3.2. Introduction

Silicones such as crosslinked poly(dimethyl siloxane) (PDMS) are often used in blood-contacting devices because of their nontoxicity, biostability, and elastomeric mechanical properties.[13,124,125] However, because of their hydrophobicity, silicones are highly susceptible to surface-induced thrombosis where nonspecific protein adsorption occurs, followed by platelet adhesion, activation, and thrombus formation.[2,3,5] This is problematic in devices such as hemodialysis catheters, where a thrombus can occlude the inner lumen, thereby reducing patency and compromising device function.[7,8,126] Thrombosis also facilitates bloodstream infections, which are a major cause of patient fatality.[3,5,127] Currently, pharmaceutical intervention with antithrombotics (e.g., heparin) is used to mitigate thrombosis. These can be administered systemically or, in the case of hemodialysis catheters, as intraluminal locking solutions.[129,130] However, pharmaceutical intervention can be costly and ineffective, as well as increase the risks of bleeding and potential hypersensitivity.[132,133,135,136] Therefore, a materials-based approach for thrombosis prevention that does not use antithrombotics would improve the safety and lifetime of blood-contacting devices.

Generally, hydrophilization of silicones to enhance fouling resistance has been attempted via the incorporation of poly(ethylene oxide) [PEO; or poly(ethylene glycol)

(PEG)].[30,37,137-140] PEO is a hydrophilic and flexible polymer with exceptional protein resistance imparted by its unique ability to form a hydration layer and to produce steric effects that creates a large excluded volume.[27-29] Additionally, PEO is used in antifouling applications because of its biocompatibility and oxidative stability.[60,141] For silicones, PEO may be conveniently incorporated via bulk-modification, but it is crucial that the PEO acts potently as a surface-modifying additive (SMA), quickly moving to and being maintained at the biological interface, in order to resist protein adsorption and subsequent thrombosis.[38,142] The efficacy of PEO in reducing protein adsorption has largely been demonstrated when applied to surfaces of physically stable substrates (e.g., gold,[24,148] silicon wafer,[26,144] and glass[23,146]). Such surface modified substrates maintain PEO chains at the surface, irrespective of the environment (i.e., air or water). However, depending on processing and fabrication parameters,[160] silicones modified with PEO via bulk-modification[30,137,140] (and even surface-grafted[37,140]) are susceptible to hydrophobic recovery due to their chain flexibility and extremely low surface energy.[149,150] Such hydrophobic recovery is likewise observed for the hydrophilic surface of plasma-treated silicone, which is not sustained after removal from an aqueous environment.[151] Moreover, we recently demonstrated the poor potential of PEO-silanes to migrate to the aqueous interface when used for bulk modification of a condensation cure silicone.[55,154,161] Thus, a PEO-based SMA that substantially and rapidly restructures to the biological interface of bulk modified silicones represents a convenient and effective strategy to minimize protein adsorption and thrombosis. Additionally, maintenance of PEO-induced surface hydrophilicity of the bulk-modified silicone must be considered, namely in terms of the

potential of the SMA to leach out and also water uptake that would cause SMA migration from the aqueous interface into the bulk.[152]

In our lab, we have developed amphiphilic PEO-based SMAs for bulk-modification of condensation cure silicones. These PEO-silane amphiphiles include a crosslinkable triethoxysilane (TEOS) group, a flexible, hydrophobic oligo(dimethyl siloxane) (ODMS) tether, and a hydrophilic PEO segment: α-$(EtO)_3$-Si-$(CH_2)_2$-$ODMS_m$-*block*-PEO_n-CH_3.[153] When incorporated into silicones, PEO-silane amphiphiles exhibited rapid and extensive water-driven restructuring to form a hydrophilic, PEO-rich surface (confirmed via atomic force microscopy[54]) with enhanced protein resistance. This was not observed when modified with the corresponding non-amphiphilic PEO-silane [α-$(EtO)_3$-Si-$(CH_2)_3$-PEO_n-CH_3]. This indicated that the unique restructuring capacity of PEO-silane amphiphiles was due to the flexible ODMS tether and the improved SMA compatibility within the silicone matrix. Additional studies investigated varying lengths of PEO (*n*; n = 3 – 16) and ODMS (*m*; m = 0 – 30) as well as SMA concentration (0 – 100 µmol/g silicone).[55,108,154,155] It was determined that water-driven restructuring and protein resistance were optimal for SMAs with a PEO segment of n = 8 and an ODMS tether of m = 13 or 30. For these SMAs, efficacy was observed at concentrations as low as 10 µmol/g.

Recently, non-crosslinkable PEO-silane amphiphile SMAs (i.e., non-TEOS end group) were used to bulk modify a condensation cure silicone to determine their efficacy and stability throughout aqueous conditioning.[157,161] Non-crosslinkable SMAs depict a situation where the hydrolytically unstable crosslinks are broken following extended

exposure to an aqueous or biological environment. Synthesis of the non-crosslinkable amphiphile also requires one less step compared to the crosslinkable variant. Thus, two PEO-silane amphiphiles were synthesized with a PEO length n = 8, one with a crosslinkable TEOS group and shorter ODMS tether (m = 13) (XL diblock, m = 13) and the other without a TEOS group and a longer ODMS tether (m = 30) (Diblock, m = 30). The longer ODMS tether was hypothesized to enhance the physical anchoring of the SMA within the silicone matrix (in the absence of covalent crosslinking) due to its chemically similar nature. These SMAs were incorporated into silicones at various concentrations: 0 – 100 μmol/g silicone. Both the XL diblock, m = 13 and Diblock, m = 30 SMAs showed effective and sustained water-driven surface restructuring as well as protein resistance at 25 μmol/g or higher. The silicones modified with Diblock, m = 30 SMAs also had minimal leaching and water uptake, comparable to that of the XL diblock, m = 13 SMAs.

These prior studies showcased the thromboresistant potential of silicones modified with PEO-silane amphiphiles. However, analyses were limited to protein adsorption tests with single protein solutions (e.g., human fibrinogen (HF) in PBS) and under static conditions, failing to parallel the complexity of thrombosis *in vivo*. Compared to plasma or whole blood, simple protein solutions do not mimic dynamic processes such as the Vroman effect or changes in protein conformation during thrombosis initiation.[115,162,163] Thus, with plasma or whole blood, various methods are used to better assess thromboresistance, including: plasma protein adsorption,[80,164-166] platelet adhesion,[80,164,166-169] thrombin generation,[166,170] as well as measuring partial thromboplastin time[168,171] and split products of the coagulation cascade.[172] A combination

of such testing methods with plasma or whole blood would be ideal for thromboresistance evaluation. Furthermore, static adhesion testing does not account for the effects of fluid flow on protein and platelet adsorption. In contrast, dynamic blood tests have been shown to better mimic the biological environment and can more accurately predict thrombosis, *in vivo*.[173,174]

Herein, silicones bulk-modified with PEO-silane amphiphile SMAs were further studied to better parallel the sequence of events that occur in thrombosis (**Figure 3-1**). These modified silicones were evaluated against whole human blood for their capacity to resist protein adsorption, platelet adhesion, and macro-scale thrombus formation. Both the XL diblock, m = 13 and Diblock, m = 30 SMAs were evaluated as they were previously shown to have effective and sustained protein resistance against a simple HF solution.[161] To determine the minimum effective concentration against whole human blood, these SMAs were synthesized and incorporated at various concentrations (5, 10, 25, and 50 μmol/g of silicone) into a condensation cure silicone. Modified silicone coatings were fabricated both in well plates and within the inner lumen of poly(ethylene vinylacetate) (PEVA) tubing. Although the former was evaluated statically, the latter was evaluated dynamically using a Chandler loop construct (**Figure 3-2**). Combined with the previous protein resistance data, these static and dynamic whole blood assessments can help establish the thromboresistance of PEO-silane amphiphile modified silicones and their potential for use in blood-contacting devices.

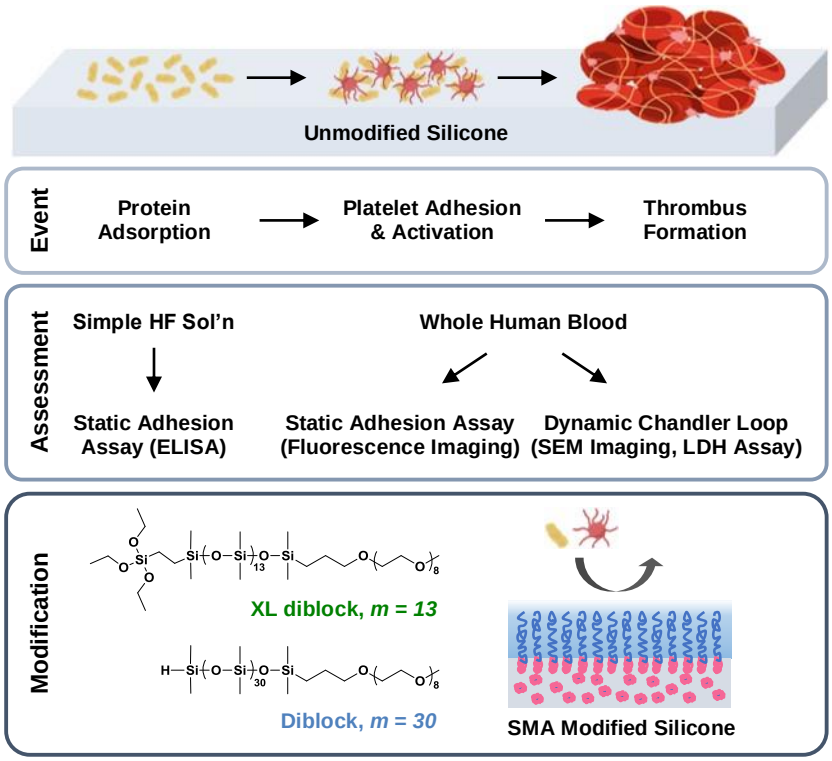

Figure 3-1. Overview of thromboresistance study described herein. Top: Simplified depiction of events leading to thrombus formation on unmodified silicone. Middle: Corresponding *in vitro* assessments for each event (as evaluated herein). Bottom: Chemical structures of crosslinkable and non-crosslinkable PEO-silane amphiphile SMAs of varying tether lengths (m = 13 and 30) for bulk modification of a condensation-cure silicone to enhance thromboresistance.

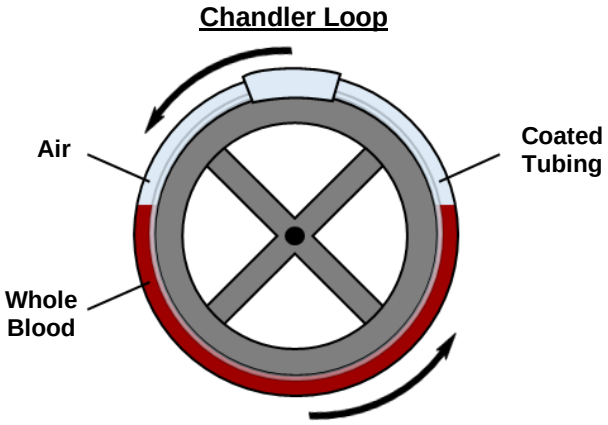

Figure 3-2. Depiction of Chandler loop construct used for dynamic whole blood adhesion study of silicones modified with PEO-silane amphiphiles.

3.3. Materials and Methods

3.3.1. Materials

Pt-divinyltetramethyldisiloxane complex in xylene (Karstedt's catalyst), tetramethyldisiloxane (TMDS), octamethylcyclotetrasiloxane (D_4), and α,ω-bis-(SiH)ODMS [$ODMS_{13}$; M_n = 1000 – 1100 g/mol per manufacturer's specifications; M_n = 1096 g/mol per ^{1}H NMR end group analysis; ^{1}H NMR (δ, ppm): 0.05-010 (m, 78H, SiC*H*$_3$), 0.18-0.19 (d, *J* = 2.7 Hz, 12H, OSi[C*H*$_3$]$_2$H) and 4.67-4.73 (m, 2H, Si*H*)] were purchased from Gelest. Polyglykol AM 450 [AM PEO_8, M_n = 292 – 644 g/mol per manufacturer's specifications; M_n = 424 g/mol per ^{1}H NMR end group analysis; ^{1}H NMR (δ, ppm): 3.37 (s, 3H, OC*H*$_3$), 3.53-3.65 (m, 32H, OC*H*$_2$C*H*$_2$), 3.99-4.02 (d, *J* = 5.4 Hz, 2H, CH_2=CHC*H*$_2$O), 5.14-5.29 (m, 2H, C*H*$_2$=CHCH_2O) and 5.84-5.96 (m, 1H, CH_2=C*H*CH_2O)] was provided by Clariant. Triflic acid, tris(triphenylphosphine)rhodium(I) chloride (Wilkinson's catalyst), 25% glutaraldehyde

(GA) solution in water, vinyltriethoxysilane (VTEOS), hexamethyldisilazane, and solvents were purchased from Sigma-Aldrich. Solvents were dried in 3 Å molecular sieves prior to use in chemical syntheses and modified silicone preparations. A medical grade, condensation cure silicone elastomer [MED-1137; per manufacturer's specifications, containing: α,ω-bis-(Si–OH)PDMS, 11 – 21% silica, < 5% methyltriacetoxysilane, < 5% ethyltriacetoxysilane, and trace amounts of acetic acid] was purchased from NuSil. Human CD-41 antibodies (R-PE conjugated), Alexa Fluor 647 conjugated HF from plasma, and Corning Costar flat bottom 96-well plates were purchased from Thermo Fisher Scientific. PEVA (1/4" OD, 1/8" ID) and poly(vinyl chloride) tubing (PVC; 3/8" OD, 1/4" ID) were purchased from McMaster-Carr.

3.3.2. Human Blood

Human blood was obtained from Student Health Services at Texas A&M University. Experiments were performed in accordance to the policies of the U.S. Office of Human Research Protections as well as the Texas A&M University Human Research Protection Program and approved by the Texas A&M University Institutional Review Board (IRB ID: IRB2016-0762D). Blood from healthy donors with informed consent was drawn into BD Vacutainer tubes [3.2% sodium citrate (blue top)]. Drawn blood was used within four hours to minimize risk of platelet dysfunction.[175]

3.3.3. Synthesis of PEO-silane Amphiphiles

3.3.3.1. Crosslinkable diblock amphiphile synthesis (m = 13; XL diblock, m = 13)

The crosslinkable diblock amphiphile (*m* = 13) was synthesized as previously reported using a two-step hydrosilylation protocol.[153] Briefly, the $ODMS_{13}$ tether was

reacted with VTEOS (1:1 molar ratio) via a Wilkinson's-catalyzed, regioselective hydrosilylation reaction. The product was then reacted with AM PEO_8 (1:1 molar ratio) via a Karstedt's-catalyzed hydrosilylation reaction.

3.3.3.2. Non-crosslinkable diblock amphiphile synthesis (m = 30; Diblock, m = 30)

The non-crosslinkable diblock amphiphile (i.e., no TEOS group; m = 30) was synthesized as previously reported.[157] Briefly, the $ODMS_{30}$ siloxane tether (m = 30) was first synthesized using a room temperature (RT), triflic acid catalyzed ring opening polymerization of TMDS and D_4.[154] The $ODMS_{30}$ tether was then reacted with AM PEO_8 (1:1 molar ratio) via a Wilkinson's-catalyzed, regioselective hydrosilylation reaction.

3.3.4. Static Adhesion Testing

3.3.4.1. Coating of well plate with modified silicones

Bulk-modified silicones were fabricated as films using a solvent casting method.[155] Casting solutions were prepared of 25 wt% MED-1137 in hexane and mixed on a shaker plate until homogeneous. For SMA-modified silicones, each amphiphile was added to casting solutions at various concentrations: 0, 5, 10, 25, and 50 μmol per 1 g of silicone. Solutions were cast into 96-well plates (100 μL per well; 4 wells per composition) and cured for 1 week at RT prior to use.

3.3.4.2. Static testing with human blood

For static testing, citrated whole human blood was first pre-treated with fluorescently labeled HF and CD41 antibodies. The HF was incubated with blood for 10 min at RT, whereas the CD41 antibodies were added immediately before use. For each composition in the modified silicone-coated well plates, 100 μL of pre-treated blood was

added to 3 wells and PBS was added to a fourth well. The blood was re-calcified by adding 10 µL of a freshly prepared 100 mM $CaCl_2$ + 75 mM $MgCl_2$ solution to each well (blood:re-calcification solution, 10:1 v/v). Samples were incubated on a shaker plate (150 rpm) at RT for 10 min. Blood was removed and wells were gently rinsed 3 times with PBS. To each well was added 200 µL of fixative solution (2.5% GA in DI water) and it was incubated on a shaker plate (150 rpm) at RT for 60 min. Wells were again rinsed 3 times prior to analysis with fluorescence microscopy. Static testing was completed for a total of 3 individual blood donors.

3.3.4.3. Fluorescence microscopy

Platelet adhesion and HF adsorption were measured via fluorescence microscopy using a Zeiss Axio Observer.Z1 microscope. Following the static testing (as noted above), images were taken of each well using an Axiocam 702 mono microscope camera and a LED illumination source (excitation/emission: 470/488 nm, 625/647 nm). Initial image analysis was performed in the Zeiss Zen 2.3 Pro (blue edition) open application development software suite. For qualitative evaluations, imaging was done with a 10X objective (Zeiss EC Plan-Neofluar 10x/0.30 M27) and ImageJ software was used to overlay the fluorescent images. For quantitative evaluations, imaging was done with a 5X objective (Zeiss N-Achroplan 5x/0.15 M27) and ImageJ software was used to calculate the fluorescence intensity. Samples were normalized to an unmodified silicone control. The reported values and corresponding error represent an average and standard deviation of three wells, respectively.

3.3.5. Dynamic Adhesion Testing

3.3.5.1. Application of modified silicones to tubing

To coat the inner lumen of tubing for Chandler loop testing, we prepared casting solutions as described above at similar MED-1137 concentration in solution (25 wt %) and SMA concentrations (0 – 50 μmol/g). PEVA tubing (40 cm) was exposed to oxygen plasma for 2 min (Harrick Plasma PDC-001) to enhance adhesion of silicone coatings. Casting solutions were immediately added (2 mL) to the treated tubing and coupled together with a PVC sleeve (1.5 cm) to form loops for fitting around the construct's rotating wheel frame. These were cured while rotating tangentially on the Chandler loop to produce a uniform coating. Tubing was cut into cross sections to verify complete coverage of the inner lumen. Samples were sputter coated using a gold target (~ 21 nm) prior to scanning electron microscopy (SEM; JEOL JCM-5000 NeoScope; accelerating voltage: 10 kV).

3.3.5.2. Chandler loop testing with human blood

A Chandler loop construct was used to evaluate thromboresistance of modified silicones against whole human blood under dynamic conditions.[164,176,177] Coated tubing was first washed with 2 mL of DI water while rotating on the Chandler loop (5 min, 15 rpm). Citrated human blood was re-calcified with a freshly prepared 100 mM $CaCl_2$ + 75 mM $MgCl_2$ solution (blood:re-calcification solution, 10:1 v/v) and immediately added to the coated tubing (1.6 mL; ~ 50 % volume). These were then rotated on the Chandler loop to simulate blood flow and circulation at RT (10 min, 15 rpm: strain rate ~ 272.5 s^{-1}).[178] The blood was then drained and the tubing was rinsed with ~ 5 mL PBS via syringe. The

tubing was sectioned into 2 cm samples, placed in PBS-filled containers, and inverted gently several times to remove non-adhered proteins and cells. Dynamic testing was performed for a total of 3 individual blood donors.

3.3.5.3. SEM imaging

One 2 cm section was obtained from each loop for SEM visualization of platelet and cell adhesion as well as thrombus formation. The tubing section was cut into two "halfpipes" and were fixed using a 2.5 % GA solution for 1 h. These were sequentially dehydrated in 70, 90, and 100% solutions of ethanol. These were then cooled to -85 ºC and lyophilized prior to SEM imaging.

3.3.5.4. LDH assay

The LDH assay was performed per standard protocols using a Pierce LDH Cytotoxicity Assay Kit.[167] Three 2 cm sections of tubing were obtained from each loop and exposed to 100 µL of 1X lysis buffer for 45 min at 37 ºC. 50 µL of each solution was then transferred to a 96-well plate before adding 50 µL of the substrate solution. After 30 min of incubation at RT, 50 µL of stop solution was added to each well. The absorbance of the reaction products were measured by microplate reader (Tecan Infinite M200 PRO). LDH positive controls were used with BSA to create a standard curve for quantification of surface protein concentration.

3.3.6. Statistical Analysis

Reported values represent an average and standard deviation of triplicate measurements. Statistical analysis was performed using two factor ANOVA and statistical significance was defined with a p-value < 0.05.

3.4. Results and Discussion

In prior work, the thromboresistant potential of silicones modified with PEO-silane amphiphile SMAs was limited to the demonstration of protein resistance with simple, single protein solutions under static conditions.[54,55,108,154,155,157,161] However, to better mimic the biological environment and predict resistance to thrombosis, the use of plasma or whole blood as well as flow conditions is necessary. In this study, silicones were bulk-modified with a crosslinkable (XL diblock, m = 13) and a non-crosslinkable (Diblock, m = 30) SMA as these were previously shown to have effective and sustained water-driven surface hydrophilicity and protein resistance.[161] Herein, these modified silicones were exposed to whole human blood, under static and flow conditions, and assessed for their capacity to resist protein adsorption, platelet adhesion, and macro-scale thrombus formation. To determine their minimum effective concentration, the SMAs were incorporated at 0, 5, 10, 25, and 50 μmol/g into a condensation cure silicone. Modified silicone coatings were formed either in well plates or on the inner lumen of PEVA tubing. The former was evaluated with fluorescent microscopy following blood exposure under static conditions, whereas the latter was evaluated dynamically using a Chandler loop construct that permits blood circulation.

3.4.1. Static Adhesion Testing

PEO-silane amphiphiles as SMAs in silicone were first assessed via a static adhesion assay against whole human blood. As coatings within well plates, SMA-modified silicones were exposed to blood and fluorescence imaging was subsequently used to observe platelet adhesion and HF adsorption. Images were analyzed both

qualitatively (**Figure 3-3a** and **3-3b**) and quantitatively (**Figure 3-3c** and **3-3d**). On the basis of the qualitative observation of the fluorescent images, the unmodified silicone control (0 µmol/g) exhibited substantial HF adsorption and platelet adhesion as expected. Modified silicones at 5 µmol/g SMA concentration showed similarly high levels of fouling for both the SMAs. At concentrations of 10 µmol/g or greater, XL diblock, *m* = 13 modified silicones exhibited substantial reduction in HF adsorption and platelet adhesion. For Diblock, *m* = 30 modified silicones, minor levels of adhesion were still observed at 10 µmol/g, whereas samples at 25 µmol/g or greater showed significantly reduced HF and platelet adhesion. For quantitative assessments of platelet adhesion and HF adsorption, images were also analyzed for their fluorescence intensities at wavelengths of 488 and 647 nm, respectively, and values were normalized to those of the unmodified silicone control (1.000) for 3 individual blood donors. Consistent with the qualitative assessment, the XL diblock, *m* = 13 modified silicones at 5 µmol/g showed high fluorescence intensities for both platelet adhesion (~ 0.969) and HF adsorption (~ 0.991) when compared to the unmodified silicone control. At concentrations of 10 µmol/g or greater, fluorescence intensity was significantly reduced for platelet adhesion (~ 0.027 average value) and HF adsorption (~ 0.014 average value). Similarly, Diblock, *m* = 30 modified silicones at 5 µmol/g showed high fluorescence intensities for platelet adhesion (~ 0.924) and HF adsorption (~ 0.676). At 10 µmol/g or greater, these intensities significantly decreased for both platelet adhesion (~ 0.047 average value) and HF adsorption (~ 0.016 average value). Thus, XL diblock, *m* = 13 and Diblock, *m* = 30 SMA-modified silicones show reduced

adhesion of proteins and platelets from whole blood under static conditions at concentrations as low as 10 µmol/g.

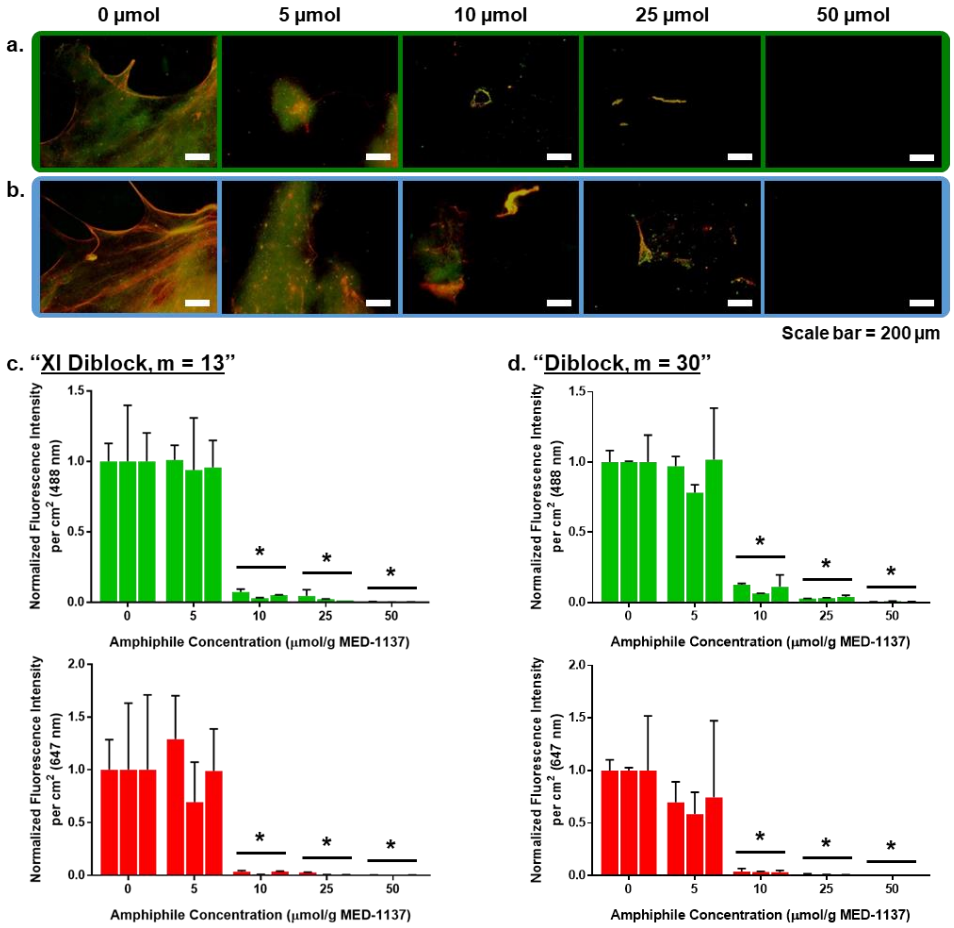

Figure 3-3. Platelet adhesion and HF adsorption following exposure to whole human blood under static conditions. Representative fluorescent images for silicones modified with (a) XL diblock, m = 13 and (b) Diblock, m = 30 at various concentrations (0 – 50 µmol/g). Platelets and HF appear green and red, respectively. Fluorescence intensity quantification of the images of (c) XL diblock, m = 13 and (d) Diblock, m = 30. "Green bars" and "red bars" correspond to platelet and HF normalized fluorescence intensities, respectively. Testing was done in triplicate and each bar represents individual blood donors (N = 3). (* indicates $p < 0.05$)

3.4.2. Dynamic Adhesion Testing

A dynamic whole human blood assessment was also performed on silicones modified with two PEO-silane amphiphile SMAs. This was done with a Chandler loop construct where whole human blood was circulated through tubing coated with a SMA-modified silicone on the inner lumen. The tubing was evaluated for adhesion of whole blood components as well as macro-scale thrombus formation using SEM imaging and an LDH assay. First, the presence of the SMA-modified silicone coatings on the inner lumen of the tubing was verified with SEM images of the tubing cross-section (**Figure 3-4**). For all coated tubing, SEM imaging confirmed a uniform coating with an approximate thickness of ~ 12 ± 2 μm.

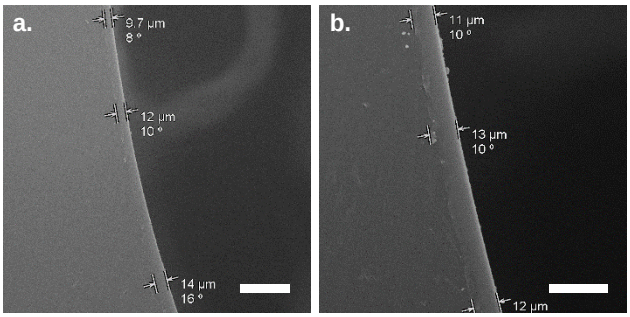

Figure 3-4. Representative SEM images of the inner lumen of tubing coated with SMA-modified silicone. Scale bar lengths are (a) 50 and (b) 25 μm.

Re-calcified whole human blood was added to the tubing and circulated on the Chandler loop for 10 min. The blood was then drained from the coated tubing and immediately rinsed with PBS. Photos were the taken to visually capture the relative levels

of blood adhesion to the coated tubing (**Figure 3-5**). Tubing coated with XL diblock, *m* = 13 or Diblock, *m* = 30 modified silicone, at just 5 µmol/g concentration, displayed high levels of blood adhesion, similar to tubing coated with unmodified silicone (0 µmol/g). In contrast, tubing coated with silicones modified with either SMA at 10 µmol/g concentrations or higher were relatively clean and showed minimal levels of adhesion.

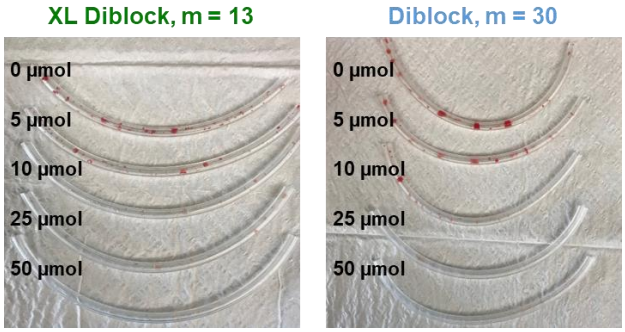

Figure 3-5. Images of the tubing coated with XL diblock, *m* = 13 (left) and Diblock, *m* = 30 (right) modified silicones following blood circulation and PBS rinse.

Following exposure to whole blood with the Chandler loop, the tubing was evaluated with SEM imaging as well as an LDH assay to further assess adhesion of blood components and thrombus formation. SEM imaging was used for qualitative assessments, with representative images selected upon viewing a series of images for each blood donor (**Figure 3-6a** and **3-6b**). The tubing coated with the unmodified silicone control (0 µmol/g) showed extensive thrombus formation, including the presence of adhered red blood cells and platelets, as well as a fibrin network. Similarly, tubing coated with XL diblock, *m* = 13 modified silicone at a 5 µmol/g concentration showed high amounts of

adhesion and thrombus formation. In contrast, at SMA concentrations of 10 µmol/g or greater, the tubing coated with modified silicones remained clean. Similar trends were observed for tubing coated with Diblock, m = 30 modified silicones.

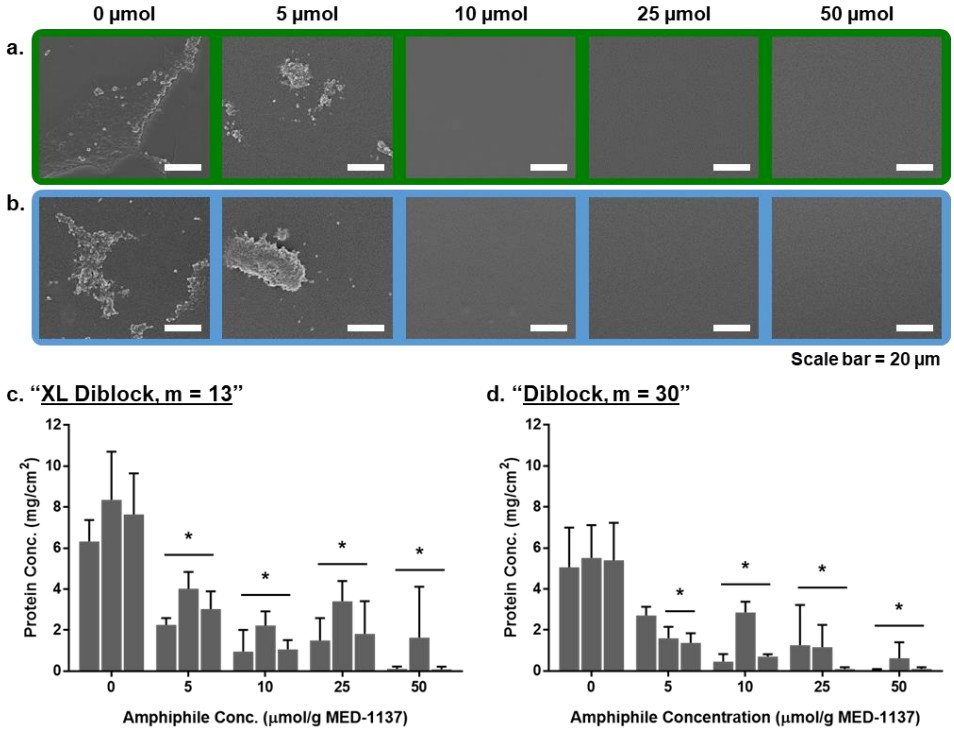

Figure 3-6. Platelet adhesion and protein adsorption following exposure to whole human blood under dynamic conditions. Representative SEM images for tubing coated with silicones modified with (a) XL diblock, m = 13 and (b) Diblock, m = 30 at various concentrations (0 – 50 µmol/g). Quantification of protein adsorption (via an LDH assay) is shown for tubing coated with silicones modified with (c) XL diblock, m = 13 and (d) Diblock, m = 30. Testing was done in triplicate and each bar represents individual blood donors (N = 3). (* indicates $p < 0.05$)

An LDH assay was also performed on exposed tubing to quantitatively assess protein adsorption (**Figure 3-6c** and **3-6d**). The unmodified silicone control (0 μmol/g) showed significant levels of protein adsorption (~ 6.38 mg/cm^2), consistent with SEM images. For tubing coated with XL diblock, *m* = 13 modified silicones, significantly reduced protein adsorption was observed at all concentrations (5 – 50 μmol/g; ~ 1.85 mg/cm^2 average value). These results coincide with SEM images of samples prepared with SMA concentrations of 10 – 50 μmol/g. However, samples prepared with 5 μmol/g showed lower protein concentrations than predicted from SEM images; this may be attributed to the random selection of imaged portions of the tube. This indicates that, at this low SMA concentration, the observed adhesion and thrombus formation was not uniformly extensive throughout the tubing unlike the unmodified control. For tubing coated with Diblock, *m* = 30 modified silicones, samples at 5 μmol/g had significantly reduced protein adsorption (~ 1.89 mg/cm^2) for only 2 of the 3 blood donors (versus the unmodified silicone). As with the XL diblock, *m* = 13 SMA, samples at this low SMA concentration appear susceptible to adhesion in various parts of the tubing. For samples at 10 – 50 μmol/g, surface protein concentration (~ 0.81 mg/cm^2 average value) was significantly lower for all donors, which was consistent with SEM imaging. Similar to the results observed in the static studies, the dynamic whole blood adhesion assays confirm the efficacy of PEO-silane amphiphiles as SMAs in silicone for thromboresistance. Tubing coated with the XL diblock, *m* = 13 and Diblock, *m* = 30 SMA-modified silicones showed significantly reduced adhesion of whole blood components as well as thrombus formation at concentrations as low as 5 μmol/g and 10 μmol/g, respectively.

3.5. Conclusions

The hydrophobic nature of silicones makes them susceptible to protein adsorption, which is followed by platelet adhesion, activation, and ultimately, thrombus formation. Previously, the efficacy and stability of PEO-silane amphiphiles as SMAs in silicone has been established for enhancement of surface hydrophilicity and protein resistance. In particular, a crosslinkable, TEOS-containing (XL diblock, m = 13) SMA and a non-crosslinkable (Diblock, m = 30) SMA were effective against HF solution in PBS. However, to better demonstrate their thromboresistance, additional assessments against blood was required. Herein, a condensation cure silicone was modified with these PEO-silane amphiphile SMAs and evaluated against whole human blood under static and dynamic conditions. Both the XL diblock, m = 13 and Diblock, m = 30 SMAs were incorporated at 5, 10, 25, and 50 μmol/g of silicone. Initial assessments were done under static conditions, where modified silicone films were prepared in well plates and evaluated with fluorescent microscopy following blood exposure. Both the XL diblock, m = 13 and the Diblock, m = 30 SMA-modified silicones showed significantly reduced HF adsorption and platelet adhesion at concentrations as low as 10 μmol/g (~ 1.7 and 2.8 wt%, respectively). For evaluation under dynamic conditions, modified silicone coatings were prepared on the inner lumen of PEVA tubing and a Chandler loop construct was used for circulation of blood. Following circulation, tubing segments were cut and assessed for surface protein concentration as well as thrombus formation. Compared to the unmodified silicone, silicones modified with XL diblock, m = 13 SMAs showed significantly reduced protein adsorption and minimal thrombus formation at concentrations as low as 5 μmol/g

(~ 0.9 wt%). For those modified with Diblock, m = 30 SMAs, significant reduction in protein adsorption and thrombus formation was consistently seen at concentrations of 10 μmol/g (~ 2.8 wt%) or greater. These results demonstrate the effectiveness of these SMA-modified silicones against whole human blood, even in the absence of crosslinking of the SMA. Future work could include investigation of SMA stability under dynamic conditions to account for the shear stress generated with blood flow. Combined with the previous studies against simple protein solutions, here we establish the potential of PEO-silane amphiphiles as SMAs to enhance the thromboresistance of silicones.

CHAPTER IV

THROMBORESISTANCE OF POLYURETHANES MODIFIED WITH PEO-SILANE AMPHIPHILES

4.1. Overview

Silicones and polyurethanes (PUs) are commonly used in blood-contacting devices; however, they are susceptible to surface-induced thrombosis. Poly(ethylene oxide) (PEO)-silane amphiphiles (PEO-SA) have previously been demonstrated to be effective surface modifying additives (SMAs) in silicones for enhanced thromboresistance. In this study, we investigated the potential of PEO-SAs as SMAs in a PU. A PEO-SA was incorporated into a PU at various concentrations (0, 5, 10, 25, 50, and 100 μmol per 1 g of PU). The resulting modified PU films were assessed in terms of mechanical properties, water-driven surface restructuring, protein resistance when subjected to simple human fibrinogen (HF) solution, and resistance to protein and platelets when exposed to whole human blood. The stability of PEO-SA modified PUs was also determined in terms of sustained surface hydrophilicity as well as film water uptake and film mass loss following conditioning in air and water. Mechanical assessments indicated the bulk-modification of PUs with PEO-SA SMAs did not result in plasticization, as evidenced by minimal changes in glass transition temperature (T_g), modulus, tensile strength, and percent strain at break. Regarding water-driven surface restructuring, PEO-SA modified PUs showed a concentration-dependent increase in hydrophilicity that was sustained following both air- and aqueous-conditioning at SMA concentrations of 25

μmol/g or greater. At all concentrations, water uptake and mass loss were minimal compared to the unmodified PU control. Lastly, although no enhanced protein resistance was observed against a simple HF solution, PEO-SA modified PUs were able to resist protein adsorption and platelet adhesion from whole human blood at concentrations ≥ 10 μmol/g PU. Overall, we demonstrate the versatility of PEO-SAs as SMAs in PU, which led to enhanced as well as sustained hydrophilicity and thromboresistance.

4.2. Introduction

Silicones and polyurethanes (PUs) are both commonly used in blood-contacting medical devices such as hemodialysis catheters, bladders of the left ventricular assist device, and vascular grafts due to their non-toxicity, biostability, as well as durability and fatigue resistance.[13,124,179,180] Unfortunately, their hydrophobicity makes them susceptible to non-specific protein adsorption, as well as subsequent platelet adhesion, activation, and thrombus formation.[2,5] Surface-induced thrombosis is problematic, particularly in devices such as hemodialysis catheters, where thrombi can reduce patency and compromise device function.[7,8,126] Thrombosis also facilitates catheter-related bloodstream infections, a major cause of patient fatalities.[3,5,127] Antithrombotic therapies (e.g. heparin) are used reduce thrombosis risk, either as systemic agents[128,130] or, in the case of hemodialysis catheters, as intraluminal locking solutions.[129,131] However, these can be costly and ineffective, as well as being associated with high bleeding risk and potential hypersensitivity.[132,133,135,136] Therefore, a thromboresistant strategy aimed towards increasing surface hydrophilicity

would reduce antithrombotic use and improve the safety and efficacy of blood-contacting devices.

Generally, the incorporation of poly(ethylene oxide) [PEO; or poly(ethylene glycol) (PEG)] into silicones and PUs has been explored towards increasing surface hydrophilicity and antifouling properties.[37,138,181,182] PEO is a hydrophilic and flexible polymer that exhibits biocompatibility and oxidative stability.[60,141] When in sufficient concentration at a material surface, PEO chains can produce exceptional protein resistance due to their ability to form a hydration layer as well as steric effects to create a large excluded volume.[27-29] Whether incorporated via surface- or bulk-modification, it is essential that PEO chains are initially present at the surface-biological interface and sustained over time in sufficient concentration to realize its antifouling effects.[38,142] Surface-modification with PEO for enhanced protein resistance has been well established on physically stable, model substrates (e.g. glass,[23,146] silicon wafer,[26,144] and gold[24,148]), where PEO chains are maintained at the surface, irrespective of the environment (i.e. air or water). However, this is not true of polymeric substrates such as PU since they are susceptible to hydrophobic recovery.[183] These effects have been observed following plasma treatment of PU surfaces.[184,185] Alternatively, PUs can be bulk-modified with PEO-based surface modifying additives (SMAs).[186] Use of SMAs requires their rapid as well as sustained restructuring of the hydrophilic PEO chains to the surface-biological interface to resist protein adsorption and thrombosis. In a series of studies, Tan and Brash synthesized and evaluated PEO-PU-PEO triblock copolymers as SMAs in PU against simple protein solutions, human plasma, as well as reconstituted human blood.[187-190] The

SMAs were incorporated at concentrations up to 20 wt% and resulted in enhanced fouling resistance of modified PUs. However, bulk-modification with SMAs at these levels are anticipated to alter the mechanical properties of the PU, but was not addressed in these studies. Furthermore, retention of antifouling properties is critical, and thus, it is essential to also monitor stability with respect to potential for SMA leaching, as well as water uptake that could cause SMA migration into the bulk and a resulting loss of surface hydrophilicity.[152]

Our group has developed PEO-silane amphiphile (PEO-SA) SMAs, originally for the bulk-modification of condensation-cure silicones.[55,108,153-155,157,161] The PEO-SA contains a triethoxysilane (TEOS) group, a flexible, hydrophobic oligo(dimethyl siloxane) (ODMS) tether, and a PEO segment: α-$(EtO)_3$-Si-$(CH_2)_2$-$ODMS_m$-*block*-PEO_n-CH_3 (**Figure 4-1a**).[153] The TEOS group is capable of crosslinking when incorporated into a condensation-cure silicone. As SMAs in such a silicone, they showed effective and sustained water-driven surface restructuring for enhanced hydrophilicity and resistance to protein adsorption (**Figure 4-1b**).[108,157,161] As this was not observed with analogous, non-amphiphilic PEO-silanes [(α-$(EtO)_3$-Si-$(CH_2)_3$-PEO_n-CH_3)],[55,154,161] the unique restructuring capacity of PEO-SAs was attributed to the flexibility and chemical compatibility of the ODMS tether with the silicone matrix. Additional studies evaluated concentration (0 – 100 µmol per 1 g of silicone) as well as the structure-property relationship of PEO-SAs of different PEO length (*n*; $n = 3 – 16$),[55,155] ODMS length (*m*; $m = 0 – 30$),[154] and crosslinkability (i.e. with or without TEOS group).[157,161] Generally, PEO-SA SMAs demonstrated increased surface hydrophilicity and resistance to human

fibrinogen (HF) adsorption (from a simple aqueous solution) at concentrations as low as 10 µmol/g. Furthermore, both a crosslinkable (m = 13, n = 8) and non-crosslinkable (m = 30, n = 8) variant could similarly sustain these properties with minimal water uptake and SMA leaching following aqueous conditioning (**Figure 4-1c** and **4-1d**). Thus, the TEOS crosslinkable group was determined to be unnecessary, highlighting the efficacy of the increased ODMS tether length to serve as a physical anchor for PEO-SA SMAs in silicone. Overall, these studies demonstrated the efficacy of PEO-SAs in silicone, but their potential to modify other polymer matrices has yet to be reported.

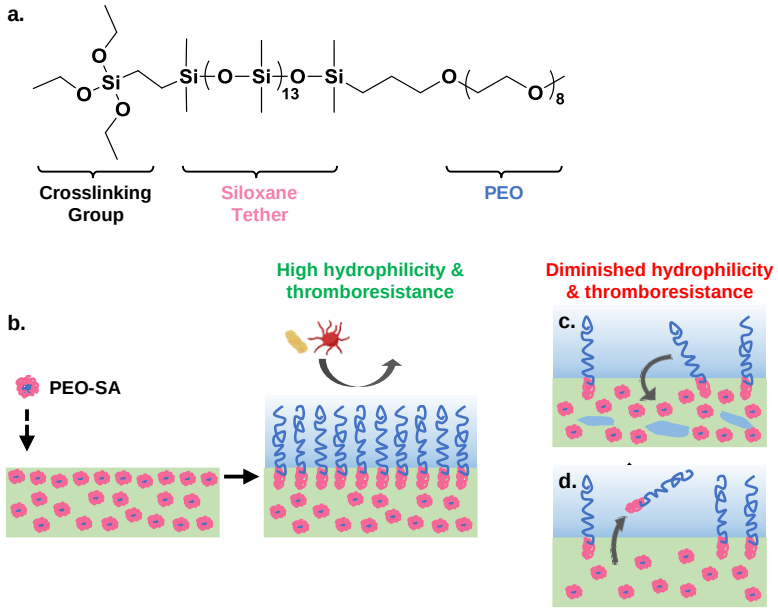

Figure 4-1. (a) Chemical structure of the PEO-SA (m = 13, n = 8). (b) In prior work with modified silicones and evaluated herein for a PU, minutes following aqueous or blood exposure, PEO-SAs restructure to form a hydrophilic and thromboresistant surface. Stability of PEO-SA modified films must resist (c) water uptake or (d) mass loss following extended aqueous exposure as the surface PEO concentration would be reduced, resulting in diminished hydrophilicity and thromboresistance.

As mentioned, PUs are another commonly used material in blood-contacting devices that are susceptible to non-specific protein adsorption and subsequent thrombosis. Herein, a PEO-SA (**Figure 4-1a**) was evaluated as a SMA in an aromatic polyether thermoplastic PU (Tecothane™, TT-1074A) at various concentrations: 0, 5, 10, 25, 50, and 100 µmol per 1 g of PU. These molar concentrations correspond to 0, 0.9, 1.7, 4.3, 8.6, and 17.1 wt% in PU, respectively. We sought to determine the minimum effective concentration of PEO-SAs as a SMA in PU as well as the stability of the modified PU surfaces. The mechanical properties of PEO-SA modified PU films were measured to determine if incorporation as SMAs led to plasticization of the PU base material. PEO-SA modified PU films were also tested for water-driven surface restructuring to form hydrophilic surfaces capable of resisting protein adsorption and thrombosis (**Figure 4-1b**). Next, films were conditioned in air and water to determine if the enhanced surface hydrophilicity could be sustained. A separate set of films were similarly conditioned in water for monitoring of mass loss as well as water uptake since prominent amounts of either would lead to diminished hydrophilicity and protein resistance (**Figure 4-1c** and **4-1d**). PEO-SA modified PUs protein resistance was assessed against a simple HF solution. Although convenient for initial assessments, simple protein solutions often fail to mimic the complexity and dynamics of protein adsorption and thrombosis, *in vivo*.[115,162,163] Thus, PEO-SA modified PUs were subjected to whole human blood and fibrinogen adsorption as well as platelet adhesion were assessed.

4.3. Materials and Methods

4.3.1. Materials

Polyglykol AM 450 [AM PEO_8, M_n = 292–644 g/mol per manufacturer's specifications; M_n = 424 g/mol per proton nuclear magnetic resonance (^{1}H NMR) end group analysis; ^{1}H NMR (δ, ppm): 3.37 (s, 3H, OC*H*$_3$), 3.53-3.65 (m, 32H, OC*H*$_2$C*H*$_2$), 3.99-4.02 (d, *J* = 5.4 Hz, 2H, CH_2=CHC*H*$_2$O), 5.14-5.29 (m, 2H, C*H*$_2$=CHCH$_2$O) and 5.84-5.96 (m, 1H, CH_2=C*H*CH$_2$O)] was provided by Clariant. Pt-divinyltetramethyldisiloxane complex in xylene (Karstedt's catalyst) and α,ω-bis-(SiH)ODMS [$ODMS_{13}$; M_n = 1000 – 1100 g/mol per manufacturer's specifications; M_n = 1096 g/mol per ^{1}H NMR end group analysis; ^{1}H NMR (δ, ppm): 0.05-010 (m, 78H, SiC*H*3), 0.18-0.19 (d, *J* = 2.7 Hz, 12H, OSi[C*H*3]$_2$H) and 4.67-4.73 (m, 2H, Si*H*)] were purchased from Gelest. Tris(triphenylphosphine)rhodium(I) chloride (Wilkinson's catalyst), vinyltriethoxysilane (VTEOS), 25% glutaraldehyde (GA) solution in water, and solvents were purchased from Sigma-Aldrich. Solvents were dried in 3 Å molecular sieves prior to use in chemical syntheses and modified PU fabrication. Tecothane™ TT-1074A (clear grade) was kindly provided by Lubrizol. Mouse anti-fibrinogen horse radish peroxidase (HRP)-conjugated monoclonal detection antibody was purchased from Abcam. Corning Costar™ flat bottom 96-well plates, Pierce 20X tris buffered saline with Tween 20 (TBS-T20), Alexa Fluor™ 647 conjugated HF from plasma, and human CD41 antibodies (R-PE conjugated) were purchased from Thermo Fisher Scientific. HF from plasma, bovine serum albumin (BSA), and TMB+ liquid 1-component substrate solution were purchased from VWR.

4.3.2. Human Blood

Human blood was acquired from the Student Health Services at Texas A&M University (TAMU). Experiments were performed in accordance to the policies of the US Office of Human Research and Protections as well as the TAMU Human Research Protection Program and approved by the TAMU Institutional Review Board (IRB ID: IRB2016-0762D). Blood was drawn from healthy, consenting donors into BD Vacutainer® tubes containing 3.2% sodium citrate (blue top) and used within four hours to minimize risk of platelet dysfunction.[175,191]

4.3.3. Synthesis of PEO-silane Amphiphile (PEO-SA; m = 13, n = 8)

The PEO-SA (*m* = 13, *n* = 8) was synthesized as previously reported using a two-step hydrosilylation protocol.[153] The synthesis was run under nitrogen (N_2) atmosphere with a Teflon-coated stir bar for mixing. First, VTEOS was reacted with the $ODMS_{13}$ tether (1:1 molar ratio) via a Wilkinson's-catalyzed, regioselective hydrosilylation reaction. The product was then reacted with AM PEO_8 (1:1 molar ratio) via a Karstedt's-catalyzed hydrosilylation reaction. The structure of the resulting PEO-SA was confirmed with ^1H NMR using an Inova 500 MHz spectrometer operating in the Fourier transform mode and a $CDCl_3$ standard.

4.3.4. Polyurethane Film Preparation

Glass slides were cleaned with dichloromethane and acetone before drying in a 120 °C oven overnight. Neat PU pellets were washed with methanol to remove processing agents and low molecular weight components. These were dried in a vacuum oven overnight at 120 °C. PU pellets were dissolved in tetrahydrofuran to form an 8 wt% solvent

casting solution. For bulk-modification as SMAs, the PEO-SA was added at 0 (unmodified PU), 5, 10, 25, 50, and 100 µmol per 1 g of PU. These were allowed to solubilize while on a shaker plate at room temperature (RT) for 3 days. Solutions were then solvent-cast onto cleaned glass slides (2 mL per slide) and allowed to cure for 1 week at RT prior to use.

4.3.5. Mechanical Properties

4.3.5.1. Glass transition temperature (T_g)

The T_g of each film composition was determined with differential scanning calorimetry (DSC; TA Instruments Q100). For each sample, PU films were removed from glass slides and a razor blade was used to cut small pieces for placement in hermetic pans. Each sample (~ 10 mg) was subjected to a heat/cool/heat protocol from -100 to 180 °C at a heating rate of 10 °C/min under N_2. T_g was determined as the midpoint of the thermal transition in the heat flow versus temperature plot of the second cycle.

4.3.5.2. Tensile testing

The tensile properties of modified PU films were measured at RT using an Instron 5944. Samples were prepared by using an ASTM D-1708 die to cut PU films that were removed from glass slides. Each specimen had a gauge area of ~ 20 mm x 5 mm x 0.05 mm and was tested with a constant strain rate (100 mm/min) in tension until break. The resulting stress strain curve was used to determine tensile strength (TS) and percent strain at break (%ε). Tensile modulus (E) was also obtained from the slope value between 20 – 100 % strain. Measurements were taken in triplicate.

4.3.6. Water-driven Surface Restructuring

Water-driven surface restructuring of PEO-SA modified PUs was assessed with static water contact angle (θ_{static}) using a CAM-200 goniometer (KSV instruments) with an autodispenser, video camera, and the Attension Theta drop-shape analysis software. A 5 µL droplet of deionized (DI) water was placed on the surface and θ_{static} was iteratively measured over a 2 min period in 15 sec intervals. The reported θ_{static} values are an average and standard deviation of three measurements made on different regions of the same film. Films were subsequently subjected to air- or water-equilibration and re-tested as described below.

4.3.6.1. Air-equilibrated PU films (i.e. conditioned in air)

Following the initial θ_{static} measurements, PU films were stored at RT in air for 2 weeks. After 2 weeks, θ_{static} was measured as previously described. For these measurements, the reported θ_{static} values are the average and standard deviation of three measurements taken at 2 min following drop placement ($\theta_{static,\ 2\ min}$).

4.3.6.2. Water-equilibrated PU films (i.e. conditioned in water)

Following the initial θ_{static} measurements, an equivalent set of PU films were submerged in ~ 30 mL of DI water in a plastic petri dish. After storage at RT for 2 weeks, these were removed, briefly dried under a stream of air, and $\theta_{static,\ 2\ min}$ was measured in triplicate as noted above.

4.3.7. Water Uptake

Water uptake of PU films was measured using thermal gravimetric analysis (TGA; TA instruments Q50). PU films were prepared in triplicate and submerged in ~ 30 mL of

DI water in a plastic petri dish at RT, as noted above. After 2 weeks, films were removed, briefly dried under a stream of air, and blotted with a paper towel. An 11 ± 3 mg segment of the film was cut using a razor blade and placed in a platinum TGA pan. The mass change was monitored as the sample was heated from RT to 150 °C at a rate of 10 °C/min. The water loss was recorded as the peak in the mass loss derivative curve between RT and approximately 140 °C. Water content in weight percent of each film was determined by measuring the mass loss percent over the bounds of that peak. The reported water uptake values are the average and standard deviation of three identically prepared films with the same submersion time.

4.3.8. Mass Loss

Mass loss was monitored by measuring changes in PU film mass following 2 weeks of conditioning in DI water. Prior to PU solvent-casting, the mass of cleaned glass slides were recorded (W_0). Once PU films were cured, the difference versus W_0 was noted as the initial PU film mass (W_i). Films were submerged in ~ 30 mL of DI water in a plastic petri dish for 2 weeks at RT before being removed and dried overnight at 50 °C under reduced pressure (30 in. Hg). The mass of each slide was measured and the difference versus W_0 was recorded as the final PU film mass (W_f). Measurements were taken in triplicate on separate films and mass loss was calculated using **Equation 4-1**.

$$\textbf{Equation 4-1.}\ Mass\ loss\ (\%) = \left[\frac{(W_i - W_f)}{W_i}\right] x\ 100$$

4.3.9. Human Fibrinogen Adsorption Testing

HF adsorption onto PU films was assessed using an immunosorbent assay.[159] To a 96-well plate, 200 µL of blocking buffer (1% BSA in PBS) was added to half of the plate

and left overnight at 4 °C. PU samples were prepared with a 6 mm biopsy punch following removal from glass slides. The blocking buffer was removed and PU samples (3 per composition) were placed in designated wells. To these, 100 µL of HF in TBS-T20 (3 mg/mL) was added. To separate wells, 100 µL of each HF standard solution (0 – 500 ng/mL) were also added. The plate was incubated for 1 hr at 37 °C before HF solutions were removed and wells were rinsed three times with 200 µL of TBS-T20 buffer. Next, 300 µL of blocking buffer was incubated in each well for 30 min at 37 °C. The blocking buffer was removed, three rinses were performed, and 100 µL of mouse anti-fibrinogen HRP-conjugated monoclonal detection antibody (1:50,000 dilution in TBS-T20 with 1% BSA) was incubated in each well for 1 hr at 37 °C. The antibody solution was removed, wells were rinsed three times, and 100 µL TMB substrate solution was incubated in each well for 10 min at 37 °C. To stop the reaction, 100 µL of 2 M H_2SO_4 was added to each well and mixed at RT for 15 min. HF adsorption was quantified by transferring 150 µL of each solution to separate, unblocked wells, and absorbance was measured at 450 nm as well as 620 nm (wavelength correction) using a Tecan M200 Infinite Pro spectrophotometer.

4.3.10. Static Adhesion Testing – Human Blood

4.3.10.1. Sample preparation – silicone isolator wells

For each PU film sample, 4 silicone isolator wells were fabricated for blood testing. Square sections (10 mm x 10 mm x 2 mm) were cut from a silicone sheet using a razor blade and an 8 mm biopsy punch was used to form wells. To prevent leakage of

solutions, these were adhered to PU films with super glue and allowed to dry 24 hr prior to use.

4.3.10.2. Human blood evaluation

Whole human blood (citrated) was pre-treated with fluorescently labelled HF and incubated at RT for 10 min. CD41 antibodies were added immediately before use. 100 μL of pre-treated blood was added to 3 wells for each composition and PBS was also added to a 4th well. To this, 10 μL of a freshly prepared 100 mM $CaCl_2$ + 75 mM $MgCl_2$ solution was added to each well to re-calcify the blood (blood:re-calcification solution, 10:1 v/v). Samples were placed on a shaker plate (150 RPM) at RT for 10 min. Blood was removed and each well was gently rinsed 3 times with PBS. Fixative solution (200 μL; 2.5% GA in DI water) was added to each well and samples were placed on a shaker plate (150 RPM) at RT for 60 min. Wells were again rinsed with PBS prior to analysis with fluorescence microscopy. Human blood evaluations were completed for three individual donors.

4.3.10.3. Fluorescence microscopy

A Zeiss Axio Observer.Z1 microscope was used to measure platelet adhesion and HF adsorption. Following the human blood evaluation, fluorescence images were taken using an Axiocam 702 mono microscope camera with a LED illumination source (excitation/emission: 470/488 nm, 625/647 nm). Initial analyses were performed with the Zeiss Zen 2.3 Pro (blue edition) open application development software suite. For qualitative evaluations, fluorescence images were taken with a 10X objective (Zeiss EC Plan-Neofluar 10x/0.30 M27) and ImageJ software was used to generate an overlay. For quantitative evaluations, images were taken with a 5X objective (Zeiss N-Achroplan

5x/0.15 M27) and ImageJ software was used for fluorescence intensity calculations. Sample intensities were normalized to an unmodified PU control. The reported values and error represent an average and standard deviation of three wells, respectively.

4.3.11. Statistical Analysis

Statistical analysis was performed using two factor ANOVA and statistical significance was defined with a p-value < 0.05.

4.4. Results and Discussion

In this study, PEO-SAs were evaluated as SMAs in PU to determine their potential for enhanced hydrophilicity, protein resistance, and thromboresistance. PU films of varying PEO-SA SMA concentration (0 – 100 µmol/g) were fabricated with a solvent-casting method and are shown in **Figure 4-2**. The unmodified control (0 µmol/g) resulted in a highly transparent film, while PEO-SA modified PUs resulted in a higher opacity as concentration was increased. This indicates some degree of immiscibility of the SMA and the PU base material.

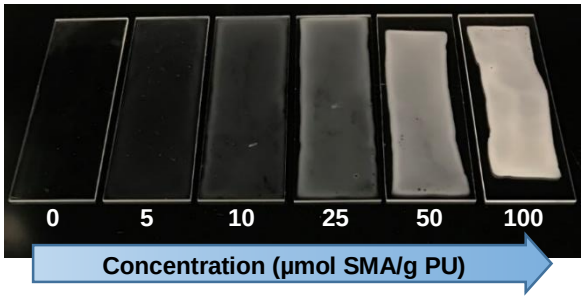

Figure 4-2. PEO-SA modified PU films after 1 week at RT following solvent casting.

Following fabrication, mechanical properties of PU films were evaluated to determine the potential impact of bulk-modification with PEO-SA SMAs (**Table 4-1**). The T_gs of the unmodified and modified PUs were first measured by DSC. Compared to the unmodified PU control (T_g ~ -41.9 °C), PEO-SA modified PUs at all concentrations had similar T_g values, ranging between -44.6 °C and -42.3 °C. This would indicate that the PU base material is not plasticized by the PEO-SA SMAs and is further supported by the tensile testing data summarized in **Table 4-1**. The unmodified PU control had E, TS, and %ε values of 24.1 kPa, 55.5 MPa, and 621%, respectively. Similarly, PEO-SA modified PUs had E, TS, and %ε values of 25.3 kPa (average value, 1.2 kPa increase), 56.5 MPa (average value, 1.0 MPa increase), and 634% (average value, 13% increase), respectively. Notably, these results show that changes in mechanical properties are minimal for PEO-SA modified PUs, even at higher SMA concentrations up to 17.1 wt%.

Table 4-1. T_g and mechanical properties of PEO-SA modified PUs.

[PEO-SA] (μmol/g)	wt%	T_g (°C)	E (kPa)	TS (MPa)	% Strain
0	0.0	-41.9 ± 1.1	24.1 ± 2.1	55.5 ± 2.8	621 ± 13
5	0.9	-44.3 ± 0.9	26.1 ± 1.4	52.0 ± 16.1	596 ± 46
10	1.7	-42.3 ± 1.4	29.2 ± 1.2	55.7 ± 17.5	596 ± 49
25	4.3	-43.2 ± 0.6	24.4 ± 1.7	65.0 ± 5.5	663 ± 9
50	8.6	-43.6 ± 0.4	23.7 ± 1.8	58.8 ± 4.4	667 ± 14
100	17.1	-44.6 ± 0.7	23.2 ± 3.0	51.0 ± 15.2	649 ± 52

As SMAs in PU, the efficacy of the PEO-SA depends on its ability to restructure to the biological interface and form a hydrophilic, PEO-rich surface for protein resistance. Following film fabrication, θ_{static} was measured to determine modified PUs initial capacity for water-driven surface restructuring (**Figure 4-3**). Initial θ_{static} values ($\theta_{static,\ initial}$) were compared with values 2 min after water drop placement ($\theta_{static,\ 2\ min}$) to assess the initial surface properties and the extent of rapid water-driven surface restructuring. The unmodified PU control was hydrophobic ($\theta_{static,\ initial}$ ~ 104 °), whereas PEO-SA modified PUs were initially hydrophilic, with samples at 5, 10, 25, 50, and 100 µmol/g showing $\theta_{static,\ initial}$ values of 78 °, 59 °, 48 °, 23 °, and 21 °, respectively. After 2 min, the unmodified PU control had a $\theta_{static,\ 2\ min}$ ~ 87°, while modified PUs at 5, 10, 25, 50, and 100 µmol/g had $\theta_{static,\ 2\ min}$ values of 71 °, 40 °, 22 °, 16 °, and 12 °, respectively. These results point to an expected concentration-dependent decrease in θ_{static} as PEO-SA concentration was increased. At concentrations ≥ 10 µmol/g, PEO-SA modified PUs exhibited statistically significant increases in water-driven surface restructuring to form hydrophilic surfaces. However, PEO-SA modified PUs at 10 µmol/g exhibited more variability than other compositions, indicative of a more heterogeneous phase separation. The lower $\theta_{static,\ initial}$ values of modified PUs versus unmodified PU indicates that PEO chains are present at the surface following fabrication. This is in contrast to modification of a silicone with this SMA, wherein $\theta_{static,\ initial}$ values of modified silicones were quite similar to that of the unmodified silicone but decreasing rapidly within seconds.[55] Thus, PEO chains of the PEO-SA (at concentrations ≥ 10 µmol/g) are initially present at the

modified PU surface, at greater levels with increased concentration, and increase in levels at the surface upon aqueous exposure.

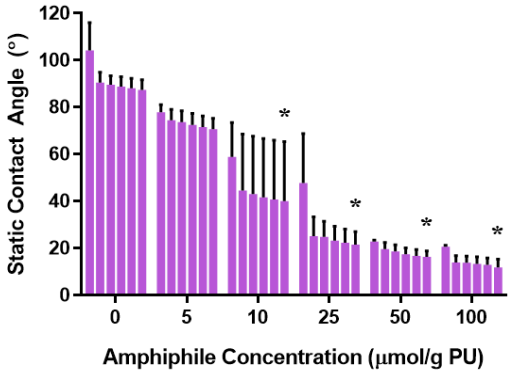

Figure 4-3. θ_{static} was measured over a 2 min period for PU modified with PEO-SA at various concentrations immediately after 1 week cure time. Bars shown represent time following drop placement: initial, 15 s, 30 s, 60 s, 90 s, and 120 s. Statistical analysis ($p < 0.05$): *sample v. unmodified at $t = 120$ s.

To ensure sustained protein- and thromboresistance, modified PUs must be able to retain their capacity for water-driven surface restructuring when conditioned in air and aqueous environments. Thus, films were conditioned at RT in air and $\theta_{static,\ 2\ min}$ values were obtained after 2 weeks (**Figure 4-4**).). Compared to the initial $\theta_{static,\ 2\ min}$ values, there was minimal change in $\theta_{static,\ 2\ min}$ for both the unmodified PU control (0.3 ° increase) and PEO-SA modified PU at 5 μmol/g (1.5 ° decrease) following conditioning. The modified PU at 10 μmol/g had an unusual, substantial decrease in $\theta_{static,\ 2\ min}$ (Δ = -20.3 °). We believe this could be due to the aforementioned heterogeneous immiscibility between the PEO-SA SMAs and the PU matrix. At concentrations ≥ 25 μmol/g, modified PUs had

slight increases in $\theta_{static,\ 2\ min}$ (7.9 ° increase, average value) after conditioning in air, but remained very hydrophilic. Thus, these results indicate that PEO-SA modified PUs at concentrations ≥ 10 µmol/g are able to retain their water-driven surface restructuring after conditioning in air and produce hydrophilic surfaces.

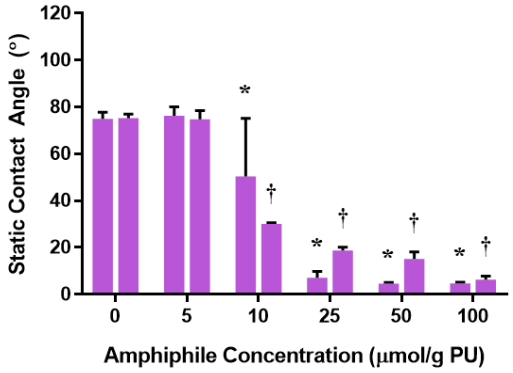

Figure 4-4. $\theta_{static,\ 2\ min}$ is shown for PEO-SA modified PUs at various concentrations after conditioning in air. Bars shown represent values initially (*left*) as well as following 2 weeks conditioning (*right*). Statistical analysis ($p < 0.05$): *sample v. unmodified (*initial*), †sample v. unmodified (*2 wk*).

A separate set of PU films were stored at RT in DI water for 2 weeks and $\theta_{static,\ 2\ min}$ was measured following conditioning (**Figure 4-5**). The unmodified PU control showed negligible changes in $\theta_{static,\ 2\ min}$ (0.4 ° decrease). In contrast, slight increases in $\theta_{static,\ 2\ min}$ values were observed for all PEO-SA modified PUs. Increases of 9.2 °, 10.9 °, 8.3 °, 17.1 °, and 8.1 ° for $\theta_{static,\ 2\ min}$ was observed for modified PUs at 5, 10, 25, 50, and 100 µmol/g, respectively, following conditioning in water. Again, the modified PU at 10 µmol/g exhibited a higher degree of variability that is attributed to a more heterogeneous

surface at this particular concentration. Overall, these small increases in $\theta_{static,\ 2\ min}$ values indicate only a minor loss in water-driven surface restructuring; however, the resulting $\theta_{static,\ 2\ min}$ values remain hydrophilic, particularly for PEO-SA modified PUs ≥ 25 µmol/g. Thus, these results demonstrate that PEO-SA modified PUs are able to retain enhanced surface hydrophilicity following 2 weeks of conditioning in DI water.

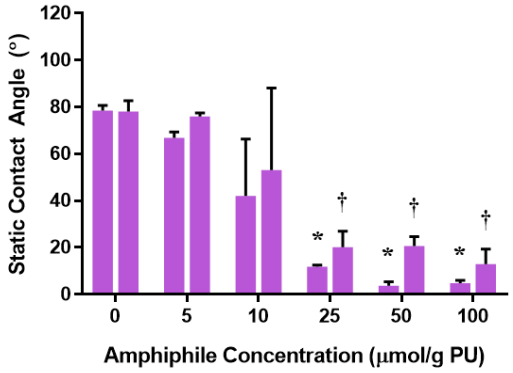

Figure 4-5. $\theta_{static,\ 2\ min}$ is shown for PEO-SA modified PU at various concentrations after conditioning in DI water. Bars shown represent values initially (*left*) as well as following 2 weeks conditioning (*right*). Statistical analysis ($p < 0.05$): *sample v. unmodified (*initial*), †sample v. unmodified (*2 wk*).

Additional PU films were conditioned at RT in DI water to evaluate their potential for water uptake. This was measured following 2 weeks of conditioning and is shown in **Figure 4-6**. The unmodified PU control had minimal water uptake (0.45 wt%) after conditioning. Similarly, PEO-SA modified PUs showed minimal amounts of water uptake at concentrations ≤ 25 µmol/g (0.43 wt%, average value). Statistically significant increases in water uptake are observed at PEO-SA concentrations of 50 (1.7 wt%) and 100

μmol/g (2.3 wt%). Although these amounts are notable compared to the unmodified PU control, overall water uptake was quite minimal for PEO-SA modified PUs at all concentrations and importantly did not lead to decreases in water-driven surface restructuring as shown in **Figure 4-5**.

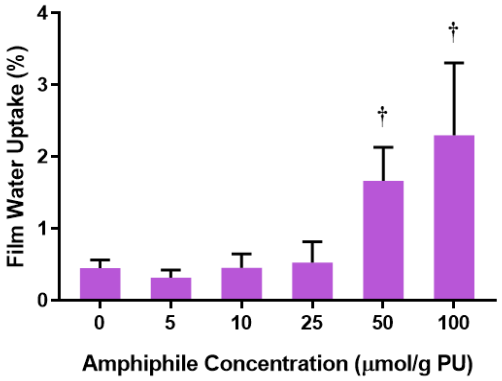

Figure 4-6. Film water uptake is shown as wt% water absorbed for PU modified with PEO-SA at various concentrations following 2 weeks of conditioning in DI water. Statistical analysis ($p < 0.05$): †sample v. unmodified.

To evaluate the potential for leaching of PEO-SA from PUs, changes in sample mass before and after 2 weeks of conditioning at RT in DI water were monitored. Mass loss was calculated using **Equation 4-1** and is shown in **Figure 4-7**. The unmodified PU control showed minimal mass loss (1.6 wt%) following conditioning. PEO-SA modified PUs at all concentrations did not display significant increases in mass loss (1.4 wt%, average value). These results indicate that SMA leaching via mass loss was minimal and did not compromise water-driven surface restructuring of PEO-SA in PU as evidenced in **Figure 4-5**.

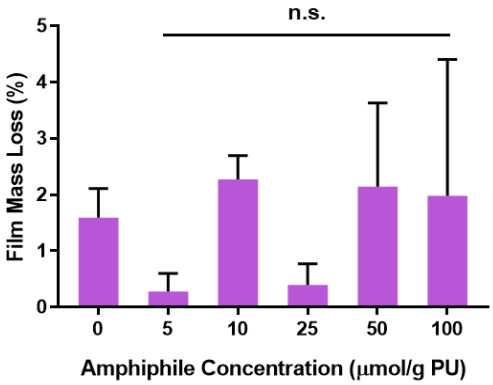

Figure 4-7. Film mass loss is shown for PU modified with PEO-SA at various concentrations following 2 weeks of conditioning in DI water.

To evaluate protein resistance of PEO-SA modified PUs, HF adsorption was measured using an immunosorbent assay (**Figure 4-8**). For the unmodified PU control, substantial amounts of HF adsorption were observed (60.9 ng/cm^2). Interestingly, PEO-SA modified PUs did not show significantly decreased HF adsorption at any concentration (54.7 ng/cm^2, average value). This result was unexpected based on the substantial increases in surface hydrophilicity (**Figure 4-3**). Thus, further assessment against a complex biological fluid such as blood was needed.

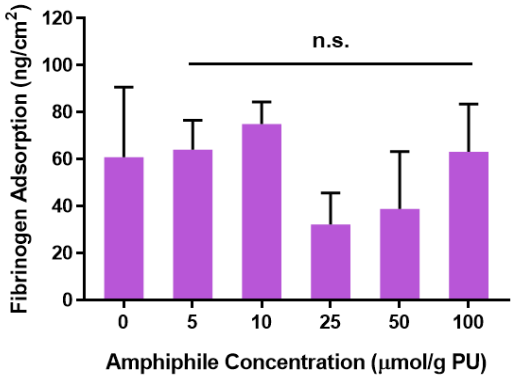

Figure 4-8. Protein adsorption from a simple HF solution is shown for PU modified with PEO-SA at various concentrations.

PEO-SA modified PU films were exposed to whole human blood and fluorescence imaging was used to observe platelet adhesion and HF adsorption, both qualitatively (**Figure 4-9a**) and quantitatively (**Figure 4-9b** and **4-9c**). Qualitative analysis of the fluorescence images indicated that the unmodified PU control and PEO-SA modified PU at 5 µmol/g showed significant levels of platelet adhesion (*green*) and HF adsorption (*red*). Modified PUs at 10 and 25 µmol/g showed minor platelet adhesion and HF adsorption, albeit markedly less than the unmodified PU control. At 50 and 100 µmol/g, no platelet adhesion or HF adsorption was observed. To quantitatively assess platelet adhesion and HF adsorption, images were analyzed for their fluorescence intensities at wavelengths of 488 nm and 647 nm, respectively. Assessments were done for three individual blood donors and values were normalized to the unmodified PU control (1.000). Consistent with the qualitative assessment, modified PUs at 5 µmol/g showed high fluorescence intensities for both platelet adhesion (~ 0.731) and HF adsorption (~ 0.906). At concentrations ≥ 10 µmol/g, significant decreases in fluorescence intensity values for platelet adhesion (~

0.039, average value) and HF adsorption (~ 0.031, average value) were observed. These results indicate that PEO-SA modified PUs, at concentrations as low as 10 µmol/g, are able to reduce platelet adhesion and HF adsorption from whole human blood under static conditions. This is in contrast to results against the simple HF solution and further highlights the need to evaluate materials with complex fluids such as whole human blood.

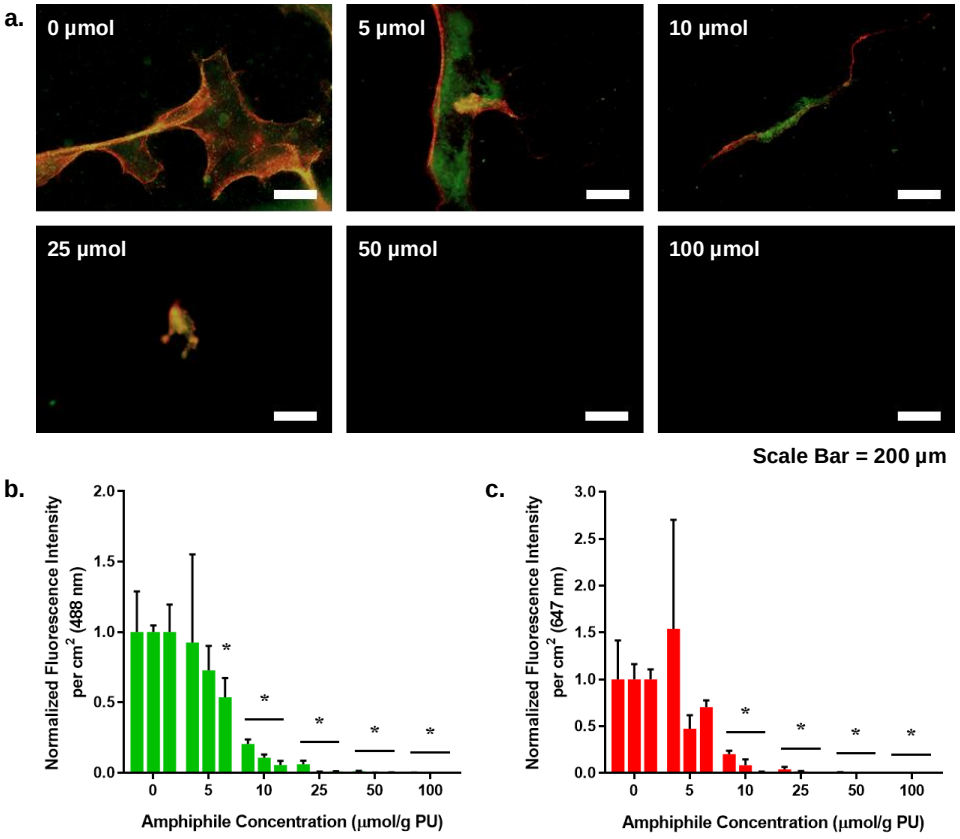

Figure 4-9. Platelet adhesion and HF adsorption following exposure to whole human blood under static conditions. (a) Representative fluorescence images are shown for PU modified with PEO-SA at various concentrations (0 – 100 µmol/g). Platelets and HF appear "green" and "red," respectively. Fluorescence intensity was quantified for (b) platelet adhesion as well as (c) HF adsorption and normalized to the unmodified PU control. Testing was done in triplicate and each bar represents an individual blood donor ($N = 3$). Statistical analysis ($p < 0.05$): *sample v. unmodified within a single blood donor.

4.5. Conclusions

The hydrophobicity of silicones and PUs makes them susceptible to protein adsorption and subsequent thrombosis. As common materials in blood-contacting devices, this can lead to device failure and adverse effects. Previously, the efficacy and stability of various PEO-SAs as SMAs in silicone was established in terms of enhanced surface hydrophilicity as well as protein resistance. However, PEO-SAs had yet to be evaluated in a PU matrix. Herein, a PEO-SA was investigated as a potential SMA in a PU and was incorporated at various concentrations (0, 5, 10, 25, 50, and 100 μmol/g), corresponding to 0, 0.9, 1.7, 4.3, 8.6, and 17.1 wt% in PU, respectively. Mechanical testing of modified PUs at these concentrations (up to 17.1 wt%) did not indicate any plasticization, as demonstrated by their similar T_g, E, TS, and %ε values compared to those of the unmodified PU control. Based on contact angle analysis, PEO chains of the PEO-SA are initially present at the modified PU surface (at concentrations ≥ 10 μmol/g) at greater levels with increased concentration. After just two minutes of aqueous contact, surfaces become even more hydrophilic as more PEO chains rapidly migrate to the surface. The retention of hydrophilicity of the resulting modified PUs following conditioning in both air and water was evaluated. Those prepared at concentrations ≥ 25 μmol/g were able to maintain this high degree of hydrophilicity following 2 weeks of air- and aqueous-conditioning. As water uptake and SMA leaching could lead to reduced hydrophilicity and thromboresistance, these were also monitored following aqueous conditioning. Compared to the unmodified PU control, PEO-SA modified PUs exhibited minimal amounts of water uptake and mass loss at all concentrations. Finally, modified PUs thromboresistant

potential was assessed with static assays against a simple HF solution and whole human blood. Assessments using a simple HF solution indicated that modified PUs did not show marked reduction in protein adsorption at any concentration. However, against whole human blood, modified PUs exhibited substantial reduction in HF adsorption and platelet adhesion at concentrations $\geq$ 10 μmol/g. These results emphasize the importance of adhesion assessments against complex biological fluids as opposed to simple protein solutions. Overall, this study demonstrates the versatility of PEO-SAs as effective SMAs in PU for enhanced and sustained surface hydrophilicity as well as resistance to protein adsorption and platelet adhesion for thromboresistance.

CHAPTER V

CONCLUSIONS

5.1. Conclusions

Polymeric matrices such as silicones and polyurethanes (PUs) are used extensively in blood-contacting medical devices for their favorable properties such as non-toxicity, durability, and mechanical properties. Unfortunately, their hydrophobicity renders them susceptible to thrombosis, which can reduce the safety and lifetime of the device. Antithrombotics are administered to address this, but also introduce bleeding risks, increased costs, and often limited efficacy. Alternatively, a materials-centered approach on enhancing surface hydrophilicity could potentially reduce thrombosis without the use of antithrombotics. There have been several reports of the bulk-modification of polymeric matrices with poly(ethylene oxide) (PEO)-based surface-modifying additives (SMAs) to increase hydrophilicity. Our group has also reported silicone modification with a PEO-silane amphiphile [PEO-SA; α-$(EtO)_3$-Si-$(CH_2)_2$-$ODMS_m$-*block*-PEO_n-CH_3] SMA. Previous studies investigated the efficacy of PEO-SAs with varying concentration (0 – 100 μmol per 1 g silicone), oligo(dimethyl siloxane) (ODMS) length (m = 0 – 30), and PEO length (n = 3 – 16). Modified silicones at 10 μmol/g or greater, showed enhanced surface hydrophilicity and protein resistance. A PEO length of n = 8 was found to be optimal, while ODMS length did not impact the minimum effective concentration.

In this work, PEO-SAs were further investigated as SMAs in both silicone and PU matrices for enhanced thromboresistance. Briefly, Chapters II and III, explored the

tunability of the PEO-SA structure to determine the impact on efficacy and stability. Several variants were prepared, including those with (*XL diblock*) and those without (*Diblock*) the crosslinkable triethoxysilane (TEOS) group. Additionally, the ODMS tether length was varied (m = 13 or 30) to determine potential impacts on modified silicone stability, while the PEO segment was kept constant, as previous studies demonstrated their efficacy at n = 8. In Chapter IV, the PEO-SA was incorporated in a PU to demonstrate not only their efficacy and stability, but also their versatility as SMAs in polymeric matrices. These studies illustrate the potential of PEO-SAs for the bulk-modification of materials in blood-contacting devices to enhance hydrophilicity and thromboresistance.

The goal of Chapter II was to investigate the efficacy and stability of PEO-SAs in a condensation-cure silicone, particularly with respect to the necessity of the crosslinkable TEOS group and the impact of the ODMS tether length. Along with a non-amphiphilic PEO-control, four PEO-SAs (*XL diblock, m = 13*; *XL diblock, m = 30*; *Diblock, m = 13*; *Diblock, m = 30*) were synthesized and incorporated as SMAs in a condensation-cure silicone at various concentrations (0 – 100 μmol/g). Efficacy was assessed in terms of surface hydrophilicity and protein resistance both before and after aqueous conditioning. To monitor stability of the modified silicones, water uptake and leaching via mass loss were also measured following aqueous conditioning. All amphiphilic PEO-SA SMAs resulted in enhanced surface hydrophilicity and resistance to HF adsorption at concentrations $\geq$ 25 μmol/g. These properties were sustained following 2 weeks of air and aqueous conditioning. Regarding stability, PEO-SA modified silicones had minimal water uptake and mass loss at all concentrations, relative to the unmodified silicone control.

Overall, this study confirmed the efficacy and stability of PEO-SA modified silicones, even in the absence of the SMA crosslinkable TEOS group. In particular, it was determined that a longer m = 30 ODMS tether could sufficiently anchor and retain the SMA in silicones. Furthermore, use of *Diblock* SMAs reduces concerns of the TEOS group hydrolyzing *in vivo*, as well as simplifying the synthesis by one step.

In Chapter III, both the *XL diblock, m = 13* and *Diblock, m = 30* PEO-SA SMAs were further evaluated for their thromboresistance against whole human blood. While the initial assessment against a simple HF solution demonstrated their potential, evaluation with more complex fluids such as whole blood would better mimic the biological environment. Thus, a condensation-cure silicone was modified with *XL diblock, m = 13* and *Diblock, m = 30* SMAs at various concentrations (0 – 50 μmol/g). Modified silicones were sequentially prepared in well plates, exposed to blood under static conditions, and protein adsorption as well as platelet adhesion were quantified with fluorescence microscopy. The *XL diblock, m = 13* and *Diblock, m = 30* SMAs effectively reduced HF adsorption and platelet adhesion at concentrations ≥ 10 μmol/g. Additionally, dynamic whole blood assessments were done using a Chandler Loop construct. For these, modified silicones were prepared as coatings on the inner lumen of PEVA tubing. Following circulation with blood, sections of tubing were evaluated for surface protein adsorption and thrombus formation. Significantly reduced protein adsorption and thrombus formation was observed for silicones modified with *XL diblock, m = 13* and *Diblock, m = 30* SMAs at concentrations as low as 5 μmol/g and 10 μmol/g, respectively. These results

demonstrated the thromboresistance of PEO-SA modified silicones against whole human blood and established their potential for use in blood-contacting devices.

Lastly, Chapter IV investigated the efficacy and stability of PEO-SAs as SMAs in a PU matrix. The *XL diblock, m = 13* PEO-SA was incorporated at various concentrations (0 – 100 μmol/g) to determine the minimum effective concentration. Similar to Chapter II, this study focused on monitoring surface hydrophilicity, water uptake, and mass loss following air and aqueous conditioning. Additionally, thromboresistance was assessed via static assays against both a simple HF solution and whole human blood. PEO-SA modified PUs showed enhanced surface hydrophilicity at concentrations as lows as 10 μmol/g. After 2 weeks conditioning in air or water, modified PUs maintained their water-driven surface restructuring at 10 μmol/g and 25 μmol/g, respectively. Notably, plasticization was not observed at any concentration, as evidenced by modified PUs minimal changes in glass transition temperature (T_g), modulus, tensile strength, and percent strain at break. Compared to the unmodified PU control, water uptake and mass loss were also minimal for all PEO-SA modified PUs. Finally, while testing against a simple HF solution was inconclusive, assessments against whole human blood showed significantly reduced platelet adhesion and HF adsorption at concentrations ≥ 10 μmol/g. Overall, these results for the modification of a PU demonstrated the versatility and efficacy of PEO-SAs as SMAs in achieving sustained hydrophilicity and thromboresistance.

5.2. Future Directions

5.2.1. PEO-SA Modified Silicones

Combined with previous studies, this work aimed to establish the potential of PEO-SAs as SMAs in silicone for increased surface hydrophilicity and thromboresistance. Moving forward, these PEO-SA modified silicones could be fabricated into catheters to demonstrate a proof-of-concept. Once fabricated, additional dynamic blood flow testing could be done, prior to evaluation in a pre-clinical porcine animal model. Silicone catheters are generally formed via extrusion methods. Currently, we are collaborating with Prof. Duncan Maitland and coworkers to test the feasibility of extruding PEO-SA modified silicones into a hollow tube as an early model of a catheter. We followed a typical extrusion process, where a two-roll mill is used to combine an addition cure silicone (two-components, part A & B; Wacker Elastosil R plus 4305/60 S) with the liquid PEO-SA SMA (**Figure 5-1**). Once incorporated, the modified silicone could be fed into an extruder to fabricate the device. To date, we have successfully mixed and extruded a simple tube with a single lumen using a PEO-SA modified silicone. In future work, in addition to dynamic blood tests, extruded catheters could be subjected to bacterial adhesion tests against species such as *S. epidermidis*, *S. aureus*, and *P. aeruginosa*, as biofilm formation can lead to device-related infection that compromises patient safety.[192,193] Ultimately, such studies would support the feasibility and efficacy of producing a hemodialysis catheter capable of resisting protein adsorption, thrombosis, as well as infection.

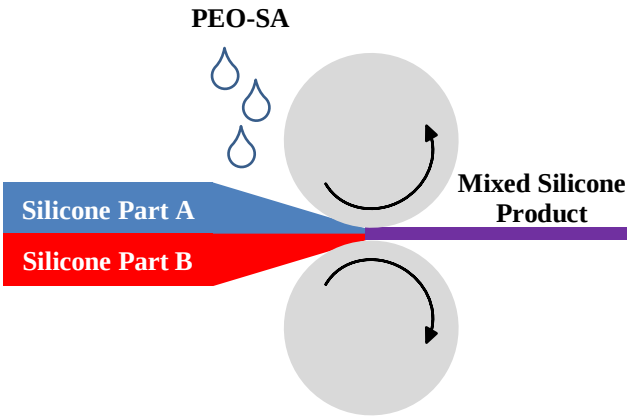

Figure 5-1. Depiction of two-roll mixing process where the PEO-SA is incorporated into silicone. The mixed silicone product can then be extruded into a device.

5.2.2. Amphiphilic SMA Structure Variants

In addition to establishing the effectiveness of PEO-SAs as SMAs in a condensation-cure silicone, these studies demonstrated the potential impacts of SMA structure optimization. We observed how minor changes to the SMA structure impacted their efficacy and stability in silicone. Therefore, future work could include further tuning of the SMA structure, such as with the replacement of the hydrophilic PEO segment. Notably, there have been recent observations of hypersensitivity reactions in patients that are exposed to PEO-containing pharmaceuticals.[194-196] Some reports have indicated this could be potentially due to nearly 25% of the population having antibodies specific to PEO,[57,197] largely due to its near-ubiquitous use. Though there is yet to be a complete understanding of the prevalence and effects of PEO antibodies,[198,199] continued and future use of PEO is potentially concerning. Some potential replacements for the PEO segment include poly(2-oxazoline)s (POx) and poly(*N*-vinyl-2-pyrrolidone) (PVP).

As introduced in Chapter I, the PEO segment could potentially be replaced by hydrophilic variants of POx such as poly(2-methyl-2-oxazoline) (PMeOx) and poly(2-ethyl-2-oxazoline) (PEtOx).[68] These POx materials were shown to be effective for increased surface hydrophilicity and protein resistance, in addition to enhanced oxidative stability compared to PEO.[68-71] Some efforts were made to prepare POx-based SMAs and incorporate them into silicones. In a collaboration with Prof. Richard Hoogenboom and co-workers (Ghent University), the initial synthesis of a PEtOx-silane amphiphile (PEtOx-SA) was successful and is depicted in **Figure 5-2a**. These were to be evaluated similarly as SMAs in a condensation-cure silicone for water-driven surface restructuring, protein resistance, and thromboresistance. However, once these were incorporated as SMAs in silicone, they failed to appreciably restructure and form a hydrophilic surface (**Figure 5-2b**). Poor restructuring could have been due to the highly hydrophilic POx segment reducing overall SMA miscibility in silicone. Additionally, the large phenoxide group could have sterically hindered SMA migration through the silicone bulk.

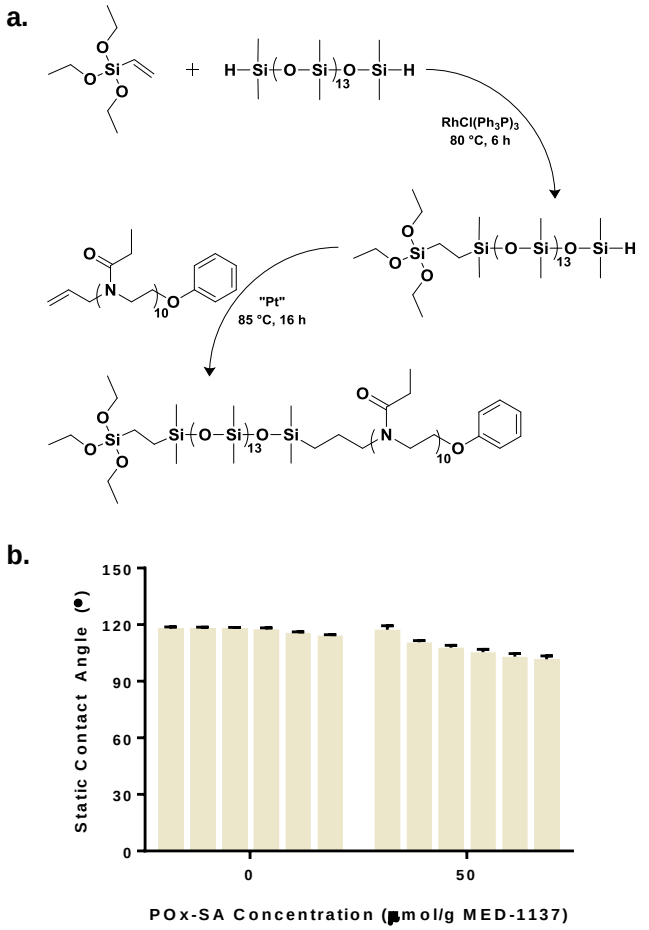

Figure 5-2. (a) Synthetic scheme for the PEtOx-SA. (b) Static contact angle was measured for PEtOx-SA modified silicones at 0 and 50 µmol/g. Bars shown represent time following drop placement: initial, 15 s, 30 s, 60 s, 120 s, and 180 s.

PVP could also serves as a potential replacement for the hydrophilic PEO segment. PVP is commonly blended in polymeric matrices to increase hydrophilicity.[200] When paired with its low cost, high lubricity and excellent hemocompatibility, these enable its use in blood-contacting applications.[201-203] However, various studies have demonstrated PVP blends are susceptible to leaching, resulting in reduced surface hydrophilicity.[204,205] Therefore, future work could look to leverage the properties of PVP, but instead as the

hydrophilic segment of an amphiphilic siloxane-containing SMA. When used to bulk-modify silicones, a PVP-silane amphiphile is hypothesized to similarly exhibit water-driven restructuring to form a hydrophilic, thromboresistant surface. As evidenced by our prior work, the siloxane tether can potentially serve as a physical anchor to enhance stability and minimize leaching of PVP. Moving forward, a PVP macromer could be synthesized using an atom transfer radical polymerization (ATRP) reaction, as proposed in **Figure 5-3**. Following their complete synthesis, PVP-silane amphiphiles could be incorporated as SMAs in silicone and tested for their capacity to increase hydrophilicity and thromboresistance. Additionally, stability of modified silicones should be investigated in terms of potential for leaching and water uptake.

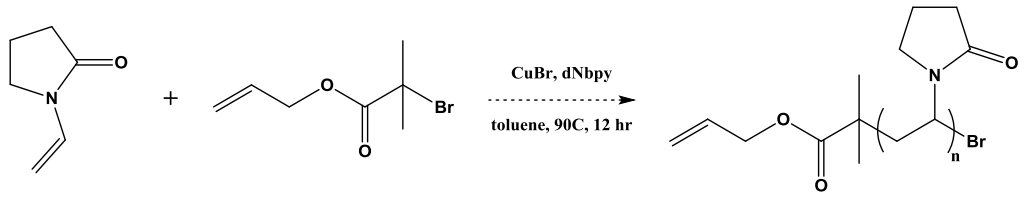

Figure 5-3. Proposed synthetic scheme for a PVP macromer.

Additional changes to SMA structure could include utilization of a PU-containing hydrophobic tether in the PEO-based SMA. As introduced in Chapter IV, PUs are also commonly used in blood-contacting devices such as hemodialysis catheters. This initial study helped demonstrate the versatility and efficacy of PEO-SAs as SMAs in PU. However, there were also indications of poor miscibility between the siloxane-containing PEO-SA and the non-silicone, PU matrix. Therefore, the development of a more

compatible, PU-containing hydrophobic tether could potentially increase SMA miscibility in PU. It is hypothesized that the incorporation of diblock PEO-PU amphiphiles as SMAs in PU would potentially lead to enhanced efficacy as well as stability. Similar evaluations should be done, including capacity for water-driven surface restructuring, protein resistance, thromboresistance, water uptake, and mass loss via leaching.

Outside of blood-contacting devices, there are other medical applications that call for antifouling materials. Implantable devices such as intraocular lens (IOL) are necessary to restore vision when patients present with cataracts or myopia.[206] Unfortunately, IOLs are generally composed of silicone- or acrylic-based materials (**Figure 5-4**), making them susceptible to fouling via lens epithelial cell on-growth and proliferation.[207,208] Otherwise known as secondary cataract formation, these are typically treated via laser capsulotomy. However, this is often expensive, increases risk to the patient, and can potentially damage the IOL that could ultimately lead to a second surgery.[209] Thus, a material with enhanced fouling resistance is necessary for IOLs and could potentially be achieved via the incorporation of amphiphilic PEO-SA SMAs. Initial work could focus on incorporation of the ODMS-containing PEO-SAs as SMAs in the silicone-based IOL material for enhanced hydrophilicity and fouling resistance. Further, a phenyl-containing siloxane tether could also be synthesized and utilized for PEO-SAs, to increase miscibility as well as ensure retention of optical properties following SMA modification. Similar studies could be conducted in acrylic-based systems, and future work could also focus on developing a chemically compatible hydrophobic segment for increased SMA miscibility.

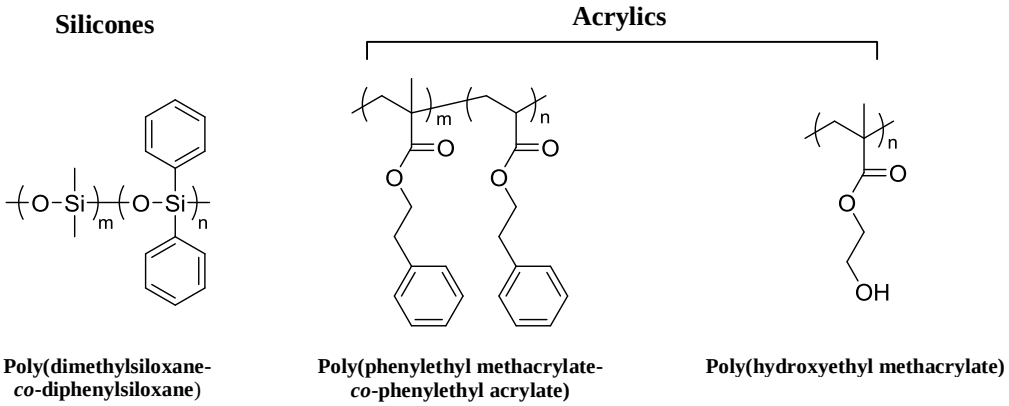

Figure 5-4. Chemical structures of common IOL materials are depicted. Shown from left to right are: silicones, hydrophobic acrylics, and hydrophilic acrylics.

REFERENCES

1. Baddour L.M., Bettmann M.A., Bolger A.F., Epstein A.E., Ferrieri P., et al. Nonvalvular cardiovascular device–related infections. *Circulation.* **2003**, *108* (16), 2015-2031.

2. Hanson S.R., Tucker E.I. Blood coagulation and blood–materials interactions In: Ratner BD, Hoffman AS, Schoen FJ, Lemons JE, eds. *Biomaterials Science.* 3rd ed. Oxford: Academic Press; **2013**:551-557.

3. Lloyd D.A., Shanbhogue L.K.R., Doherty P.J., Sunderland D., Hart C.A., et al. Does the fibrin coat around a central venous catheter influence catheter-related sepsis? *J Pediatr Surg.* **1993**, *28* (3), 345-349.

4. Pereda D., Conte J.V. Left ventricular assist device driveline infections. *Cardiol Clin.* **2011**, *29* (4), 515-527.

5. Raad I., Luna M., Khalil S.M., Costerton J.W., Lam C., et al. The relationship between the thrombotic and infectious complications of central venous catheters. *J Am Med Assoc.* **1994**, *271* (13), 1014-1016.

6. Rose E.A., Gelijns A.C., Moskowitz A.J., Heitjan D.F., Stevenson L.W., et al. Long-term use of a left ventricular assist device for end-stage heart failure. *N Engl J Med.* **2001**, *345* (20), 1435-1443.

7. Jaffer I.H., Fredenburgh J.C., Hirsh J., Weitz J.I. Medical device-induced thrombosis: What causes it and how can we prevent it? *J Thromb Haemost.* **2015**, *13* (S1), S72-S81.

8. Werner C., Maitz M.F., Sperling C. Current strategies towards hemocompatible coatings. *J Mater Chem.* **2007**, *17* (32), 3376-3384.

9. Avula M.N., Rao A.N., McGill L.D., Grainger D.W., Solzbacher F. Modulation of the foreign body response to implanted sensor models through device-based delivery of the tyrosine kinase inhibitor, masitinib. *Biomaterials.* **2013**, *34* (38), 9737-9746.

10. Gifford R., Kehoe J.J., Barnes S.L., Kornilayev B.A., Alterman M.A., et al. Protein interactions with subcutaneously implanted biosensors. *Biomaterials.* **2006**, *27* (12), 2587-2598.

11. Klueh U., Frailey J.T., Qiao Y., Antar O., Kreutzer D.L. Cell based metabolic barriers to glucose diffusion: Macrophages and continuous glucose monitoring. *Biomaterials.* **2014**, *35* (10), 3145-3153.

12. Ratner B.D., Bryant S.J. Biomaterials: Where we have been and where we are going. *Annu Rev Biomed Eng.* **2004**, *6* (1), 41-75.

13. Brown J.M. Polyurethane and silicone: Myths and misconceptions. *J Intraven Nurs.* **1995**, *18* (3), 120-123.

14. Tal M.G., Ni N. Selecting optimal hemodialysis catheters: Material, design, advanced features, and preferences. *Tech Vasc Interv Radiol.* **2008**, *11* (3), 186-191.

15. Banerjee I., Pangule R.C., Kane R.S. Antifouling coatings: recent developments in the design of surfaces that prevent fouling by proteins, bacteria, and marine organisms. *Adv Mater.* **2011**, *23* (6), 690-718.

16. Liu X., Yuan L., Li D., Tang Z., Wang Y., et al. Blood compatible materials: State of the art. *J Mater Chem B.* **2014**, *2* (35), 5718-5738.

17. Magin C.M., Cooper S.P., Brennan A.B. Non-toxic antifouling strategies. *Mater Today.* **2010**, *13* (4), 36-44.

18. Worz A., Berchtold B., Moosmann K., Prucker O., Ruhe J. Protein-resistant polymer surfaces. *J Mater Chem.* **2012**, *22* (37), 19547-19561.

19. Yu Q., Zhang Y., Wang H., Brash J., Chen H. Anti-fouling bioactive surfaces. *Acta Biomater.* **2011**, *7* (4), 1550-1557.

20. Ratner B.D., Hoffman A.S. Physicochemical surface modification of materials used in medicine. In: Ratner BD, Hoffman AS, Schoen FJ, Lemons JE, eds. *Biomaterials Science.* 3rd ed. Oxford: Academic Press; **2013**:259-276.

21. Nakanishi K., Sakiyama T., Imamura K. On the adsorption of proteins on solid surfaces, a common but very complicated phenomenon. *J Biosci Bioeng.* **2001**, *91* (3), 233-244.

22. Gong P., Grainger D.W. Nonfouling surfaces: A review of principles and applications for microarray capture assay designs. *Methods Mol Biol.* **2007**, *381*, 59-92.

23. Jo S., Park K. Surface modification using silanated poly(ethylene glycol)s. *Biomaterials.* **2000**, *21* (6), 605-616.

24. Prime K., Whitesides G. Self-assembled organic monolayers: Model systems for studying adsorption of proteins at surfaces. *Science.* **1991**, *252* (5009), 1164-1167.

25. Prime K.L., Whitesides G.M. Adsorption of proteins onto surfaces containing end-attached oligo(ethylene oxide): A model system using self-assembled monolayers. *J Am Chem Soc.* **1993**, *115* (23), 10714-10721.

26. Sofia S.J., Premnath V., Merrill E.W. Poly(ethylene oxide) grafted to silicon surfaces: Grafting density and protein adsorption. *Macromolecules.* **1998**, *31* (15), 5059-5070.

27. Sefton M.V., Gemmell C.H., Gorbet M.B. Nonthrombogenic treatments and strategies. In: Ratner BD, Hoffman AS, Schoen FJ, Lemons JE, eds. *Biomaterials Science.* 3rd ed. Oxford: Academic Press; **2013**:1488-1509.

28. van Oss C.J. The primary interactions. In: *Interfacial Forces in Aqueous Media.* New York: Marcel Dekker; **1994**:231-236.

29. Jeon S.I., Lee J.H., Andrade J.D., De Gennes P.G. Protein-surface interactions in the presence of polyethylene oxide. *J Colloid Interface Sci.* **1991**, *142* (1), 149-158.

30. Chen H., Brook M.A., Sheardown H. Silicone elastomers for reduced protein adsorption. *Biomaterials.* **2004**, *25* (12), 2273-2282.

31. Green R.J., Davies M.C., Roberts C.J., Tendler S.J.B. A surface plasmon resonance study of albumin adsorption to PEO–PPO–PEO triblock copolymers. *J Biomed Mater Res.* **1998**, *42* (2), 165-171.

32. Anderson J.M., Kottke-Marchant K. Platelet interactions with biomaterials and artificial devices. In: *Anonymous CRC Reviews in Biocompatibility.* Boca Raton: CRC; **1987**:111-204.

33. Salzman E.W., Lindon J., Brier D., Merrill E.W. Surface-induced platelet adhesion, aggregation, and release. *Ann N Y Acad Sci.* **1977**, *283* (1), 114-126.

34. Chang T.M.S. Platelet-surface interaction: Effect of albumin coating or heparin complexing on thrombogenic surfaces. *Can J Physiol Pharmacol.* **1974**, *52* (2), 275-285.

35. Andrade J.D., Hlady V. Protein adsorption and materials biocompatibility: A tutorial review and suggested hypotheses. In: *Biopolymers/Non-Exclusion HPLC.* Berlin, Heidelberg: Springer Berlin Heidelberg; **1986**:1-63.

36. Matsuda T., Takano H., Hayashi K., Taenaka Y., Takaichi S., et al. The blood interface with segmented polyurethanes: "Multilayered protein passivation mechanism". *ASAIO J.* **1984**, *30* (1), 353-358.

37. Chen H., Zhang Z., Chen Y., Brook M.A., Sheardown H. Protein repellant silicone surfaces by covalent immobilization of poly(ethylene oxide). *Biomaterials.* **2005**, *26* (15), 2391-2399.

38. Malmsten M., Emoto K., Van Alstine J.M. Effect of chain density on inhibition of protein adsorption by poly(ethylene glycol) based coatings. *J Colloid Interface Sci.* **1998**, *202* (2), 507-517.

39. Murthy R., Shell C.E., Grunlan M.A. The influence of poly(ethylene oxide) grafting via siloxane tethers on protein adsorption. *Biomaterials.* **2009**, *30* (13), 2433-2439.

40. Xu L.-C., Siedlecki C.A. Protein adsorption, platelet adhesion, and bacterial adhesion to polyethylene-glycol-textured polyurethane biomaterial surfaces. *J Biomed Mater Res, Part B.* **2017**, *105* (3), 668-678.

41. Norde W., Gage D. Interaction of bovine serum albumin and human blood plasma with PEO-tethered surfaces: Influence of PEO chain length, grafting density, and temperature. *Langmuir.* **2004**, *20* (10), 4162-4167.

42. Rufin M.A., Grunlan M.A. Surface-grafted polymer coatings. In: Wu L, Baghdachi J, eds. *Functional Polymer Coatings.* New Jersey: John Wiley & Sons, Inc; **2015**:218-238.

43. Chang Y., Shih Y.-J., Ko C.-Y., Jhong J.-F., Liu Y.-L., et al. Hemocompatibility of poly(vinylidene fluoride) membrane grafted with network-like and brush-like antifouling layer controlled via plasma-induced surface PEGylation. *Langmuir.* **2011**, *27* (9), 5445-5455.

44. Zamfir M., Rodriguez-Emmenegger C., Bauer S., Barner L., Rosenhahn A., et al. Controlled growth of protein resistant PHEMA brushes via S-RAFT polymerization. *J Mater Chem B.* **2013**, *1* (44), 6027-6034.

45. Yuan B., Chen Q., Ding W.-Q., Liu P.-S., Wu S.-S., et al. Copolymer coatings consisting of 2-methacryloyloxyethyl phosphorylcholine and 3-methacryloxypropyl trimethoxysilane via ATRP to improve cellulose biocompatibility. *ACS Appl Mater Inter.* **2012**, *4* (8), 4031-4039.

46. Chen W.-L., Cordero R., Tran H., Ober C.K. 50th anniversary perspective: Polymer brushes: Novel surfaces for future materials. *Macromolecules.* **2017**, *50* (11), 4089-4113.

47. Olivier A., Meyer F., Raquez J.-M., Damman P., Dubois P. Surface-initiated controlled polymerization as a convenient method for designing functional polymer brushes: From self-assembled monolayers to patterned surfaces. *Prog Polym Sci.* **2012**, *37* (1), 157-181.

48. Park J.H., Bae Y.H. Hydrogels based on poly(ethylene oxide) and poly(tetramethylene oxide) or poly(dimethyl siloxane): Synthesis, characterization, in vitro protein adsorption and platelet adhesion. *Biomaterials.* **2002**, *23* (8), 1797-1808.

49. Ratner B.D., Hoffman A.S., Hanson S.R., Harker L.A., Whiffen J.D. Blood-compatibility-water-content relationships for radiation-grafted hydrogels. *J Polym Sci, Polym Symp.* **1979**, *66* (1), 363-375.

50. Seifert L.M., Greer R.T. Evaluation of in vivo adsorption of blood elements onto hydrogel-coated silicone rubber by scanning electron microscopy and fourier transform infrared spectroscopy. *J Biomed Mater Res.* **1985**, *19* (9), 1043-1071.

51. Decher G. Fuzzy nanoassemblies: Toward layered polymeric multicomposites. *Science.* **1997**, *277* (5330), 1232-1237.

52. Lu Y., Sarshar M.A., Du K., Chou T., Choi C.-H., et al. Large-amplitude, reversible, pH-triggered wetting transitions enabled by layer-by-layer films. *ACS Appl Mater Inter.* **2013**, *5* (23), 12617-12623.

53. Richardson J.J., Björnmalm M., Caruso F. Technology-driven layer-by-layer assembly of nanofilms. *Science.* **2015**, *348* (6233), 411-422.

54. Hawkins M.L., Rufin M.A., Raymond J.E., Grunlan M.A. Direct observation of the nanocomplex surface reorganization of antifouling silicones containing a highly mobile PEO-silane amphiphile. *J Mater Chem B.* **2014**, *2* (34), 5689-5697.

55. Rufin M.A., Gruetzner J.A., Hurley M.J., Hawkins M.L., Raymond E.S., et al. Enhancing the protein resistance of silicone via surface-restructuring PEO-silane amphiphiles with variable PEO length. *J Mater Chem B.* **2015**, *3* (14), 2816-2825.

56. Tanzi M.C. Bioactive technologies for hemocompatibility. *Expert Rev Med Devices.* **2005**, *2* (4), 473-492.

57. Garay R.P., El-Gewely R., Armstrong J.K., Garratty G., Richette P. Antibodies against polyethylene glycol in healthy subjects and in patients treated with PEG-conjugated agents. *Expert Opin Drug Delivery.* **2012**, *9* (11), 1319-1323.

58. Herold D.A., Keil K., Bruns D.E. Oxidation of polyethylene glycols by alcohol dehydrogenase. *Biochem Pharmacol.* **1989**, *38* (1), 73-76.

59. Hucknall A., Rangarajan S., Chilkoti A. In pursuit of zero: Polymer brushes that resist the adsorption of proteins. *Adv Mater.* **2009**, *21* (23), 2441-2446.

60. Browning M.B., Cereceres S.N., Luong P.T., Cosgriff-Hernandez E.M. Determination of the in vivo degradation mechanism of PEGDA hydrogels. *J Biomed Mater Res, Part A.* **2014**, *102* (12), 4244-4251.

61. Utrata-Wesołek A., Wałach W., Anioł J., Sieroń A.L., Dworak A. Multiple and terminal grafting of linear polyglycidol for surfaces of reduced protein adsorption. *Polymer.* **2016**, *97*, 44-54.

62. Weinhart M., Becherer T., Schnurbusch N., Schwibbert K., Kunte H.-J., et al. Linear and hyperbranched polyglycerol derivatives as excellent bioinert glass coating materials. *Adv Eng Mater.* **2011**, *13* (12), B501-B510.

63. Weinhart M., Grunwald I., Wyszogrodzka M., Gaetjen L., Hartwig A., et al. Linear poly(methyl glycerol) and linear polyglycerol as potent protein and cell resistant alternatives to poly(ethylene glycol). *Chem - Asian J.* **2010**, *5* (9), 1992-2000.

64. Kainthan R.K., Zou Y., Chiao M., Kizhakkedathu J.N. Self-assembled monothiol-terminated hyperbranched polyglycerols on a gold surface: A comparative study on the structure, morphology, and protein adsorption characteristics with linear poly(ethylene glycol)s. *Langmuir.* **2008**, *24* (9), 4907-4916.

65. Lukowiak M.C., Wettmarshausen S., Hidde G., Landsberger P., Boenke V., et al. Polyglycerol coated polypropylene surfaces for protein and bacteria resistance. *Polym Chem.* **2015**, *6* (8), 1350-1359.

66. Wyszogrodzka M., Haag R. Synthesis and characterization of glycerol dendrons, self-assembled monolayers on gold: A detailed study of their protein resistance. *Biomacromolecules.* **2009**, *10* (5), 1043-1054.

67. Siegers C., Biesalski M., Haag R. Self-assembled monolayers of dendritic polyglycerol derivatives on gold that resist the adsorption of proteins. *Chem - Eur J.* **2004**, *10* (11), 2831-2838.

68. Knop K., Hoogenboom R., Fischer D., Schubert U.S. Poly(ethylene glycol) in drug delivery: Pros and cons as well as potential alternatives. *Angew Chem, Int Ed.* **2010**, *49* (36), 6288-6308.

69. Zalipsky S., Hansen C.B., Oaks J.M., Allen T.M. Evaluation of blood clearance rates and biodistribution of poly(2-oxazoline)-grafted liposomes. *J Pharm Sci.* **1996**, *85* (2), 133-137.

70. Bai L., Tan L., Chen L., Liu S., Wang Y. Preparation and characterizations of poly(2-methyl-2-oxazoline) based antifouling coating by thermally induced immobilization. *J Mater Chem B.* **2014**, *2* (44), 7785-7794.

71. Konradi R., Acikgoz C., Textor M. Polyoxazolines for nonfouling surface coatings — A direct comparison to the gold standard PEG. *Macromol Rapid Commun.* **2012**, *33* (19), 1663-1676.

72. Zhu Z., Li X. Silicone hydrogels based on a novel amphiphilic poly(2-methyl-2-oxazoline)-b-poly(dimethyl siloxane) copolymer. *J Appl Polym Sci.* **2014**, *131* (3), n/a-n/a.

73. Zhang Z., Chen S., Chang Y., Jiang S. Surface grafted sulfobetaine polymers via atom transfer radical polymerization as superlow fouling coatings. *J Phys Chem B.* **2006**, *110* (22), 10799-10804.

74. Chou Y.-N., Wen T.-C., Chang Y. Zwitterionic surface grafting of epoxylated sulfobetaine copolymers for the development of stealth biomaterial interfaces. *Acta Biomater.* **2016**, *40*, 78-91.

75. Jiang S., Cao Z. Ultralow-fouling, functionalizable, and hydrolyzable zwitterionic materials and their derivatives for biological applications. *Adv Mater.* **2010**, *22* (9), 920-932.

76. Vaisocherová H., Yang W., Zhang Z., Cao Z., Cheng G., et al. Ultralow fouling and functionalizable surface chemistry based on a zwitterionic polymer enabling sensitive and specific protein detection in undiluted blood plasma. *Anal Chem.* **2008**, *80* (20), 7894-7901.

77. Wang W., Lu Y., Luo M., Zhao Q., Wang Y., et al. Zwitterionic-polymer-functionalized poly(vinyl alcohol-co-ethylene) nanofiber membrane for resistance to the adsorption of bacteria and protein. *J Appl Polym Sci.* **2016**, *133* (44), n/a-n/a.

78. Yang W., Sundaram H.S., Ella J.-R., He N., Jiang S. Low-fouling electrospun PLLA films modified with zwitterionic poly(sulfobetaine methacrylate)-catechol conjugates. *Acta Biomater.* **2016**, *40*, 92-99.

79. Zhang Z., Vaisocherová H., Cheng G., Yang W., Xue H., et al. Nonfouling behavior of polycarboxybetaine-grafted surfaces: Structural and environmental effects. *Biomacromolecules.* **2008**, *9* (10), 2686-2692.

80. Zhang Z., Zhang M., Chen S., Horbett T.A., Ratner B.D., et al. Blood compatibility of surfaces with superlow protein adsorption. *Biomaterials.* **2008**, *29* (32), 4285-4291.

81. Chang Y., Chang W.-J., Shih Y.-J., Wei T.-C., Hsiue G.-H. Zwitterionic sulfobetaine-grafted poly (vinylidene fluoride) membrane with highly effective blood compatibility via atmospheric plasma-induced surface copolymerization. *ACS Appl Mater Inter.* **2011**, *3* (4), 1228-1237.

82. Zhang Z., Chao T., Chen S., Jiang S. Superlow fouling sulfobetaine and carboxybetaine polymers on glass slides. *Langmuir.* **2006**, *22* (24), 10072-10077.

83. Zhang Z., Chen S., Jiang S. Dual-functional biomimetic materials: Nonfouling poly(carboxybetaine) with active functional groups for protein immobilization. *Biomacromolecules.* **2006**, *7* (12), 3311-3315.

84. Zhang L., Cao Z., Bai T., Carr L., Ella-Menye J.-R., et al. Zwitterionic hydrogels implanted in mice resist the foreign-body reaction. *Nat Biotechnol.* **2013**, *31* (6), 553-556.

85. Grainger S.J., El-Sayed M.E. Stimuli-sensitive particles for drug delivery. In: Jabbari E, Khademhosseini, A, ed. *Biologically-Responsive Hybrid Biomaterials.* Boston: MA: Artech Publishing; **2010**:171-190.

86. Karlsson E., Hirsh I. Ion exchange chromatography. In: Janson JC, ed. *Protein Purification.* New York: John Wiley & Sons, Inc.; **2011**:93-133.

87. Guo S., Jańczewski D., Zhu X., Quintana R., He T., et al. Surface charge control for zwitterionic polymer brushes: Tailoring surface properties to antifouling applications. *J Colloid Interface Sci.* **2015**, *452*, 43-53.

88. Chien H.-W., Tsai C.-C., Tsai W.-B., Wang M.-J., Kuo W.-H., et al. Surface conjugation of zwitterionic polymers to inhibit cell adhesion and protein adsorption. *Colloids Surf B.* **2013**, *107*, 152-159.

89. Xiang T., Wang R., Zhao W.-F., Sun S.-D., Zhao C.-S. Covalent deposition of zwitterionic polymer and citric acid by click chemistry-enabled layer-by-layer assembly for improving the blood compatibility of polysulfone membrane. *Langmuir.* **2014**, *30* (18), 5115-5125.

90. Roach P., Shirtcliffe N.J., Newton M.I. Progess in superhydrophobic surface development. *Soft Matter.* **2008**, *4* (2), 224-240.

91. Barthlott W., Neinhuis C. Purity of the sacred lotus, or escape from contamination in biological surfaces. *Planta.* **1997**, *202* (1), 1-8.

92. Shirtcliffe N.J., Roach P. Superhydrophobicity for antifouling microfluidic surfaces. *Methods Mol Biol.* **2013**, *949*, 269-281.

93. Zheng J., Song W., Huang H., Chen H. Protein adsorption and cell adhesion on polyurethane/Pluronic® surface with lotus leaf-like topography. *Colloids Surf B.* **2010**, *77* (2), 234-239.

94. Lord M.S., Foss M., Besenbacher F. Influence of nanoscale surface topography on protein adsorption and cellular response. *Nano Today.* **2010**, *5* (1), 66-78.

95. May R.M., Magin C.M., Mann E.E., Drinker M.C., Fraser J.C., et al. An engineered micropattern to reduce bacterial colonization, platelet adhesion and fibrin sheath formation for improved biocompatibility of central venous catheters. *Clin Trans Med.* **2015**, *4* (9), 1-8.

96. Burns K.E., McLaren A. A critical review of thromboembolic complications associated with central venous catheters. *Can J Anaesth.* **2008**, *55* (8), 532-541.

97. Pittet D., Tarara D., Wenzel R.P. Nosocomial bloodstream infection in critically ill patients: Excess length of stay, extra costs, and attributable mortality. *J Am Med Assoc.* **1994**, *271* (20), 1598-1601.

98. Chen Y., Zhao X., He C. Dual-mode antifouling ability of PVDF membrane with a surface-anchored amphiphilic polymer. *RSC Adv.* **2015**, *5* (84), 68998-69005.

99. Colak S., Tew G.N. Amphiphilic polybetaines: The effect of side-chain hydrophobicity on protein adsorption. *Biomacromolecules.* **2012**, *13* (5), 1233-1239.

100. Gan D., Mueller A., Wooley K.L. Amphiphilic and hydrophobic surface patterns generated from hyperbranched fluoropolymer/linear polymer networks: Minimally adhesive coatings via the crosslinking of hyperbranched fluoropolymers. *J Polym Sci, Part A: Polym Chem.* **2003**, *41* (22), 3531-3540.

101. Jiang J., Fu Y., Zhang Q., Zhan X., Chen F. Novel amphiphilic poly(dimethylsiloxane) based polyurethane networks tethered with carboxybetaine and their combined antibacterial and anti-adhesive property. *Appl Surf Sci.* **2017**, *412*, 1-9.

102. Lei Y., Lin Y., Zhang A. The synthesis and protein resistance of amphiphilic PDMS-b-(PDMS-g-cysteine) copolymers. *Appl Surf Sci.* **2017**, *419*, 393-398.

103. Mazl Chanova E., Pop-Georgievski O., Kumorek M.M., Janouskova O., Machova L., et al. Polymer brushes based on PLLA-b-PEO colloids for the

preparation of protein resistant PLA surfaces. *Biomater Sci.* **2017**, *5* (6), 1130-1143.

104. Peng J., Su Y., Shi Q., Chen W., Jiang Z. Protein fouling resistant membrane prepared by amphiphilic pegylated polyethersulfone. *Bioresour Technol.* **2011**, *102* (3), 2289-2295.

105. Pollack K.A., Imbesi P.M., Raymond J.E., Wooley K.L. Hyperbranched fluoropolymer-polydimethylsiloxane-poly(ethylene glycol) cross-linked terpolymer networks designed for marine and biomedical applications: Heterogeneous nontoxic antibiofouling surfaces. *ACS Appl Mater Inter.* **2014**, *6* (21), 19265-19274.

106. Zhan X., Zhang G., Zhang Q., Chen F. Preparation, surface wetting properties, and protein adsorption resistance of well-defined amphiphilic fluorinated diblock copolymers. *J Appl Polym Sci.* **2014**, *131* (23), 1-12.

107. Zhao X., Su Y., Li Y., Zhang R., Zhao J., et al. Engineering amphiphilic membrane surfaces based on PEO and PDMS segments for improved antifouling performances. *J Membr Sci.* **2014**, *450*, 111-123.

108. Hawkins M.L., Grunlan M.A. The protein resistance of silicones prepared with a PEO-silane amphiphile. *J Mater Chem.* **2012**, *22* (37), 19540-19546.

109. Mark J.E. Silicon-containing polymers. In: Zeigler JM, Fearon FWG, eds. *Silicon-Based Polymer Science.* Vol 224. Washington, DC: American Chemical Society; **1989**:47-68.

110. Li J.-H., Li M.-Z., Miao J., Wang J.-B., Shao X.-S., et al. Improved surface property of PVDF membrane with amphiphilic zwitterionic copolymer as membrane additive. *Appl Surf Sci.* **2012**, *258* (17), 6398-6405.

111. Wang C., Ma C., Mu C., Lin W. A novel approach for synthesis of zwitterionic polyurethane coating with protein resistance. *Langmuir.* **2014**, *30* (43), 12860-12867.

112. Yang J., Li L., Ma C., Ye X. Degradable polyurethane with poly(2-ethyl-2-oxazoline) brushes for protein resistance. *RSC Adv.* **2016**, *6* (74), 69930-69938.

113. Park K., Shim H.S., Dewanjee M.K., Eigler N.L. In vitro and in vivo studies of PEO-grafted blood-contacting cardiovascular prostheses. *J Biomater Sci Polym, Ed.* **2000**, *11* (11), 1121-1134.

114. Rodriguez Emmenegger C., Brynda E., Riedel T., Sedlakova Z., Houska M., et al. Interaction of blood plasma with antifouling surfaces. *Langmuir.* **2009**, *25* (11), 6328-6333.

115. Horbett T.A. Principles underlying the role of adsorbed plasma proteins in blood interactions with foreign materials. *Cardiovasc Pathol.* **1993**, *2* (3), 137-148.

116. Ladd J., Zhang Z., Chen S., Hower J.C., Jiang S. Zwitterionic polymers exhibiting high resistance to nonspecific protein adsorption from human serum and plasma. *Biomacromolecules.* **2008**, *9* (5), 1357-1361.

117. Adams G.A., Feuerstein I.A. How much fibrinogen or fibronectin is enough for platelet adhesion? *Trans - Am Soc Artif Intern Organs.* **1981**, *27*, 219-224.

118. Tsai W.-B., Grunkemeier J.M., McFarland C.D., Horbett T.A. Platelet adhesion to polystyrene-based surfaces preadsorbed with plasmas selectively depleted in fibrinogen, fibronectin, vitronectin, or von Willebrand's factor. *J Biomed Mater Res.* **2002**, *60* (3), 348-359.

119. Cheng G., Li G., Xue H., Chen S., Bryers J.D., et al. Zwitterionic carboxybetaine polymer surfaces and their resistance to long-term biofilm formation. *Biomaterials.* **2009**, *30* (28), 5234-5240.

120. Product Datasheet. *Human fibrinogen ELISA kit.* AB208036:1-6.

121. User Manual. *Human fibrinogen ELISA kit (sandwich ELISA).* LS-F22853:1-22.

122. Product Datasheet. *Fibrinogen (human) ELISA kit*. ADI-900-230:1-2.

123. Bard A.J., Inzelt G., Scholz F. Q. In: *Electrochemical Dictionary.* 1st ed. Berlin, Heidelberg: Springer-Verlag; **2008**:559-563.

124. Curtis J., Colas A. Medical applications of silicones. In: Hoffman AS, Schoen FJ, Lemons JE, eds. *Biomaterials Science.* 3rd ed. Oxford: Academic Press; **2013**:1106-1116.

125. VanDyke M.E., Clarson S.J., Arshady R. Silicone biomaterials. In: Arshady R, ed. *An Introduction to Polymeric Biomaterials.* Vol 1. London: Citrus Books; **2003**:109-135.

126. Ratner B.D., Horbett T.A. Evaluation of blood–materials interactions. In: Ratner BD, Hoffman AS, Schoen FJ, Lemons JE, eds. *Biomaterials Science.* 3rd ed. Oxford: Academic Press; **2013**:617-634.

127. Kumar V., Rauscher H., Brétagnol F., Arefi-Khonsari F., Pulpytel J., et al. Preventing biofilm formation on biomedical surfaces. In: Rauscher H, Perucca M, Buyle G, eds. *Plasma Technology for Hyperfunctional Surfaces.* Weinheim: Wiley-VCH Verlag GmbH & Co. KGaA; **2010**:183-223.

128. Abdul-Rahman I.S., Al-Howaish A.K. Warfarin versus aspirin in preventing tunneled hemodialysis catheter thrombosis: a prospective randomized study. *Hong Kong J Nephrol.* **2007**, *9* (1), 23-30.

129. Grudzinski L., Quinan P., Kwok S., Pierratos A. Sodium citrate 4% locking solution for central venous dialysis catheters—An effective, more cost-efficient alternative to heparin. *Nephrol Dial Transplant.* **2007**, *22* (2), 471-476.

130. Obialo C.I., Conner A.C., Lebon L.F. Maintaining patency of tunneled hemodialysis catheters. *Scand J Urol Nephrol.* **2003**, *37* (2), 172-176.

131. Willicombe M.K., Vernon K., Davenport A. Embolic complications from central venous hemodialysis catheters used with hypertonic citrate locking solution. *Am J Kidney Dis.* **2010**, *55* (2), 348-351.

132. Bircher A.J., Harr T., Hohenstein L., Tsakiris D.A. Hypersensitivity reactions to anticoagulant drugs: Diagnosis and management options. *Allergy.* **2006**, *61* (12), 1432-1440.

133. Karaaslan H., Peyronnet P., Benevent D., Lagarde C., Rince M., et al. Risk of heparin lock- related bleeding when using indwelling venous catheter in haemodialysis. *Nephrol Dial Transplant.* **2001**, *16* (10), 2072-2074.

134. Levine M.N., Raskob G., Landefeld S., Kearon C. Hemorrhagic complications of anticoagulant treatment. *Chest.* **2001**, *119* (1_suppl), 108s-121s.

135. Rogacka R., Chieffo A., Michev I., Airoldi F., Latib A., et al. Dual antiplatelet therapy after percutaneous coronary intervention with stent implantation in patients taking chronic oral anticoagulation. *JACC-Cardiovasc Inte.* **2008**, *1* (1), 56-61.

136. Scherer K., Tsakiris D.A., Bircher A.J. Hypersensitivity reactions to anticoagulant drugs. *Curr Pharm Design.* **2008**, *14* (27), 2863-2873.

137. Chen H., Brook M.A., Chen Y., Sheardown H. Surface properties of PEO–silicone composites: Reducing protein adsorption. *J Biomater Sci Polym, Ed.* **2005**, *16* (4), 531-548.

138. Lee S., Vörös J. An aqueous-based surface modification of poly(dimethylsiloxane) with poly(ethylene glycol) to prevent biofouling. *Langmuir.* **2005**, *21* (25), 11957-11962.

139. Papra A., Bernard A., Juncker D., Larsen N.B., Michel B., et al. Microfluidic networks made of poly(dimethylsiloxane), Si, and Au coated with polyethylene glycol for patterning proteins onto surfaces. *Langmuir.* **2001**, *17* (13), 4090-4095.

140. Thompson D.B., Fawcett A.S., Brook M.A. Simple strategies to manipulate hydrophilic domains in silicones. In: Ganachaud F, Boileau S, Boury B, eds. *Silicon Based Polymers: Advances in Synthesis and Supramolecular Organization.* 1st ed. Netherlands: Springer; **2008**:29-38.

141. Harris J.M., ed *Poly(ethylene glycol) chemistry: Biotechnical and biomedical applications.* New York: Plenum Press; **1992**.

142. Kingshott P., Thissen H., Griesser H.J. Effects of cloud-point grafting, chain length, and density of PEG layers on competitive adsorption of ocular proteins. *Biomaterials.* **2002**, *23* (9), 2043-2056.

143. Papra A., Gadegaard N., Larsen N.B. Characterization of ultrathin poly(ethylene glycol) monolayers on silicon substrates. *Langmuir.* **2001**, *17* (5), 1457-1460.

144. Zhang M., Desai T., Ferrari M. Proteins and cells on PEG immobilized silicon surfaces. *Biomaterials.* **1998**, *19* (10), 953-960.

145. Zhang M., Ferrari M. Hemocompatible polyethylene glycol films on silicon. *Biomed Microdevices.* **1998**, *1* (1), 81-89.

146. Lee S.-W., Laibinis P.E. Protein-resistant coatings for glass and metal oxide surfaces derived from oligo(ethylene glycol)-terminated alkyltrichlorosilanes. *Biomaterials.* **1998**, *19* (18), 1669-1675.

147. Feldman K., Hähner G., Spencer N.D., Harder P., Grunze M. Probing resistance to protein adsorption of oligo(ethylene glycol)-terminated self-assembled monolayers by scanning force microscopy. *J Am Chem Soc.* **1999**, *121* (43), 10134-10141.

148. Pale-Grosdemange C., Simon E.S., Prime K.L., Whitesides G.M. Formation of self-assembled monolayers by chemisorption of derivatives of oligo(ethylene glycol) of structure $HS(CH_2)_{11}(OCH_2CH_2)_mOH$ on gold. *J Am Chem Soc.* **1991**, *113* (1), 12-20.

149. Lane T., Burns S. Silica, silicon and silicones... Unraveling the mystery. In: Potter M, Rose NR, eds. *Immunology of silicones.* Heidelberg: Springer; **1996**:3-12.

150. Owen M.J. Surface chemistry and applications. In: Clarson SJ, Semlyen JA, eds. *Siloxane Polymers.* Englewood Cliffs: Prentice Hall; **1993**:309.

151. Owen M.J., Smith P.J. Plasma treatment of polydimethylsiloxane. *J Adhes Sci Technol.* **1994**, *8* (10), 1063-1075.

152. Lopez-Donaire M.L., Santerre J.P. Surface modifying oligomers used to functionalize polymeric surfaces: Consideration of blood contact applications. *J Appl Polym Sci.* **2014**, *131* (14), 40328.

153. Murthy R., Cox C.D., Hahn M.S., Grunlan M.A. Protein-resistant silicones: Incorporation of poly(ethylene oxide) via siloxane tethers. *Biomacromolecules.* **2007**, *8* (10), 3244-3252.

154. Hawkins M.L., Schott S.S., Grigoryan B., Rufin M.A., Ngo B.K.D., et al. Anti-protein and anti-bacterial behavior of amphiphilic silicones. *Polym Chem.* **2017**, *8* (34), 5239-5251.

155. Rufin M.A., Barry M.E., Adair P.A., Hawkins M.L., Raymond J.E., et al. Protein resistance efficacy of PEO-silane amphiphiles: Dependence on PEO-segment length and concentration. *Acta Biomater.* **2016**, *41*, 247-252.

156. Zhai Q., Zhou C., Zhao S., Peng C., Han Y. Kinetic study of alkoxysilane hydrolysis under acidic conditions by fourier transform near infrared spectroscopy combined with partial least-squares model. *Ind Eng Chem Res.* **2014**, *53* (35), 13598-13609.

157. Rufin M.A., Ngo B.K.D., Barry M.E., Page V.M., Hawkins M.L., et al. Antifouling silicones based on surface-modifying additive amphiphiles. *Green Mater.* **2017**, *5* (1), 4-13.

158. Brinker C.J. Hydrolysis and condensation of silicates: Effects on structure. *J Non-Cryst Solids.* **1988**, *100* (1-3), 31-50.

159. Maitz M.F., Gago R., Abendroth B., Camero M., Caretti I., et al. Hemocompatibility of low-friction boron–carbon–nitrogen containing coatings. *J Biomed Mater Res, Part B.* **2006**, *77B* (1), 179-187.

160. Wang C., Nair S.S., Veeravalli S., Moseh P., Wynne K.J. Sticky or slippery wetting: Network formation conditions can provide a one-way street for water

flow on platinum-cured silicone. *ACS Appl Mater Inter.* **2016**, *8* (22), 14252-14262.

161. Ngo B.K.D., Lim K.K., Stafslien S.J., Grunlan M.A. Stability of silicones modified with PEO-silane amphiphiles: Impact of structure and concentration. *Polym Degrad Stab.* **2019**, *163*, 136-142.

162. Morrissey B.W. The adsorption and conformation of plasma proteins: A physical approach. *Ann N Y Acad Sci.* **2006**, *283*, 50-64.

163. Vroman L. The life of an artificial device in contact with blood: Initial events and their effect on its final state. *Bull N Y Acad Med.* **1988**, *64* (4), 352-357.

164. Haraguchi K., Takehisa T., Mizuno T., Kubota K. Antithrombogenic properties of amphiphilic block copolymer coatings: Evaluation of hemocompatibility using whole blood. *ACS Biomat Sci Eng.* **2015**, *1* (6), 352-362.

165. Lorenzetti M., Bernardini G., Luxbacher T., Santucci A., Kobe S., et al. Surface properties of nanocrystalline TiO2 coatings in relation to the in vitro plasma protein adsorption. *Biomed Mater.* **2015**, *10* (4), 045012.

166. Sperling C., Fischer M., Maitz M.F., Werner C. Blood coagulation on biomaterials requires the combination of distinct activation processes. *Biomaterials.* **2009**, *30* (27), 4447-4456.

167. Tamada Y., Kulik E.A., Ikada Y. Simple method for platelet counting. *Biomaterials.* **1995**, *16* (3), 259-261.

168. Xiong Z., Liu F., Lin H., Li J., Wang Y. Covalent bonding of heparin on the crystallized poly(lactic acid) (PLA) membrane to improve hemocompability via surface cross-linking and glycidyl ether reaction. *ACS Biomat Sci Eng.* **2016**, *2* (12), 2207-2216.

169. Zhao J., Bai L., Muhammad K., Ren X.-k., Guo J., et al. Construction of hemocompatible and histocompatible surface by grafting antithrombotic peptide ACH11 and hydrophilic PEG. *ACS Biomat Sci Eng.* **2019**, *5* (6), 2846-2857.

170. Keuren J.F., Wielders S.J., Driessen A., Verhoeven M., Hendriks M., et al. Covalently-bound heparin makes collagen thromboresistant. *Arterioscler Thromb Vasc Biol.* **2004**, *24* (3), 613-617.

171. Han D.K., Jeong S.Y., Kim Y.H., Min B.G., Cho H.I. Negative cilia concept for thromboresistance: Synergistic effect of PEO and sulfonate groups grafted onto polyurethanes. *J Biomed Mater Res.* **1991**, *25* (5), 561-575.

172. Frank R.D., Muller U., Lanzmich R., Groeger C., Floege J. Anticoagulant-free genius haemodialysis using low molecular weight heparin-coated circuits. *Nephrol Dial Transplant.* **2006**, *21* (4), 1013-1018.

173. Chatterjee M.S., Denney W.S., Jing H., Diamond S.L. Systems biology of coagulation initiation: Kinetics of thrombin generation in resting and activated human blood. *PLOS Comput Biol.* **2010**, *6* (9), e1000950.

174. van Oeveren W. Obstacles in haemocompatibility testing. *Scientifica.* **2013**, *2013*, 14.

175. Cattaneo M., Hayward C.P., Moffat K.A., Pugliano M.T., Liu Y., et al. Results of a worldwide survey on the assessment of platelet function by light transmission aggregometry: A report from the platelet physiology subcommittee of the SSC of the ISTH. *J Thromb Haemost.* **2009**, *7* (6), 1029.

176. Krajewski S., Prucek R., Panacek A., Avci-Adali M., Nolte A., et al. Hemocompatibility evaluation of different silver nanoparticle concentrations employing a modified chandler-loop in vitro assay on human blood. *Acta Biomater.* **2013**, *9* (7), 7460-7468.

177. McClung W.G., Babcock D.E., Brash J.L. Fibrinolytic properties of lysine-derivatized polyethylene in contact with flowing whole blood (chandler loop model). *J Biomed Mater Res, Part A.* **2007**, *81A* (3), 644-651.

178. Touma H., Sahin I., Gaamangwe T., Gorbet M.B., Peterson S.D. Numerical investigation of fluid flow in a chandler loop. *J Biomech Eng.* **2014**, *136* (7), 071004.

179. Wildgruber M., Lueg C., Borgmeyer S., Karimov I., Braun U., et al. Polyurethane versus silicone catheters for central venous port devices implanted at the forearm. *Eur J Cancer.* **2016**, *59*, 113-124.

180. Zdrahala R.J., Zdrahala I.J. Biomedical applications of polyurethanes: A review of past promises, present realities, and a vibrant future. *J Biomater Appl.* **1999**, *14* (1), 67-90.

181. Li D., Chen H., Glenn McClung W., Brash J.L. Lysine-PEG-modified polyurethane as a fibrinolytic surface: Effect of PEG chain length on protein interactions, platelet interactions and clot lysis. *Acta Biomater.* **2009**, *5* (6), 1864-1871.

182. Park K.D., Kim Y.S., Han D.K., Kim Y.H., Lee E.H.B., et al. Bacterial adhesion on PEG modified polyurethane surfaces. *Biomaterials.* **1998**, *19* (7), 851-859.

183. Domansky K., Leslie D.C., McKinney J., Fraser J.P., Sliz J.D., et al. Clear castable polyurethane elastomer for fabrication of microfluidic devices. *Lab Chip.* **2013**, *13* (19), 3956-3964.

184. Kostov K.G., dos Santos A.L.R., Honda R.Y., Nascente P.A.P., Kayama M.E., et al. Treatment of PET and PU polymers by atmospheric pressure plasma generated in dielectric barrier discharge in air. *Surf Coat Technol.* **2010**, *204* (18), 3064-3068.

185. Sanchis M.R., Calvo O., Fenollar O., Garcia D., Balart R. Characterization of the surface changes and the aging effects of low-pressure nitrogen plasma treatment in a polyurethane film. *Polym Test.* **2008**, *27* (1), 75-83.

186. Lee J.H., Ju Y.M., Kim D.M. Platelet adhesion onto segmented polyurethane film surfaces modified by addition and crosslinking of PEO-containing block copolymers. *Biomaterials.* **2000**, *21* (7), 683-691.

187. Tan J., Brash J.L. Nonfouling biomaterials based on polyethylene oxide-containing amphiphilic triblock copolymers as surface modifying additives: Adsorption of proteins from human plasma to copolymer/polyurethane blends. *J Biomed Mater Res, Part A.* **2009**, *90A* (1), 196-204.

188. Tan J., L. Brash J. Nonfouling biomaterials based on polyethylene oxide-containing amphiphilic triblock copolymers as surface modifying additives: Synthesis and characterization of copolymers and surface properties of copolymer–polyurethane blends. *J Appl Polym Sci.* **2008**, *108* (3), 1617-1628.

189. Tan J., McClung W.G., Brash J.L. Nonfouling biomaterials based on polyethylene oxide-containing amphiphilic triblock copolymers as surface modifying additives: Protein adsorption on PEO-copolymer/polyurethane blends. *J Biomed Mater Res, Part A.* **2008**, *85A* (4), 873-880.

190. Tan J., McClung W.G., Brash J.L. Non-fouling biomaterials based on blends of polyethylene oxide copolymers and polyurethane: Simultaneous measurement of platelet adhesion and fibrinogen adsorption from flowing whole blood. *J Biomater Sci Polym, Ed.* **2013**, *24* (4), 497-506.

191. Huskens D., Sang Y., Konings J., van der Vorm L., de Laat B., et al. Standardization and reference ranges for whole blood platelet function measurements using a flow cytometric platelet activation test. *PLoS One.* **2018**, *13* (2), e0192079-e0192079.

192. Percival S.L., Suleman L., Vuotto C., Donelli G. Healthcare-associated infections, medical devices and biofilms: Risk, tolerance and control. *J Med Microbiol.* **2015**, *64* (4), 323-334.

193. Wu H., Moser C., Wang H.-Z., Hoiby N., Song Z.-J. Strategies for combating bacterial biofilm infections. *Int J Oral Sci.* **2015**, *7* (1), 1-7.

194. Moghimi S.M., Hamad I., Andresen T.L., Jørgensen K., Szebeni J. Methylation of the phosphate oxygen moiety of phospholipid-methoxy(polyethylene glycol) conjugate prevents PEGylated liposome-mediated complement activation and anaphylatoxin production. *FASEB J.* **2006**, *20* (14), 2591-2593.

195. Shah S., Prematta T., Adkinson N.F., Ishmael F.T. Hypersensitivity to polyethylene glycols. *J Clin Pharmacol.* **2013**, *53* (3), 352-355.

196. Wenande E., Garvey L.H. Immediate-type hypersensitivity to polyethylene glycols: A review. *Clin Exp Allergy.* **2016**, *46* (7), 907-922.

197. Armstrong J.K. The occurrence, induction, specificity and potential effect of antibodies against poly(ethylene glycol). In: Veronese FM, ed. *PEGylated Protein Drugs: Basic Science and Clinical Applications.* Basel: Birkhäuser Basel; **2009**:147-168.

198. Schellekens H., Hennink W.E., Brinks V. The immunogenicity of polyethylene glycol: Facts and fiction. *Pharm Res.* **2013**, *30* (7), 1729-1734.

199. Yang Q., Lai S.K. Anti-PEG immunity: Emergence, characteristics, and unaddressed questions. *Wiley Interdiscip Rev Nanomed Nanbiotechnol.* **2015**, *7* (5), 655-677.

200. Hayama M., Yamamoto K.-i., Kohori F., Uesaka T., Ueno Y., et al. Nanoscopic behavior of polyvinylpyrrolidone particles on polysulfone/polyvinylpyrrolidone film. *Biomaterials.* **2004**, *25* (6), 1019-1028.

201. Xu C., Huang W., Lu X., Yan D., Chen S., et al. Preparation of PVDF porous membranes by using PVDF-g-PVP powder as an additive and their antifouling property. *Radiat Phys Chem.* **2012**, *81* (11), 1763-1769.

202. Higuchi A., Shirano K., Harashima M., Yoon B.O., Hara M., et al. Chemically modified polysulfone hollow fibers with vinylpyrrolidone having improved blood compatibility. *Biomaterials.* **2002**, *23* (13), 2659-2666.

203. Wang B.-L., Liu X.-S., Ji Y., Ren K.-F., Ji J. Fast and long-acting antibacterial properties of chitosan-Ag/polyvinylpyrrolidone nanocomposite films. *Carbohydr Polym.* **2012**, *90* (1), 8-15.

204. Wan L.-S., Xu Z.-K., Wang Z.-G. Leaching of PVP from polyacrylonitrile/PVP blending membranes: A comparative study of asymmetric and dense membranes. *J Polym Scie, Part B: Polym Phys.* **2006**, *44* (10), 1490-1498.

205. Yang Q., Chung T.-S., Weber M. Microscopic behavior of polyvinylpyrrolidone hydrophilizing agents on phase inversion polyethersulfone hollow fiber membranes for hemofiltration. *J Membr Sci.* **2009**, *326* (2), 322-331.

206. Moreau K.L., King J.A. Protein misfolding and aggregation in cataract disease and prospects for prevention. *Trends Mol Med.* **2012**, *18* (5), 273-282.

207. Wormstone I.M., Wang L., Liu C.S.C. Posterior capsule opacification. *Exp Eye Res.* **2009**, *88* (2), 257-269.

208. Mohamed Ismail M., Alió J.L., Ruiz Moreno J.M. Prevention of secondary cataract by antimitotic drugs: Experimental study. *Ophthalmic Res.* **1996**, *28* (1), 64-69.

209. Aslam T.M., Devlin H., Dhillon B. Use of Nd:YAG laser capsulotomy. *Surv Ophthalmol.* **2003**, *48* (6), 594-612.

APPENDIX A

^{1}H NMR SPECTRA OF SYNTHETIC PRODUCTS

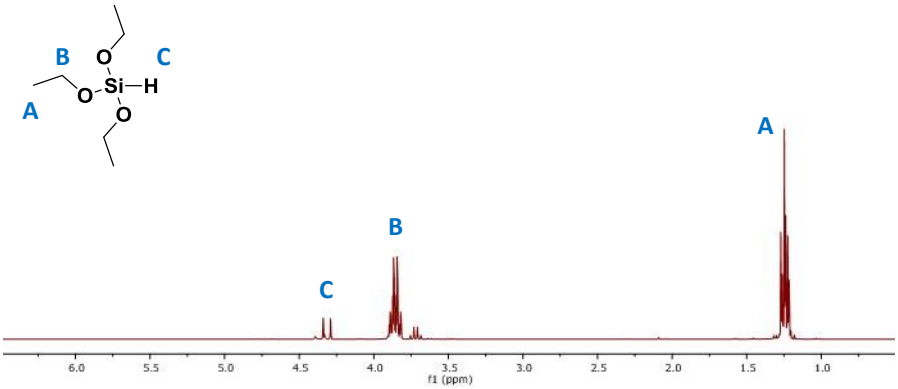

Figure A-1. ^{1}H NMR of "***triethoxysilane***," (δ, ppm): 1.19-1.29 (t, *J* = 7.0 Hz, 9H, [C*H*$_3$CH$_2$O]$_3$SiH), 3.80-3.92 (q, *J* = 7.0 Hz, 6H, [CH$_3$C*H*$_2$O]$_3$SiH), and 4.24-4.41 (m, 1H, [CH$_3$CH$_2$O]$_3$Si*H*)

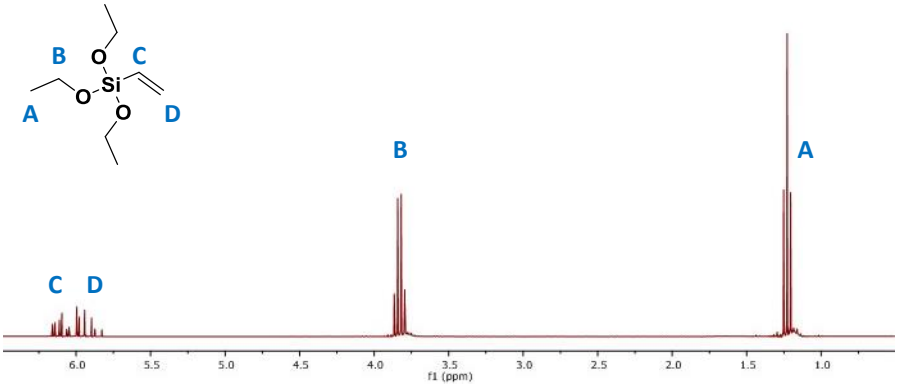

Figure A-2. ^{1}H NMR of "***vinyltriethoxysilane***," (δ, ppm): 1.19-1.26 (t, *J* = 7.0 Hz, 9H, [C*H*$_3$CH$_2$O]$_3$Si), 3.78-3.88 (q, *J* = 7.0 Hz, 6H, [CH$_3$C*H*$_2$O]$_3$Si), 5.87-6.07 (m, 2H, SiCH=C*H*$_2$), and 6.09-6.17 (m, 1H, SiC*H*=CH$_2$)

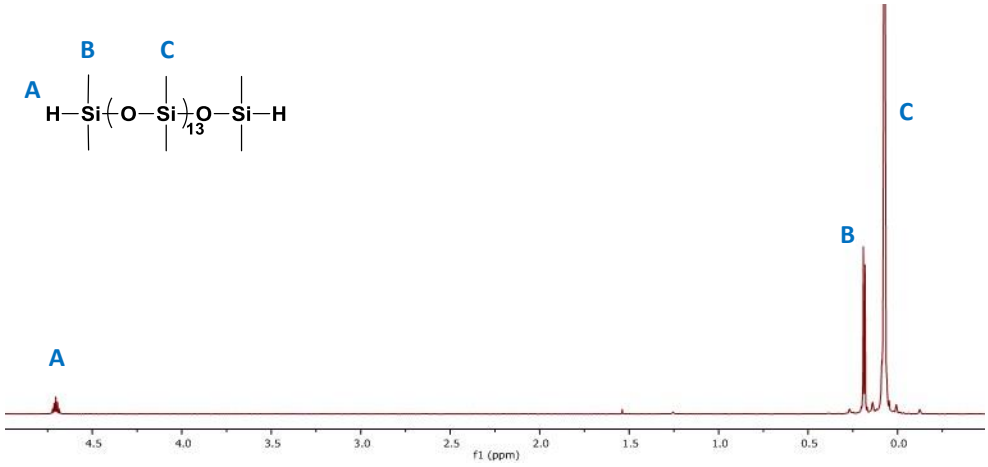

Figure A-3. ^{1}H NMR of "***m* = *13***" ODMS tether, (δ, ppm): 0.05-0.10 (m, 78H, SiC*H*$_3$), 0.17-0.19 (d, *J* = 2.8 Hz, 12H, OSi[C*H*$_3$]$_2$H), and 4.65-4.75 (m, 2H, Si*H*).

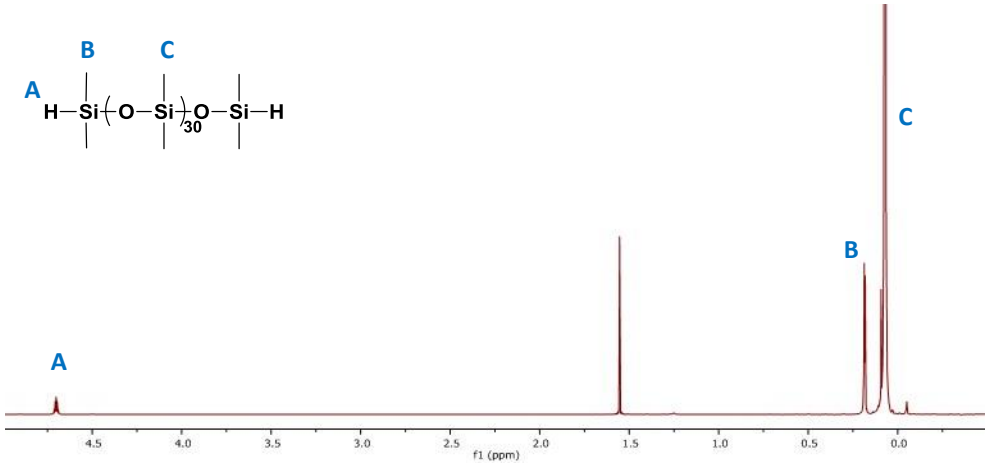

Figure A-4. ^{1}H NMR of "***m* = *30***" ODMS tether, (δ, ppm): 0.05-0.10 (m, 180H, SiC*H*$_3$), 0.17-0.19 (d, *J* = 2.8 Hz, 12H, OSi[C*H*$_3$]$_2$H), and 4.65-4.75 (m, 2H, Si*H*).

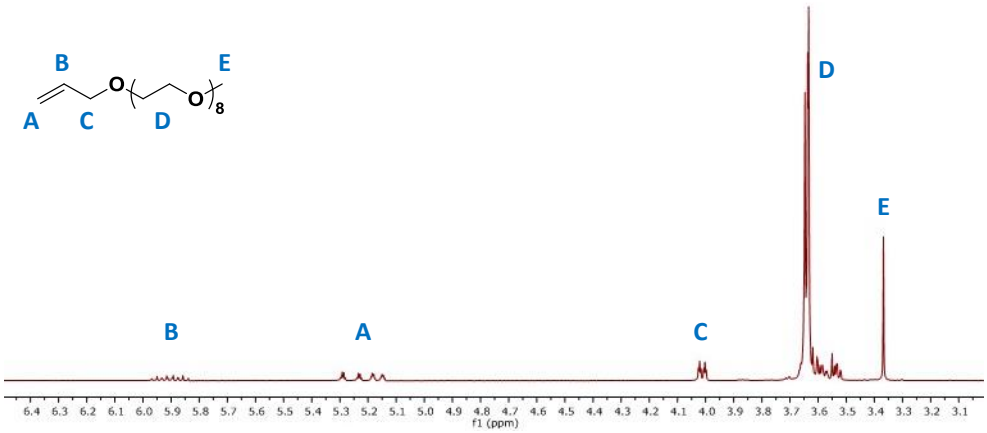

Figure A-5. ^{1}H NMR of "***allyl methyl PEO, n = 8***," (δ, ppm): 3.37 (s, 3H, OC*H*$_3$), 3.51-3.72 (m, 32H, C*H*$_2$C*H*$_2$O), 3.98-4.04 (m, 2H, CH$_2$=CHC*H*$_2$O), 5.13-5.31 (m, 2H, C*H*$_2$=CHCH$_2$O), and 5.82-5.99 (m, 1H, CH$_2$=C*H*CH$_2$O).

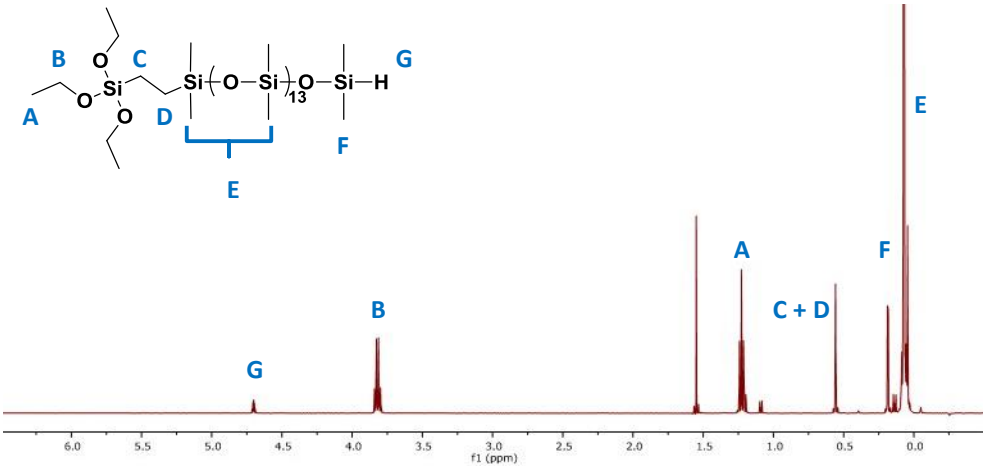

Figure A-6. ^{1}H NMR of "***Step 1, m = 13***" intermediate of PEO-SA, (δ, ppm): 0.05-0.10 (m, 84H, SiC*H*$_3$), 0.17-0.19 (d, *J* = 2.8 Hz, 6H, OSi[C*H*$_3$]$_2$H), 0.55-0.57 (m, 3H, SiC*H*$_2$C*H*$_2$), 1.15-1.19 (m, 1H, SiC*H*$_2$C*H*$_2$), 1.19-1.26 (t, *J* = 7.0 Hz, 9H, [C*H*$_3$CH$_2$O]$_3$Si), 3.78-3.86 (q, *J* = 7.0 Hz, 6H, [CH$_3$C*H*$_2$O]$_3$Si), and 4.65-4.75 (m, 1H, Si*H*).

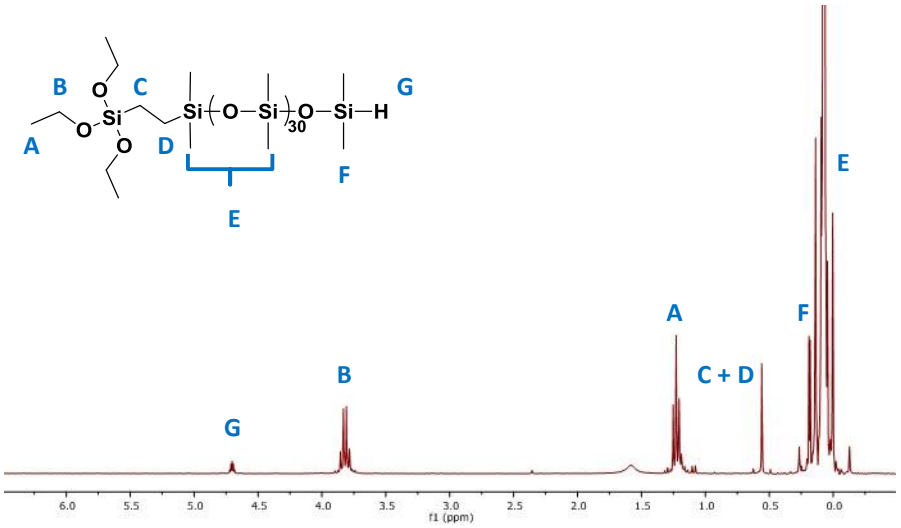

Figure A-7. ^{1}H NMR of "***Step 1, m = 30***" intermediate of PEO-SA, (δ, ppm): 0.05-0.10 (m, 186H, SiC*H*$_3$), 0.17-0.19 (d, *J* = 2.8 Hz, 6H, OSi[C*H*$_3$]$_2$H), 0.55-0.57 (m, 3H, SiC*H*$_2$C*H*$_2$), 1.15-1.19 (m, 1H, SiC*H*$_2$C*H*$_2$), 1.19-1.26 (t, *J* = 7.0 Hz, 9H, [C*H*$_3$CH$_2$O]$_3$Si), 3.78-3.86 (q, *J* = 7.0 Hz, 6H, [CH$_3$C*H*$_2$O]$_3$Si), and 4.65-4.75 (m, 1H, Si*H*).

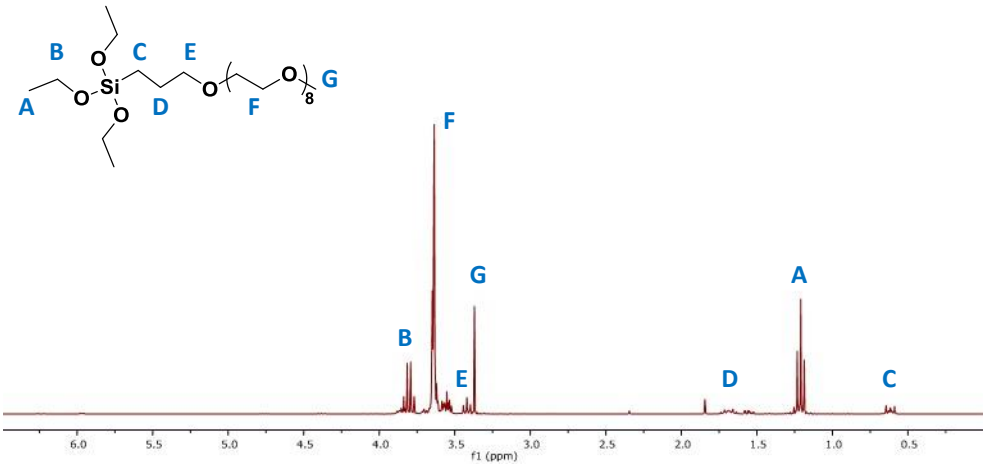

Figure A-8. ^{1}H NMR of non-amphiphilic, "***PEO-control, n = 8***" SMA, (δ, ppm): 0.56-0.67 (m, 2H, SiC*H*$_2$CH$_2$CH$_2$), 1.16-1.26 (t, *J* = 6.9 Hz, 9H, [C*H*$_3$CH$_2$O]$_3$Si), 1.61-1.76 (m, 2H, SiCH$_2$C*H*$_2$CH$_2$), 3.37 (s, 3H, OC*H*$_3$), 3.39-3.45 (t, *J* = 7.0 Hz, 2H, SiCH$_2$CH$_2$C*H*$_2$), 3.51-3.68 (m, 32H, C*H*$_2$C*H*$_2$O) and 3.75-3.86 (q, *J* = 7.0 Hz, 6H, [CH$_3$C*H*$_2$O]$_3$Si).

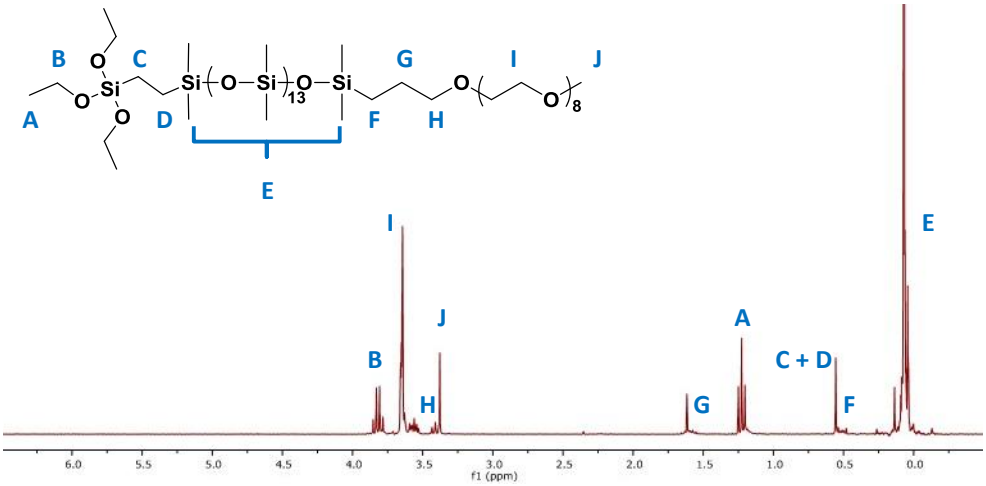

Figure A-9. ^{1}H NMR of "***XL Diblock, m = 13***" PEO-SA, (δ, ppm): 0.05-0.10 (m, 90H, SiCH_3), 0.47-0.55 (m, 2H, SiCH_2CH$_2$CH$_2$), 0.55-0.57 (m, 3H, SiCH_2CH_2), 1.15-1.19 (m, 1H, SiCH_2CH_2), 1.19-1.26 (t, *J* = 7.0 Hz, 9H, [CH_3CH$_2$O]$_3$Si), 1.54-1.66 (m, 2H, SiCH$_2$CH_2CH$_2$), 3.38 (s, 3H, OCH_3), 3.39-3.45 (t, *J* = 6.9 Hz, 2H, SiCH$_2$CH$_2$CH_2), 3.50-3.70 (m, 32H, CH_2CH_2O) and 3.78-3.86 (q, *J* = 7.0 Hz, 6H, [CH$_3$CH_2O]$_3$Si).

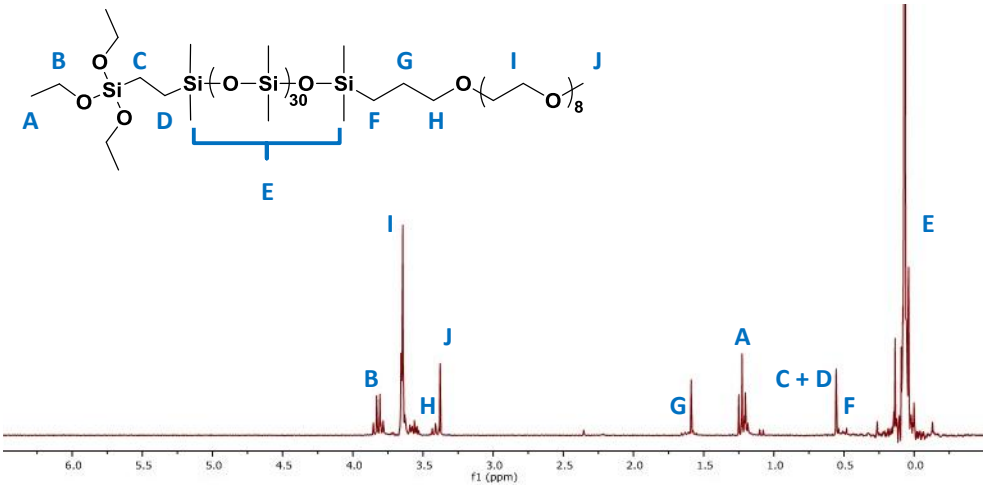

Figure A-10. ^{1}H NMR of "***XL Diblock, m = 30***" PEO-SA, (δ, ppm): 0.05-0.10 (m, 192H, SiCH_3), 0.47-0.55 (m, 2H, SiCH_2CH$_2$CH$_2$), 0.55-0.57 (m, 3H, SiCH_2CH_2), 1.15-1.19 (m, 1H, SiCH_2CH_2), 1.19-1.26 (t, *J* = 7.0 Hz, 9H, [CH_3CH$_2$O]$_3$Si), 1.54-1.66 (m, 2H, SiCH$_2$CH_2CH$_2$), 3.38 (s, 3H, OCH_3), 3.39-3.45 (t, *J* = 6.9 Hz, 2H, SiCH$_2$CH$_2$CH_2), 3.50-3.70 (m, 32H, CH_2CH_2O) and 3.78-3.86 (q, *J* = 7.0 Hz, 6H, [CH$_3$CH_2O]$_3$Si).

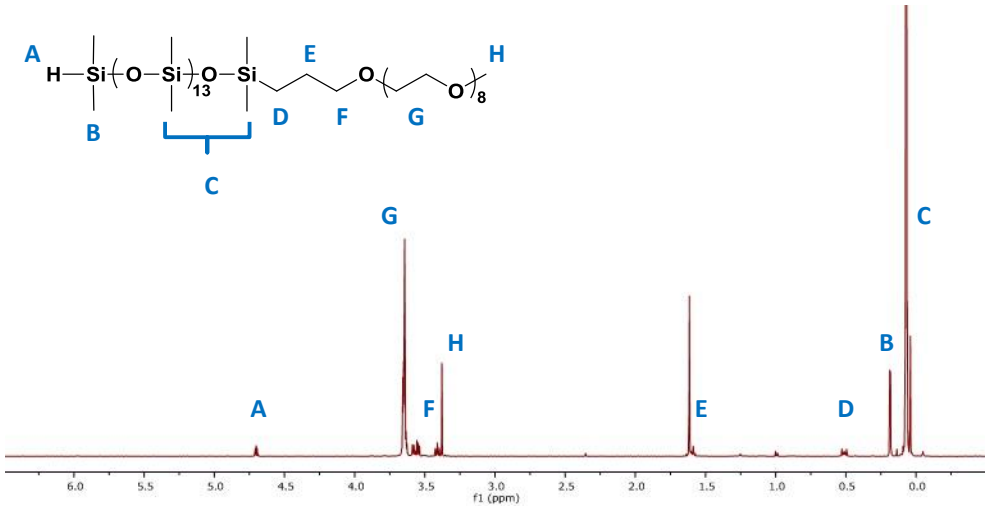

Figure A-11. ^{1}H NMR of "***Diblock, m = 13***" PEO-SA, (δ, ppm): 0.05-0.10 (m, 84H, SiC*H*$_3$), 0.17-0.19 (d, *J* = 2.8 Hz, 6H, OSi[C*H*$_3$]$_2$H), 0.47-0.55 (m, 2H, SiC*H*$_2$CH$_2$CH$_2$), 1.56-1.64 (m, 2H, SiCH$_2$C*H*$_2$CH$_2$), 3.38 (s, 3H, OC*H*$_3$), 3.39-3.44 (t, *J* = 6.9 Hz, 2H, SiCH$_2$CH$_2$C*H*$_2$), 3.52-3.70 (m, 32H, C*H*$_2$C*H*$_2$O) and 4.65-4.75 (m, 1H, Si*H*).

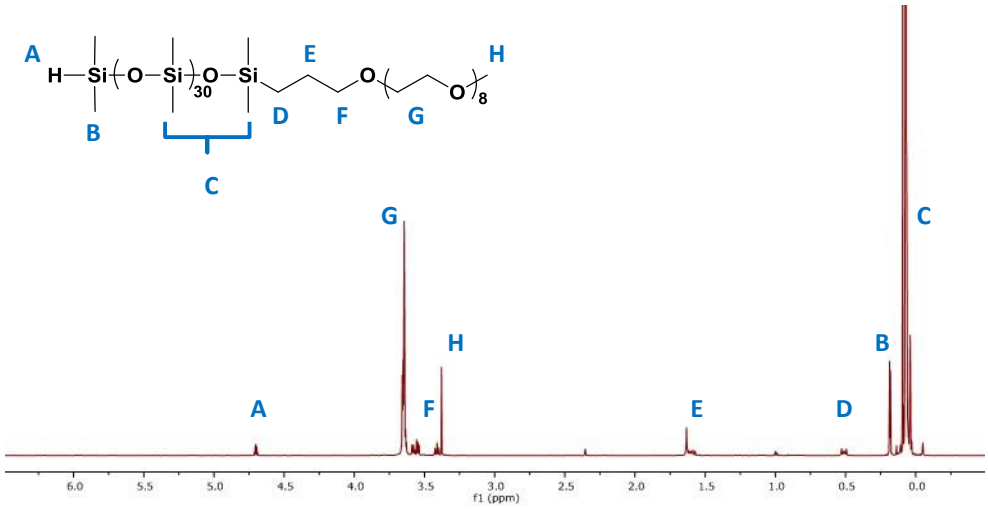

Figure A-12. ^{1}H NMR of "***Diblock, m = 30***" PEO-SA, (δ, ppm): 0.05-0.10 (m, 186H, SiC*H*$_3$), 0.17-0.19 (d, *J* = 2.8 Hz, 6H, OSi[C*H*$_3$]$_2$H), 0.47-0.55 (m, 2H, SiC*H*$_2$CH$_2$CH$_2$), 1.56-1.64 (m, 2H, SiCH$_2$C*H*$_2$CH$_2$), 3.38 (s, 3H, OC*H*$_3$), 3.39-3.44 (t, *J* = 6.9 Hz, 2H, SiCH$_2$CH$_2$C*H*$_2$), 3.52-3.70 (m, 32H, C*H*$_2$C*H*$_2$O) and 4.65-4.75 (m, 1H, Si*H*).

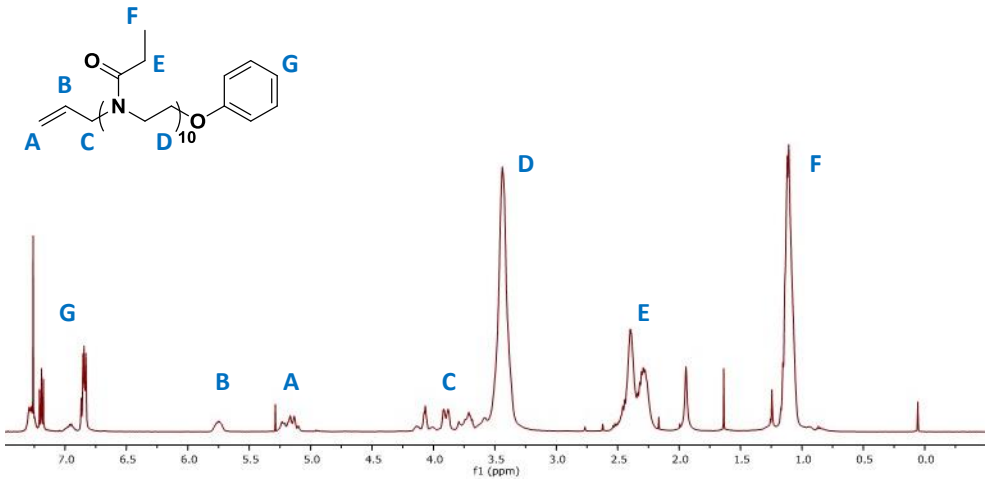

Figure A-13. ^{1}H NMR of "***allyl-PEtOx-phenoxide***," (δ, ppm): 0.90-1.30 (m, 30H, NCO-CH_2CH_3), 2.10-2.60 (m, 20H, NCO-CH_2CH_3), 3.20-3.65 (m, 40H, CH_2CH_2N), 3.84-3.95 (d, J = 15.5 Hz, 2H, CH_2=$CHCH_2N$), 5.07-5.27 (m, 2H, CH_2=$CHCH_2N$), 5.68-5.82 (m, 2H, CH_2=$CHCH_2N$), and 6.80-7.22 (m, 5H, C_6H_5).

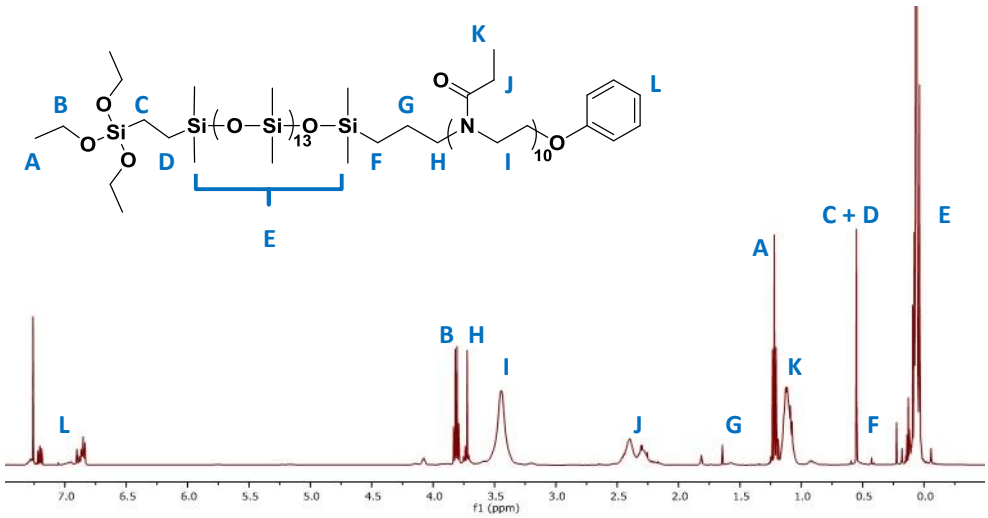

Figure A-14. ^{1}H NMR of "***PEtOx-silane Amphiphile***," (δ, ppm): 0.05 – 0.10 (m, 90H, SiCH_3), 0.39-0.45 (m, 2H, Si$CH_2CH_2CH_2$), 0.54-0.56 (m, 4H, SiCH_2CH_2), 0.84-1.17 (m, 30H, NCO-CH_2CH_3), 1.20-1.24 (t, J = 7.0 Hz, 9H, $[CH_3CH_2O]_3Si$), 1.50-1.70 (m, 2H, $SiCH_2CH_2CH_2$), 2.10-2.60 (m, 20H, NCO-CH_2CH_3), 3.15-3.65 (m, 40H, CH_2CH_2N), 3.72-3.76 (m, 2H, $SiCH_2CH_2CH_2$), 3.78-3.84 (q, J = 7.0 Hz, 6H, $[CH_3CH_2O]_3Si$), and 6.80-7.23 (m, 5H, C_6H_5).

APPENDIX B

DATA TABLES FOR BAR GRAPHS

Table B-1. $\theta_{static,\ 2\ min}$ values for modified silicones (air-equilibrated) in **Figure 2-2**.

	0 μmol/g	**5 μmol/g**	**10 μmol/g**	**25 μmol/g**	**50 μmol/g**	**100 μmol/g**
			PEO-Control			
t = initial	114.6° ± 1.2°	113.4° ± 0.4°	111.9° ± 0.3°	112.1° ± 1.3°	95.0° ± 0.8°	73.7° ± 0.2°
t = 1 wks	114.5° ± 0.5°	113.9° ± 0.3°	112.6° ± 1.9°	112.2° ± 1.9°	95.9° ± 0.7°	89.9° ± 1.6°
t = 2 wks	114.6° ± 2.2°	114.2° ± 0.5°	113.0° ± 0.3°	112.4° ± 2.7°	96.9° ± 0.4°	89.4° ± 1.2°
			"XL Diblock, m = 13"			
t = initial	114.6° ± 1.2°	109.4° ± 1.0°	94.8° ± 1.5°	58.6° ± 0.7°	35.2° ± 1.1°	25.3° ± 0.9°
t = 1 wks	114.5° ± 0.5°	110.4° ± 0.9°	98.9° ± 0.4°	57.6° ± 1.0°	35.4° ± 1.6°	21.8° ± 0.8°
t = 2 wks	114.6° ± 2.2°	112.3° ± 1.7°	101.3° ± 0.2°	58.3° ± 1.4°	34.0° ± 4.0°	19.9° ± 0.3°
			"XL Diblock, m = 30"			
t = initial	114.6° ± 1.2°	113.4° ± 2.4°	101.0° ± 1.7°	58.7° ± 1.0°	42.7° ± 0.6°	35.1° ± 0.2°
t = 1 wks	114.5° ± 0.5°	113.4° ± 1.0°	101.6° ± 0.3°	58.8° ± 1.2°	42.7° ± 0.2°	35.5° ± 0.3°
t = 2 wks	114.6° ± 2.2°	113.5° ± 1.9°	103.7° ± 0.6°	58.4° ± 0.4°	42.9° ± 0.3°	36.7° ± 1.1°
			"Diblock, m = 13"			
t = initial	114.6° ± 1.2°	112.4° ± 0.5°	90.2° ± 0.8°	49.6° ± 2.9°	14.9° ± 0.7°	13.5° ± 0.5°
t = 1 wks	114.5° ± 0.5°	112.2° ± 0.2°	90.1° ± 0.7°	44.2° ± 3.1°	16.7° ± 1.0°	14.4° ± 0.7°
t = 2 wks	114.6° ± 2.2°	112.6° ± 0.6°	91.2° ± 0.8°	44.0° ± 1.6°	15.3° ± 0.9°	14.4° ± 0.5°
			"Diblock, m = 30"			
t = initial	114.6° ± 1.2°	110.8° ± 0.5°	88.8° ± 0.1°	43.4° ± 0.4°	22.1° ± 1.5°	24.3° ± 1.2°
t = 1 wks	114.5° ± 0.5°	111.0° ± 0.3°	89.1° ± 0.3°	42.1° ± 2.8°	17.3° ± 1.4°	20.6° ± 3.6°
t = 2 wks	114.6° ± 2.2°	111.1° ± 1.0°	89.2° ± 0.5°	41.7° ± 1.7°	17.2° ± 0.6°	22.5° ± 0.8°

Table B-2. $\theta_{static,\ 2\ min}$ values for modified silicones (water-equilibrated) in **Figure 2-3**.

	0 µmol/g	5 µmol/g	10 µmol/g	25 µmol/g	50 µmol/g	100 µmol/g
			PEO-Control			
t = initial	116.9° ± 0.3°	112.1° ± 0.4°	107.7° ± 0.8°	97.8° ± 0.3°	90.9° ± 0.5°	87.9° ± 1.5°
t = 6 d	117.1° ± 1.3°	116.7° ± 0.5°	113.5° ± 0.5°	113.3° ± 0.3°	114.3° ± 1.2°	113.1° ± 0.9°
t =15 d	115.8° ± 1.2°	116.5° ± 1.5°	114.7° ± 0.3°	113.4° ± 0.4°	114.5° ± 2.2°	110.7° ± 3.3°
			"XL Diblock, m = 13"			
t = initial	116.9° ± 0.3°	111.8° ± 0.6°	93.4° ± 0.7°	49.6° ± 0.8°	37.7° ± 0.7°	28.2° ± 0.4°
t = 6 d	117.1° ± 1.3°	113.7° ± 1.0°	100.7° ± 1.1°	55.3° ± 0.8°	41.3° ± 0.9°	35.9° ± 1.5°
t =15 d	115.8° ± 1.2°	113.6° ± 0.7°	105.5° ± 0.3°	58.7° ± 0.9°	43.2° ± 0.5°	35.4° ± 1.7°
			"XL Diblock, m = 30"			
t = initial	116.9° ± 0.3°	113.1° ± 0.7°	101.0° ± 1.8°	55.3° ± 0.6°	42.5° ± 1.5°	37.0° ± 1.0°
t = 6 d	117.1° ± 1.3°	113.3° ± 0.7°	104.1° ± 0.2°	60.1° ± 0.3°	44.7° ± 0.3°	40.0° ± 0.4°
t =15 d	115.8° ± 1.2°	112.4° ± 0.3°	106.5° ± 0.7°	64.5° ± 0.6°	46.6° ± 1.1°	39.6° ± 1.4°
			"Diblock, m = 13"			
t = initial	116.9° ± 0.3°	110.4° ± 0.5°	85.2° ± 1.3°	37.9° ± 0.6°	20.7° ± 0.7°	14.1° ± 0.8°
t = 6 d	117.1° ± 1.3°	111.6° ± 1.5°	94.4° ± 0.4°	44.4° ± 1.8°	35.1° ± 1.9°	17.3° ± 3.8°
t =15 d	115.8° ± 1.2°	111.4° ± 0.3°	98.7° ± 0.3°	47.1° ± 2.9°	35.2° ± 1.6°	21.0° ± 3.4°
			"Diblock, m = 30"			
t = initial	116.9° ± 0.3°	109.7° ± 0.2°	84.1° ± 0.4°	43.2° ± 0.4°	28.3° ± 0.8°	24.8° ± 0.6°
t = 6 d	117.1° ± 1.3°	111.9° ± 0.3°	90.9° ± 0.4°	48.8° ± 0.9°	36.4° ± 0.7°	26.5° ± 1.8°
t =15 d	115.8° ± 1.2°	111.9° ± 1.3°	94.4° ± 1.2°	51.5° ± 2.6°	37.6° ± 0.5°	34.0° ± 0.2°

Table B-3. Water uptake values (wt% water) for samples from **Figure 2-4**.

	0 µmol/g	5 µmol/g	10 µmol/g	25 µmol/g	50 µmol/g	100 µmol/g
			PEO-Control			
t = 1 d	0.22 ± 0.04	0.27 ± 0.05	0.33 ± 0.02	0.81 ± 0.28	2.86 ± 0.21	7.54 ± 0.78
t = 6 d	0.33 ± 0.04	0.27 ± 0.06	0.32 ± 0.03	0.97 ± 0.63	3.12 ± 0.60	12.9 ± 0.20
t =15 d	0.31 ± 0.07	0.27 ± 0.05	0.33 ± 0.03	1.25 ± 0.59	3.61 ± 0.20	13.5 ± 0.29
			"XL Diblock, m = 13"			
t = 1 d	0.22 ± 0.04	0.24 ± 0.02	0.26 ± 0.05	0.38 ± 0.04	0.46 ± 0.06	0.99 ± 0.26
t = 6 d	0.33 ± 0.04	0.29 ± 0.02	0.31 ± 0.06	0.42 ± 0.06	0.40 ± 0.06	2.30 ± 0.58
t =15 d	0.31 ± 0.07	0.27 ± 0.01	0.29 ± 0.07	0.42 ± 0.02	0.34 ± 0.01	1.81 ± 0.20
			"XL Diblock, m = 30"			
t = 1 d	0.22 ± 0.04	0.32 ± 0.07	0.40 ± 0.05	0.43 ± 0.06	0.42 ± 0.09	0.60 ± 0.05
t = 6 d	0.33 ± 0.04	0.30 ± 0.04	0.37 ± 0.05	0.41 ± 0.03	1.69 ± 0.39	2.57 ± 0.30
t =15 d	0.31 ± 0.07	0.30 ± 0.04	0.35 ± 0.05	0.41 ± 0.03	1.60 ± 0.05	3.22 ± 0.71
			"Diblock, m = 13"			
t = 1 d	0.22 ± 0.04	0.30 ± 0.04	0.38 ± 0.02	0.41 ± 0.05	0.68 ± 0.22	0.78 ± 0.30
t = 6 d	0.33 ± 0.04	0.33 ± 0.04	0.40 ± 0.03	0.45 ± 0.07	1.57 ± 0.57	4.50 ± 1.14
t =15 d	0.31 ± 0.07	0.36 ± 0.06	0.40 ± 0.04	0.73 ± 0.28	2.35 ± 0.53	7.46 ± 1.88
			"Diblock, m = 30"			
t = 1 d	0.22 ± 0.04	0.26 ± 0.05	0.25 ± 0.01	0.24 ± 0.04	0.39 ± 0.04	0.59 ± 0.18
t = 6 d	0.33 ± 0.04	0.28 ± 0.04	0.29 ± 0.01	0.38 ± 0.12	1.68 ± 0.16	4.13 ± 0.08
t =15 d	0.31 ± 0.07	0.28 ± 0.03	0.28 ± 0.01	0.57 ± 0.14	3.12 ± 0.14	6.81 ± 0.30

Table B-4. Film mass loss values (%) for samples from **Figure 2-5**.

	0 µmol/g	5 µmol/g	10 µmol/g	25 µmol/g	50 µmol/g	100 µmol/g
PEO-Control	0.29 ± 0.05	0.36 ± 0.01	0.66 ± 0.18	1.18 ± 0.01	2.22 ± 0.07	3.95 ± 0.16
XL Diblock, m = 13	0.29 ± 0.05	0.64 ± 0.05	0.77 ± 0.21	0.84 ± 0.08	1.36 ± 0.03	1.44 ± 0.12
XL Diblock, m = 30	0.29 ± 0.05	0.44 ± 0.09	0.44 ± 0.04	0.73 ± 0.15	0.50 ± 0.03	1.01 ± 0.16
Diblock, m = 13	0.29 ± 0.05	0.59 ± 0.08	0.25 ± 0.14	0.53 ± 0.08	0.96 ± 0.15	1.72 ± 0.17
Diblock, m = 30	0.29 ± 0.05	0.36 ± 0.07	0.42 ± 0.09	0.52 ± 0.10	0.85 ± 0.08	1.10 ± 0.16

Table B-5. HF adsorption values (ng/cm^2) for samples from **Figure 2-6**.

	0 µmol/g	5 µmol/g	10 µmol/g	25 µmol/g	50 µmol/g	100 µmol/g
			PEO-Control			
t = initial	402.9 ± 23.2	345.8 ± 46.3	297.2 ± 15.9	281.0 ± 23.1	287.8 ± 21.4	294.7 ± 2.4
t = 2 wks	269.6 ± 20.2	307.5 ± 14.5	288.2 ± 19.2	285.5 ± 8.5	283.1 ± 11.6	250.3 ± 34.6
			"XL Diblock, m = 13"			
t = initial	402.9 ± 23.2	309.9 ± 23.2	82.6 ± 9.4	39.0 ± 16.2	15.7 ± 7.5	0.2 ± 0.1
t = 2 wks	269.6 ± 20.2	289.3 ± 17.2	131.3 ± 17.3	33.4 ± 2.1	20.8 ± 9.4	1.7 ± 0.1
			"XL Diblock, m = 30"			
t = initial	402.9 ± 23.2	280.5 ± 3.5	48.2 ± 10.8	14.9 ± 5.3	6.1 ± 3.4	5.3 ± 1.3
t = 2 wks	269.6 ± 20.2	305.0 ± 19.9	107.3 ± 13.5	36.3 ± 4.3	1.4 ± 0.9	14.0 ± 5.3
			"Diblock, m = 13"			
t = initial	402.9 ± 23.2	303.5 ± 17.8	93.2 ± 16.1	22.5 ± 6.1	16.2 ± 1.3	0.9 ± 0.1
t = 2 wks	269.6 ± 20.2	285.3 ± 21.8	207.0 ± 25.2	28.6 ± 7.1	35.4 ± 8.1	21.8 ± 3.5
			"Diblock, m = 30"			
t = initial	402.9 ± 23.2	286.8 ± 12.2	66.1 ± 5.3	14.4 ± 3.5	3.5 ± 2.2	3.6 ± 4.8
t = 2 wks	269.6 ± 20.2	270.3 ± 20.3	129.8 ± 6.2	28.6 ± 5.7	27.7 ± 10.8	4.1 ± 2.5

Table B-6. Normalized platelet and HF fluorescence intensity values for "***XL diblock, m = 13***" modified silicones in **Figure 3-3c**.

	0 µmol/g	5 µmol/g	10 µmol/g	25 µmol/g	50 µmol/g
			Platelet Adhesion (*green*, 488 nm)		
Donor 1	1.0000 ± 0.1288	1.0109 ± 0.1040	0.0738 ± 0.0194	0.0445 ± 0.0451	0.0040 ± 0.0015
Donor 2	1.0000 ± 0.3981	0.9400 ± 0.3696	0.0294 ± 0.0043	0.0225 ± 0.0025	0.0018 ± 0.0003
Donor 3	1.0000 ± 0.2028	0.9564 ± 0.1930	0.0510 ± 0.0027	0.0133 ± 0.0001	0.0030 ± 0.0003
			HF Adsorption (*red*, 647 nm)		
Donor 1	1.0000 ± 0.2857	1.2901 ± 0.4115	0.0353 ± 0.0103	0.0268 ± 0.0031	0.0030 ± 0.0005
Donor 2	1.0000 ± 0.6318	0.6939 ± 0.3783	0.0088 ± 0.0017	0.0061 ± 0.0017	0.0007 ± 0.0001
Donor 3	1.0000 ± 0.7096	0.9882 ± 0.3997	0.0363 ± 0.0050	0.0055 ± 0.0004	0.0025 ± 0.0003

Table B-7. Normalized platelet and HF fluorescence intensity values for "***Diblock, m = 30***" modified silicones in **Figure 3-3d**.

	0 µmol/g	5 µmol/g	10 µmol/g	25 µmol/g	50 µmol/g
			Platelet Adhesion (*green*, 488 nm)		
Donor 1	1.0000 ± 0.0826	0.9702 ± 0.0703	0.1274 ± 0.0084	0.0277 ± 0.0007	0.0048 ± 0.0002
Donor 2	1.0000 ± 0.0064	0.7824 ± 0.0560	0.0649 ± 0.0008	0.0316 ± 0.0031	0.0095 ± 0.0008
Donor 3	1.0000 ± 0.1929	1.0184 ± 0.3673	0.1120 ± 0.0853	0.0408 ± 0.0102	0.0058 ± 0.0010
			HF Adsorption (*red*, 647 nm)		
Donor 1	1.0000 ± 0.1032	0.6978 ± 0.1951	0.0388 ± 0.0294	0.0133 ± 0.0046	0.0013 ± 0.0006
Donor 2	1.0000 ± 0.0275	0.5842 ± 0.2097	0.0347 ± 0.0074	0.0111 ± 0.0020	0.0012 ± 0.0003
Donor 3	1.0000 ± 0.5188	0.7450 ± 0.7294	0.0322 ± 0.0179	0.0068 ± 0.0035	0.0007 ± 0.0003

Table B-8. Protein adsorption values (mg/cm^2; via LDH assay) for "***XL diblock, m = 13***" and "***Diblock, m = 30***" modified silicones in **Figure 3-6c and 3-6d**, respectively.

	0 µmol/g	5 µmol/g	10 µmol/g	25 µmol/g	50 µmol/g
			"XL Diblock, m = 13"		
Donor 1	6.33 ± 1.05	2.26 ± 0.33	0.96 ± 1.05	1.50 ± 1.10	0.11 ± 0.11
Donor 2	8.35 ± 2.35	4.03 ± 0.82	2.22 ± 0.69	3.41 ± 1.00	1.63 ± 2.49
Donor 3	7.64 ± 2.01	3.03 ± 0.86	1.06 ± 0.45	1.82 ± 1.59	0.09 ± 0.13
			"Diblock, m = 30"		
Donor 1	5.06 ± 1.94	2.71 ± 0.43	0.46 ± 0.37	1.26 ± 1.97	0.04 ± 0.06
Donor 2	5.51 ± 1.60	1.59 ± 0.56	2.85 ± 0.53	1.17 ± 1.08	0.63 ± 0.78
Donor 3	5.40 ± 1.82	1.37 ± 0.47	0.71 ± 0.11	0.10 ± 0.09	0.11 ± 0.08

Table B-9. θ_{static} values for modified PUs immediately after fabrication, in **Figure 4-3**.

	0 µmol/g	5 µmol/g	10 µmol/g	25 µmol/g	50 µmol/g	100 µmol/g
t = 0 s	104.2° ± 11.9°	78.0° ± 3.2°	59.0° ± 14.5°	47.9° ± 21.0°	22.9° ± 0.6°	20.6° ± 0.6°
t = 15 s	90.5° ± 4.4°	74.6° ± 4.6°	44.7° ± 23.9°	25.2° ± 8.2°	19.6° ± 2.8°	14.0° ± 2.9°
t = 30 s	89.6° ± 3.9°	73.7° ± 4.8°	43.2° ± 24.6°	24.9° ± 6.5°	18.7° ± 2.7°	13.8° ± 2.8°
t = 60 s	88.9° ± 4.2°	72.5° ± 4.9°	41.7° ± 25.0°	23.3° ± 6.1°	17.5° ± 2.7°	13.4° ± 3.0°
t = 90 s	88.1° ± 4.2°	71.6° ± 4.8°	40.9° ± 25.2°	22.3° ± 5.8°	16.7° ± 2.7°	12.9° ± 3.0°
t = 120 s	87.5° ± 4.2°	70.7° ± 4.6°	40.1° ± 25.3°	21.5° ± 5.5°	16.3° ± 2.5°	11.8° ± 3.5°

Table B-10. $\theta_{static,\ 2\ min}$ values for modified PUs after both air- and water-equilibration, in **Figure 4-4** and **4-5**, respectively.

	0 µmol/g	5 µmol/g	10 µmol/g	25 µmol/g	50 µmol/g	100 µmol/g
			Air-equilibrated			
t = initial	75.0° ± 2.8°	76.3° ± 3.8°	50.4° ± 24.8°	7.1° ± 2.7°	4.5° ± 0.6°	4.7° ± 0.6°
t = 2 wks	75.3° ± 1.6°	74.8° ± 3.7°	30.1° ± 0.5°	18.8° ± 1.4°	15. 1° ± 3.1°	6.4° ± 1.4°
			Water-Equilibrated			
t = initial	78.4° ± 2.2°	66.8° ± 2.5°	42.1° ± 24.3°	11.9° ± 0.7°	3.6° ± 1.8°	4.9° ± 1.2°
t = 2 wks	78.0° ± 4.6°	76.0° ± 1.5°	53.0° ± 35.1°	20.2° ± 6.8°	20.7° ± 4.0°	13.0° ± 6.4°

Table B-11. Water uptake (wt% water), film mass loss (%), and HF adsorption (ng/cm^2) values for modified PUs from **Figure 4-6**, **4-7**, and **4-8**, respectively.

	Water Uptake (wt%)	Film Mass Loss (%)	HF Adsorption (ng/cm^2)
0 µmol/g	0.45 ± 0.11	1.59 ± 0.52	60.9 ± 29.9
5 µmol/g	0.32 ± 0.11	0.28 ± 0.32	64.2 ± 12.5
10 µmol/g	0.45 ± 0.19	2.27 ± 0.43	75.1 ± 9.4
25 µmol/g	0.53 ± 0.29	0.40 ± 0.37	32.3 ± 13.5
50 µmol/g	1.67 ± 0.47	2.14 ± 1.49	38.9 ± 24.4
100 µmol/g	2.30 ± 1.01	1.98 ± 2.43	63.2 ± 20.3

Table B-12. Normalized platelet and HF fluorescence intensity values for modified PUs in **Figure 4-9b** and **4-9c**, respectively.

	0 µmol/g	5 µmol/g	10 µmol/g	25 µmol/g	50 µmol/g	100 µmol/g
	Platelet Adhesion (*green*, 488 nm)					
Donor 1	1.0000 ± 0.2894	0.9259 ± 0.6268	0.2046 ± 0.0325	0.0611 ± 0.0247	0.0114 ± 0.0028	0.0013 ± 0.0004
Donor 2	1.0000 ± 0.0477	0.7288 ± 0.1731	0.1074 ± 0.0231	0.0068 ± 0.0023	0.0013 ± 0.0002	0.0004 ± 0.0001
Donor 3	1.0000 ± 0.1956	0.5382 ± 0.1365	0.0559 ± 0.0285	0.0096 ± 0.0011	0.0029 ± 0.0007	0.0004 ± 0.0001
	HF Adsorption (*red*, 647 nm)					
Donor 1	1.0000 ± 0.4170	1.5407 ± 1.1645	0.2028 ± 0.0357	0.0411 ± 0.0265	0.0086 ± 0.0023	0.0003 ± 0.0001
Donor 2	1.0000 ± 0.1628	0.4733 ± 0.1463	0.0856 ± 0.0611	0.0181 ± 0.0047	0.0002 ± 0.0001	0.0001 ± 0.0001
Donor 3	1.0000 ± 0.1068	0.7046 ± 0.0717	0.0103 ± 0.0067	0.0008 ± 0.0004	0.0002 ± 0.0001	0.0001 ± 0.0001